Chem Soc Rev

RSC Publishing

REVIEW ARTICLE

View Article Online
View Journal

Arylamine organic dyes for dye-sensitized solar cells

Cite this: DOI: 10.1039/c3cs35372a

Mao Liang†[ab] and Jun Chen*[b]

Arylamine organic dyes with donor (D), π-bridge (π) and acceptor (A) moieties for dye-sensitized solar cells (DSCs) have received great attention in the last decade because of their high molar absorption coefficient, low cost and structural variety. In the early stages, the efficiency of DSCs with arylamine organic dyes with D–π–A character was far behind that of DSCs with ruthenium(II) complexes partly due to the lack of information about the relationship between the chemical structures and the photovoltaic performance. However, exciting progress has been recently made, and power conversion efficiencies over 10% were obtained for DSCs with arylamine organic dyes. It is thus that the recent research and development in the field of arylamine organic dyes employing an iodide/triiodide redox couple or polypyridyl cobalt redox shuttles as the electrolytes for either DSCs or solid-state DSCs has been summarized. The cell performance of the arylamine organic dyes are compared, providing a comprehensive overview of arylamine organic dyes, demonstrating the advantages/disadvantages of each class, and pointing out the field that needs to reinforce the research direction in the further application of DSCs.

Received 5th September 2012

DOI: 10.1039/c3cs35372a

www.rsc.org/csr

1. Introduction

Fossil fuels such as coal, oil, and natural gas have generated most of the energy consumed globally for over a century, paving the way for continued advancement and new inventions. However, the fossil fuel age has also created two significant issues for the world to deal with: climate change mitigation and the

[a] Department of Applied Chemistry, Tianjin University of Technology, Tianjin 300384, People's Republic of China
[b] Key Laboratory of Advanced Energy Materials Chemistry (KLAEMC) (Ministry of Education), Chemistry College, Nankai University, Tianjin, 300071, People's Republic of China. E-mail: chenabc@nankai.edu.cn; Fax: +86-22-23509571; Tel: +86-22-23506808
† M.L. is a visiting professorial scholar at KLAEMC.

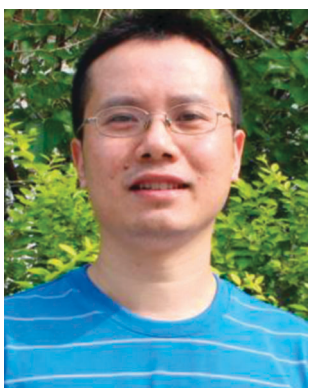

Mao Liang

Mao Liang was born in Sichuan, China, in 1976. He received his PhD in inorganic chemistry under the supervision of Prof. Jun Chen from Nankai University in 2007. He is presently an associated professor at the Department of Applied Chemistry, Tianjin University of Technology. He is also a visiting professorial scholar at KLAEMC. His current research interest is focused on the design and synthesis of dye sensitizers for dye-sensitized solar cells (DSCs).

Jun Chen

Jun Chen was born in Anhui, China, in 1967. He obtained his BSc and MSc degrees from Nankai University in 1989 and 1992, respectively, and his PhD from Wollongong University (Australia) in 1999. He held the NEDO fellowship at National Institute of AIST Kansai Center (Japan) from 1999 to 2002. He was appointed the specially-appointed Professor of Energy Materials Chemistry at Nankai University in 2002, the Outstanding Young Scientist from NSFC in 2003, Cheung Kong Scholar from Ministry of Education in 2005, and the Chief Scientist of the National Nano Key Science Research in 2010. He is the director of KLAEMC. He was awarded the National Natural Science Award (2nd prize) in 2011. His research expertise is energy conversion and storage with solar cells, fuel cells, and batteries.

security of energy supply. To solve these problems, there has been recently a trend towards the increased commercialization of various renewable energy sources. In particular, solar cells are one of the most favorable ways to convert solar energy into electricity and have received considerable attention. As a new type of photovoltaic technology, dye-sensitized solar cells (DSCs) have been considered to be a credible alternative to conventional inorganic silicon-based solar cells, because of their easy fabrication, high efficiency and low cost, since the pioneering report by O'Regan and Grätzel.[1] To date, a 12.3% efficiency of DSCs has been achieved by employing a combination of a zinc porphyrin dye (YD2–*o*–C8) and an organic dye (Y123) in conjunction with a tris(2,2′-bipyridine)cobalt(II/III) redox couple,[2] speeding up the large-scale practical application of DSCs.

Typically, a DSC contains the following key components: (1) a conductive mechanical support such as fluorine-doped SnO_2 (FTO) over layer, (2) a mesoporous semiconductor metal oxide (such as nanocrystalline TiO_2) film, (3) a sensitizer (dye), (4) an electrolyte/hole transporter, and (5) a counter electrode, which is usually made of noble-metal platinum or carbon on FTO, as schematically shown in Fig. 1. In the DSCs system, light is absorbed by the dye anchored on the TiO_2 surface and then electrons from the excited dye inject into the conduction band (CB) of the TiO_2, generating an electric current, while the ground state of the dye is regenerated by the electrolyte to give efficient charge separation. The iodide is regenerated in turn by the reduction of triiodide at the counter electrode and the circuit is completed *via* electron migration through the external load. The voltage generated under illumination corresponds to the difference between the Fermi level of the electron in the solid and the redox potential of the electrolyte.[3] Thus, the device generates electric power from light continuously. A unique feature of DSCs compared with the other solar cell technologies is that they separate the function of light absorption from charge carrier transport,[4] allowing optimization of the device by careful screening of the light absorber and charge transport materials.

The sensitizer, which acts as the light harvesting antennae, is essential for efficient light harvesting and electron generation/transfer. Generally, the ideal photosensitizer should fulfill the following essential characteristics: (1) the dye displays a very broad absorption spectrum with a high molar extinction coefficient (ε) to enable efficient light harvesting with thinner TiO_2 films, namely panchromatic absorption; (2) the dye shows appropriate steric properties to suppress charge recombination at the TiO_2/electrolyte interface and dye aggregation, both of which have an adverse effect on the photocurrent and photovoltage; (3) the lowest unoccupied molecular orbital (LUMO) of the dye should be more negative than the conduction band of TiO_2 (−0.5 V *vs.* NHE), to provide sufficient driving forces (at least 0.2 eV[5]) for electron injection; (4) the highest occupied molecular orbital (HOMO) of the dye should be more positive than the energy level of the redox mediator, to provide sufficient driving forces (at least 0.15 eV[6]) for the efficient regeneration of the oxidized dye; (5) the dye should have suitable anchoring groups, such as carboxylates or phosphonates, for grafting the dye on the semiconductor surface, to ascertain the intimate electronic coupling between the excited state wave function and the conduction band manifold of the semiconductor;[7] (6) the photo- and heat-stability of the dye should be high enough to ensure a long lifetime of DSCs.

Based on these requirements, many different photosensitizers, including metal complexes, porphyrins, phthalocyanines and metal-free organic dyes, have been designed and applied to DSCs in the past two decades.[8] In particular, N719 $(Bu_4N)_2[Ru(dcbpyH)_2(NCS)_2]$ possesses a superior photovoltaic performance to other metal complexes.[8] On the other hand, metal-free organic dyes have received great attention for their low cost, high molar absorption coefficient, high efficiency and easy synthesis. Generally, metal-free organic sensitizers are constituted by donor (D), π-bridge (π) and acceptor (A) moieties, so called D–π–A character. This push–pull structure can induce the intramolecular charge transfer (ICT) from subunit A to D through the π-bridge when a dye absorbs light (Fig. 2), which is important for light harvesting. Moreover, it is easy to tune the absorption spectra as well as the HOMO and LUMO levels of the dyes by variation of the D, π and A moieties. By this way, hundreds of metal-free organic dyes with tailor-made photophysical, electrochemical, and other properties have been obtained and successfully adopted to act as sensitizers for DSCs over the past ten years. Among the metal-free organic dyes, the arylamine organic dyes, holding the record for validated efficiency of over 10.3%, are promising candidates for highly efficient DSCs.[9]

Arylamine derivatives are well known electron-rich compounds that are widely used in hole transporting materials and light emitters in the field of optoelectronics, such as in organic light-emitting diodes (OLEDs), organic field-effect transistors, non-linear materials and organic solar cells.[10] The family of arylamines

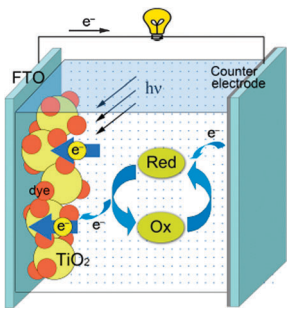

Fig. 1 Schematic working principle of a DSC.

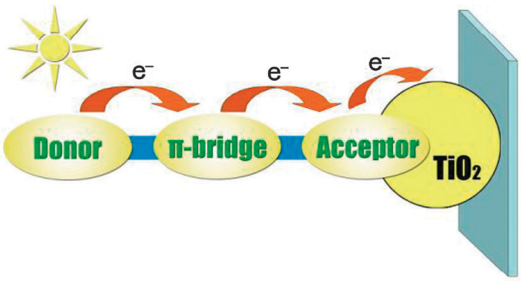

Fig. 2 Schematic of the D–π–A structure of an organic dye.

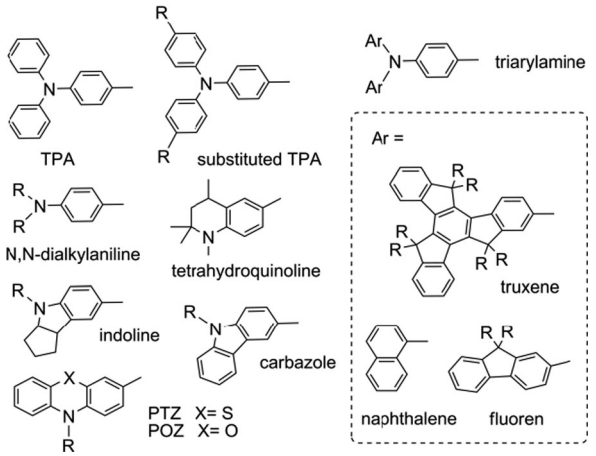

Fig. 3 Molecular structure of arylamine donors.

has also many favorable properties such as redox, ion transfer processes, and photoelectrochemical behavior as well as their excellent electronic properties.[11] In recent years, it has been found that the arylamine derivatives are desirable for organic sensitizers. As shown in Fig. 3, representative arylamine donors, including triphenylamine (TPA),[21–52] substituted TPA,[53–98] triarylamine (fluoren-substituted aniline,[110–128] naphthalene-substituted aniline[129–136] and truxene-substituted aniline[137–142]), indoline,[143–162] *N*,*N*-dialkylaniline,[163–166] tetrahydroquinoline,[167–169] phenothiazine (PTZ)/phenoxazine (POZ)[171–188] and carbazole,[189–201] have been developed as organic dyes for DSCs.

Like metal complexes, porphyrins and other organic dyes, arylamine organic dyes also suffer from a series of scientific problems with respect to higher efficiency. The main issues include: (1) lack of absorption in the near-infrared region, (2) charge recombination at the TiO_2/electrolyte interface, (3) dye aggregation on the TiO_2 film, and (4) the energy level mismatch between the dye, TiO_2 and electrolyte.

The bathochromic shift of the absorption maxima is one of the most important challenges to improve the DSCs performance. Snaith proposed that with the loss-in-potential of the present state-of-the-art DSCs (0.75 eV), a maximum efficiency of 13.4% is achievable employing a sensitizer with an absorption onset at 840 nm.[12] Reducing the loss-in-potential to that of the least ''lossy'' DSC reported to date (0.66 eV) results in a maximum efficiency of 15.1% with an absorption onset at 920 nm. The first issue could be fulfilled by the introduction of electron-donating groups onto the donors, introduction of electron-rich and electron-withdrawing groups onto the π-bridges, or incorporation of a longer conjugated segment in the push–pull system. Moreover, co-sensitization using multiple dyes, to have complementary absorption features, is also an efficient approach, which is beyond the scope of this review. For the second and third issue, an efficient strategy is the introduction of sterically hindered substituents (bulky groups) such as long alkyl chains and aromatic units onto the donors or π-bridges. On the other hand, co-adsorbents such as deoxycholic acid (DCA) have been successfully utilized to avoid the charge recombination and dye aggregation. As for the final issue, a typical case is the potential mismatch between the I^-/I_3^- redox potential and the HOMO level of the photosensitizer. In other words, a more negative potential of the I^-/I_3^- redox couple strongly leads to a reduction in photovoltage value.[13] To avoid the efficiency loss in DSCs, the HOMOs and LUMOs of dyes should match the conduction band edge of TiO_2 and the redox potential of the electrolyte, respectively. This could be realized by chemical modification of each component.

It is necessary to point out that the aforementioned issues are closely related to each other. In other words, it is easy to deal with one or two problems, but difficult to control all of them. In this context, much effort has been dedicated to the design and synthesis of different types of arylamine organic dyes and the investigation of structure–function relationships.

Herein, we intend to review the fundamentals and the most recent and significant scientific progress made in the fields relevant to arylamine-based organic dyes, with emphasis placed on the structure–function relationships. The survey of intensively investigated arylamine organic dyes, and the discussion of the design and optimization of molecular structure will be sequentially presented in the following sections with the final conclusion remarks being on future challenges and perspectives. The aim is to provide promising design principles for the future development of new organic molecules for the dyes of DSCs.

2. Photovoltaic parameters of DSCs

There are two widely used techniques for photovoltaic characterisations: current–voltage measurements under simulated sunlight (producing *J*–*V* curves) and monochromatic light generated current measurements (producing incident photon-to-current conversion efficiency (IPCE) spectra). The photovoltaic parameters including short-circuit photocurrent density (J_{SC}), open-circuit voltage (V_{OC}), fill factor (FF) and overall power conversion efficiency (PCE) can be obtained by the current–voltage measurements.[3,4] Generally, the standard solar spectrum used for the efficiency measurements of solar cells is AM 1.5 irradiation, corresponding to the irradiance of 100 mW cm^{-2}, namely, P_{in} = 100 mW cm^{-2}. A typical *J*–*V* curve is shown in Fig. 4.

The J_{SC} is the photocurrent per unit area (mA cm^{-2}) when the applied bias potential is zero. When no current is flowing through the cell, the potential equals the V_{OC}. The FF is defined as the maximum power output ($J_{max} \times V_{max}$) divided by the product of J_{SC} and V_{OC}: FF = ($J_{max} \times V_{max}$)/($J_{SC} \times V_{OC}$). The FF quantifies the quality of the DSCs, it is the ratio between the areas of the two rectangles shown in Fig. 4. The PCE can be calculated from eqn (1).

$$\mathrm{PCE} = \frac{J_{SC} V_{OC} \mathrm{FF}}{P_{in}} \quad (1)$$

To better evaluate the J_{SC}, another important parameter, the IPCE, has to be taken into account. The IPCE value corresponds to the photocurrent density that is produced in the external circuit under monochromatic illumination of the cell divided by the photon flux that strikes the cell.[8] A typical IPCE spectrum is shown in Fig. 5. Generally, a low IPCE value results in low J_{SC}.

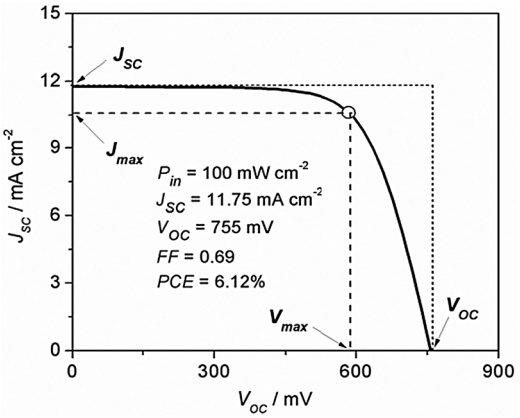

Fig. 4 A typical *J–V* curve of a DSC.

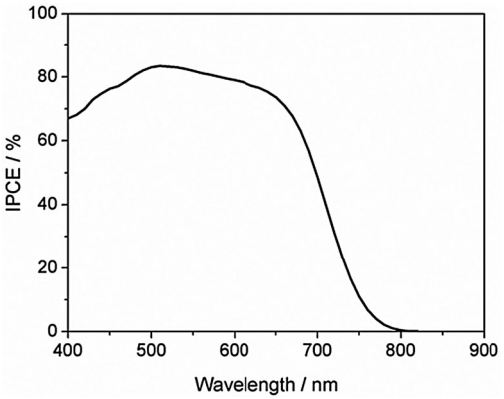

Fig. 5 A typical IPCE curve of a DSC.

The IPCE is expressed by the product of the absorbed photon-to-current conversion efficiency (APCE) and the light harvesting efficiency (LHE):[14,15]

$$\mathrm{IPCE}\ (\lambda) = \mathrm{APCE} \times \mathrm{LHE} = \Phi_{\mathrm{inj}} \times \eta_{\mathrm{col}} \times \mathrm{LHE} \qquad (2)$$

where APCE should be divided into two terms: the overall charge collective efficiency (η_{col}) and the overall electron injection efficiency (Φ_{inj}). The LHE at the maximum absorption wavelength can be estimated using the following equation: LHE = $1–10^{-A}$,[16] where A is the absorbance of the dye on TiO_2 at the maximum wavelength. Therefore, IPCE is determined by the light harvesting ability, the amount of adsorbed dyes on the TiO_2 surface, the overall charge collective efficiency and the overall electron injection efficiency. It is noted that the maximum IPCEs for DSCs generally should be smaller than 90% because of the reflection and absorption loss due to the FTO glass.

On the other hand, the value of V_{OC} is determined by the potential difference between the Fermi-level of TiO_2 ($E_{\mathrm{F,n}}$) and the Fermi-level of a redox electrolyte ($E_{\mathrm{F,redox}}$) as shown in Fig. 6. The V_{OC} and $E_{\mathrm{F,n}}$ can be expressed as:[17]

$$V_{\mathrm{OC}} = E_{\mathrm{F,redox}} - E_{\mathrm{F,n}} \qquad (3)$$

$$E_{\mathrm{F,n}} = E_{\mathrm{CB}} + k_{\mathrm{B}}T \ln\left(\frac{n_{\mathrm{c}}}{N_{\mathrm{c}}}\right) \qquad (4)$$

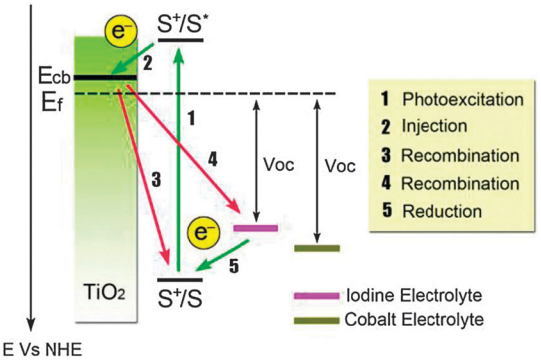

Fig. 6 Simple energy level diagram and basic electron transfer processes for a DSC.

where k_{B} is the Boltzmann constant, T is the temperature (293 K in this work), n_{c} is the free electron density and N_{c} is the density of accessible states in the conduction band.[18] Considering that $E_{\mathrm{F,redox}}$ would not change strongly in DSCs with a fixed redox electrolyte, V_{OC} is intimately correlated to the E_{CB} and n_{c}. The E_{CB} is determined by the surface charge of the TiO_2 and the n_{c} is determined by the balance between electron injection (process 2 in Fig. 6) and electron recombination (processes 3 and 4 in Fig. 6). Therefore, dyes affect the conduction band edge position of TiO_2 differently, since any change in the surface charge will shift the conduction band edge position.[19] Furthermore, any change of the surface blocking of the dyes on the TiO_2 surface leads to different amounts of electron recombination (process 4 in Fig. 6). Finally, electrolyte–dye interactions may lead to enhancing the electron recombination. Therefore, the dyes have an important impact not only on both the J_{SC} and V_{OC}, but also on the performance of the devices.

It is also pointed out that the use of the iodide/triiodide electrolyte as a redox shuttle limits the attainable V_{OC} to 0.7 to 0.8 V. To further improve the V_{OC}, and hence the PCE of DSCs, alternative redox couples such as the Co-complex based redox couples have been explored, enabling the attainment of high photovoltages (Fig. 6). The exploration of arylamine organic dyes for DSCs employing cobalt electrolytes will be discussed in detail in Section 11.

3. The developing map of arylamine organic dyes

As mentioned above, arylamine derivatives are promising materials for electron donors. The donor groups can not only affect the absorption spectra but also adjust the energy levels of the sensitizers. Therefore, choosing a suitable donor group in the D–π–A system is very critical to balance between photovoltage, driving forces and spectral response for the preparation of high efficiency dyes.[20] To enhance the donor ability of TPA and suppress the charge recombination at the TiO_2/electrolyte interface and dye aggregation, substituted TPA dyes were developed.[53–98] To engineer the organic sensitizers with an enhanced stability and a reduced tendency toward aggregation, a successful approach was

introduced by incorporating a triarylamine moiety into the organic framework. As demonstrated, triarylamine dyes not only suppress the aggregation but also increase the molar extinction coefficient of the organic sensitizer and retard the charge recombination.[110,113,141] On the other hand, PTZ/POZ is a well-known heterocyclic compound with electron-rich sulfur and nitrogen heteroatoms.[170] The PTZ/POZ ring is nonplanar with a butterfly conformation in the ground state, which can impede the molecular aggregation and the formation of intermolecular excimers.[180] To red-shift the maximum absorption band to a longer wavelength, arylamines with alkyl substituents such as *N*,*N*-dialkylaniline[20,166] and indoline[20] were introduced as donors for the organic dyes. Like TPA, carbazole was utilized as an electron donor due to its stronger electron-donating ability and excellent hole-transporting ability.[188–193] Thus, minor changes in the geometry of the donor structure could result in interesting photophysical, electrochemical, and other properties.

4. TPA and substituted TPA dyes

4.1 TPA dyes

The TPA unit is well-known for its strong electron-donating ability and hole-transport properties. A very large number of triarylamine dyes with a variation of π-bridges have been developed and most of them have shown good power conversion efficiencies in DSCs.[21–52]

Originally, double bonds and triple bonds were introduced as spacers for the expansion of the π-conjugated system (Fig. 7). Yanagida and co-workers first introduced the TPA unit as an electron donor in organic dyes and obtained a PCE of 3.3% and 5.3% for dyes **1** and **2**, respectively (for reference: **N719**, 7.7%).[21] The bathochromic shift of the absorption spectrum of **2** was achieved by increasing the number of methine units, thus leading to higher efficiency. Yang, Wang, Sun and co-workers further synthesized two TPA dyes (**4**, PCE = 4.3% and **6**, PCE = 5%) with triple bonds as π-spacers. Two TPA dyes (**3**, PCE = 5.73% and **5**, PCE = 6.25%) with double bonds were applied in DSCs to study the influence of triple bonds as π-spacer units on their photoelectrochemical properties and DSCs performance.[22] In comparison to the DSCs performance of reference dyes without a triple bond, the introduction of the triple bond improved the PCE slightly because of a slight enhancement of J_{SC}, but the introduction of a double bond could improve the PCE dramatically because of a large enhancement of J_{SC}. The lower J_{SC} of the DSCs sensitized by the dyes with a triple bond was attributed to their narrower absorption spectra than that of the dyes with a double bond. In spite of that, it does not mean that the double bond is always better than the triple bond. For example, when organic dyes were bridged by anthracene-containing π-conjugations, a higher PCE was obtained for the DSC sensitized by **8** (PCE = 6.78%) than that by **7** (PCE = 5.14%).[23] With the appearance of a triple bond and a double bond, the dihedral angles in **8** and **7** are 0° and 48.4°, respectively. Better molecular planar conjugation of **8** than that of **7** leads to a broader absorption spectrum and thus a higher J_{SC} and PCE of the DSC sensitized by **8**. This result revealed that suitable planar conjugation was essential for high J_{SC} realization.

To further design and develop more efficient TPA dyes with a phenylene bridge, Yang, Hagfeldt, Sun and co-workers reported a series of TPA dyes (**3**, PCE = 5.73%; **9**, PCE = 4.36%; **10**, PCE = 3.86%; **11**, PCE = 0.44%; and **12**, PCE = 3.49%) consisting of the phenylene with different substitutes.[24] Compared to **3**, the introduction of different electron-withdrawing substitutes on the phenylene units (**9**, **10** and **11**) used as the π-spacers, to act as the electron acceptor in the molecular structures, can give bathochromic shifts of the absorption spectra. However, a negative effect on the DSCs performance was observed because the electron-withdrawing units on the π-spacers suppressed the electron injection from the LUMO level to the TiO_2 CB. On the other hand, the relatively low photovoltaic performance of **12** was attributed to its narrow range of visible spectrum response. In contrast, when methoxy was introduced as an electron-donating group (**13**, PCE = 6.49%), an improved PCE was reported by Park, Kim and co-workers.[25,26]

Considering the stability of the chromophores is less affected than that of polyene linkers,[27] Hagfeldt, Sun and co-workers further optimized the TPA dye by introducing thiophene to extend the number of π-conjugations,[28] based on dye **5**.[29] The dyes (**1**, PCE = 1.55%; **5**, PCE = 3.08%; and **14**, PCE = 2.73%) show satisfactory efficiencies on thin TiO_2 films (3 μm), demonstrating the advantage of chromophores with higher extinction coefficients. By increasing the π-conjugation of the linker, the HOMO and LUMO energy levels were tuned. The longer linker conjugation gave an enhanced spectral response but increased the recombination of electrons to the triiodide (*e.g.* **5** *vs.* **14**), leading to lower IPCEs.

In a study on the V_{OC} of DSCs using the three dyes (**1**, 710 mV; **5**, 640 mV; **14**, 585 mV), Mori, Hagfeldt and co-workers discussed

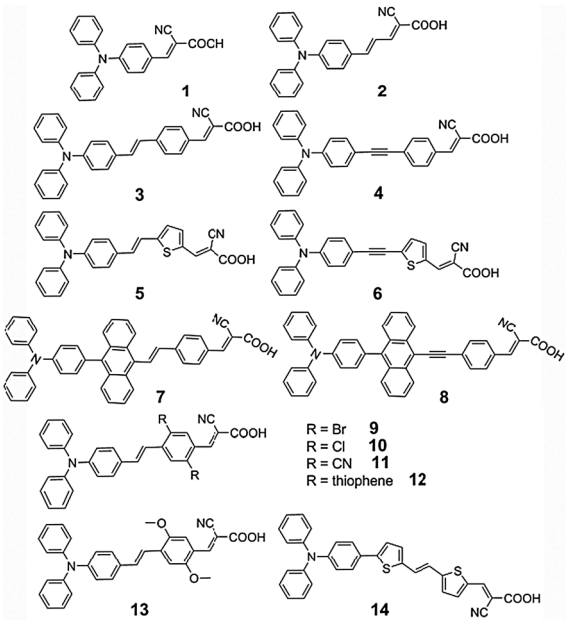

Fig. 7 Representative TPA dyes **1–14**.

the factors that affect the V_{OC} and electron lifetimes.[19] They claimed that the surface blocking of the dye layer could be improved by reducing the dye size. Good surface blocking means a high V_{OC} and long electron lifetimes. They also pointed out that there was an interaction between the **14** dye molecular structure and I_3^- and/or I_2. This finding demonstrated that enhancing the efficiency of the dyes by simple expansion of the π-conjugated system through increasing the number of electron-rich segments (such as thiophene) was not an effective strategy, because the halogen bonding between iodine and some electron-rich segments of the dye molecules could cause a larger charge recombination rate at the titania/electrolyte interface.

In parallel with the studies on double bonds and triple bonds, efforts were made to explore more utilizable thiophene derivatives (Fig. 8). With the goal of developing simple organic dyes based on TPA, Chi, Chou and co-workers designed and synthesized a series of TPA dyes (**15–17**) containing thiophene derivatives,[30] such as 3,4-ethylenedioxythiophene (EDOT) or 3,4-bis[2-(2-methoxyethoxy)ethoxy]thiophene (BMEET). Dyes **16** (λ_{max} = 426 nm) and **17** (λ_{max} = 420 nm) showed a bathochromic shift compared with **15** (λ_{max} = 410 nm) due to the strong electron-donating ability of the alkoxy group. Relative to **15** and **17**, the higher PCE of **16** (7.3%) was attributed to a broader spectral response, higher molar absorption coefficient and higher amounts of dye adsorbed on the TiO_2 films. The side chain of **17** suppressed the dark current from the free TiO_2 conduction-band to the counter electrolyte, while the long side chain also led to less dye-uptake and hence a low J_{SC}. The same research group also prepared dyes **18–20** containing EDOT plus various functionalized phenylenes as spacers.[31] These organic sensitizers exhibited much higher molar extinction coefficients than the parent **16** dye, as well as revealing a remarkable fluorine substituent effect. **20**, with fluoro substitution at the *meta* position relative to cyanoacrylic acid, possesses a lower S_0–S_1 gap and weaker coupling with the TiO_2 electrode (*cf.* **18** and **19**). Conversely, due to the resonance effect with respect to cyanoacrylic acid, the *ortho*-F-substituted **20** has a larger energy gap but stronger TiO_2 affinity. As a result, **20** showed better DSC performance with J_{SC} = 15.58 mA cm^{-2}, V_{OC} = 787 mV, FF = 0.67 and PCE = 8.22%.

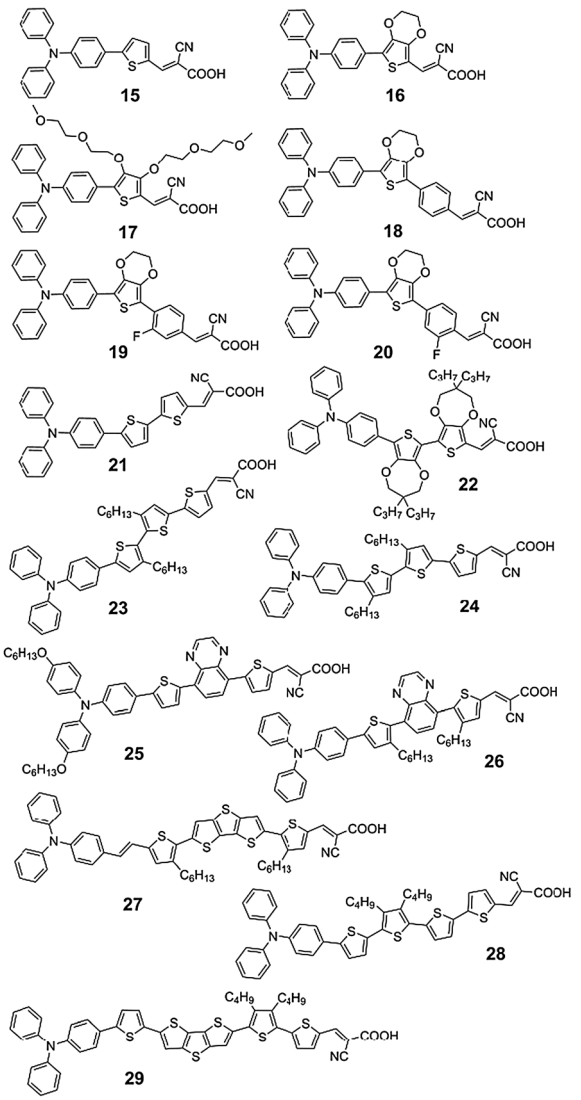

Fig. 8 Representative TPA dyes **15–29**.

As discussed above, the complex formation between dye molecules and I_2 or I_3^- is a determining factor for the V_{OC} of DSCs. In order to alleviate the strong interaction between sensitizers and acceptor species in the electrolyte, our attempts to develop high-efficiency TPA dyes focus on the retardation of charge recombination by introducing appropriate steric hindrance to the sensitizer backbone, namely, the passivation of the sensitizers rather than the entire TiO_2 surface. The three-dimensional (3D) branched structures of the functionalized 3,4-propylenedioxythiophene (ProDOT) not only disfavor π–π packing but also block other molecules (*e.g.*, I_3^-) from approaching.[32] As a result, the V_{OC} of **22** (V_{OC} = 797 mV, PCE = 5.3%) is much higher than that with a thiophene congener **21** (V_{OC} = 720 mV, PCE = 4.36%) under similar conditions. This finding provides a novel strategy for the multi-functionalization of organic dyes, as well as for the retardation of charge recombination in DSCs.

Mori, Yamashita and co-workers proposed a new strategy to improve the V_{OC} of TPA dyes with a long π-conjugation unit, namely, increasing steric hindrance by attaching obstacle units to the π-linker without a significant increase of polarizability.[33] Their studies showed that the addition of an alkyl chain to the dyes increased the electron lifetime. Further increase of the electron lifetime was obtained by introducing a twisted structure. Compared with **24** (V_{OC} = 720 mV, J_{SC} = 11.9 mA cm^{-2}, PCE = 6.3%), the two hexyl groups introduced to the opposable 3,3′-positions of a bithiophene spacer in **23** (V_{OC} = 750 mV, J_{SC} = 10.1 mA cm^{-2}, PCE = 5.7%) successfully realized an increase in V_{OC} by 30 mV. They also suggested that the twisted structure is not essential, but having a 3D structure to increase the distance between the dyes and acceptors is important to increase the electron lifetime.

However, the twisted spacer structure may interrupt the conjugation system and weaken the ICT interactions, resulting

in a hypsochromic shift of the maximum absorption band as well as low J_{SC}. Interestingly, the adverse impact of a twisted spacer structure on the absorption of dye is still distinct, even inserting a quinoxaline unit into the opposable 3,3′-positions of a bithiophene spacer. For example, the DSCs based on **25** (V_{OC} = 676 mV, J_{SC} = 14.6 mA cm^{-2}, PCE = 7.4%) showed an improved light harvesting efficiency and therefore photogenerated current due to its much broader absorption spectra in comparison to that of **26** (V_{OC} = 735 mV, J_{SC} = 5.70 mA cm^{-2}, PCE = 3.2%).[34] As the inserting spacer changes from quinoxaline to dithieno-[3,2-*b*:2′,3′-*d*]thiophene (DTT), this effect arises from the two 3-hexylthiophenes attenuation. Dye **27** (V_{OC} = 697 mV, J_{SC} = 14.4 mA cm^{-2}, PCE = 7.3%) in CH_2Cl_2 showed a strong broad absorption maximum around 490 nm.[35]

In addition to the 3-alkyl-thiophene moieties, 3,4-dialkyl-thiophene rings also enable high steric hindrance and thus decrease the dye aggregation and enhance the tolerance towards water in the electrolyte. The introduction of a 3,4-dibutyl-thiophene ring into dyes **28** and **29** reduced the sensitizer aggregation and allowed the preparation of solar cells with PCEs of 7.17% and 6.27% without the use of coadsorbant agents.[36]

Fluorene derivatives have been used as the spacer in organic dyes (Fig. 9) because of their electron-rich nature, good stability and the suppressing of the charge recombination and inter-molecular interaction ability. Dye **31** (λ_{max} = 510 nm) provided a more red shifted value than that of **30** (λ_{max} = 443 nm), though both of them possess a similar π-conjugation length.[37] This result can be understood by considering their molecular geometries. The increased twist angle between the fluorene entity and the EDOT ring led to a less effective π-conjugation length and, consequently, blue shifted λ_{max}. Nevertheless, the efficiency of **31** (PCE = 4.4%) is lower than that of **30** (PCE = 5.8%) because of strong charge recombination. In contrast, spirobifluorene was found to be less efficient due to low J_{SC} and V_{OC}.[38,39]

Considering the furan ring with smaller resonance energy (furan, 16 kcal mol^{-1}; thiophene, 29 kcal mol^{-1}; benzene, 36 kcal mol^{-1}) can provide more effective conjugation, Lin, Yeh and co-workers incorporated a furan ring between a TPA donor and a cyanoacrylic acid acceptor to yield **32** and **33**.[40] The cells based on the two dyes exhibited high conversion efficiencies (7.36 and 6.3%, respectively), reaching ~96% of a **N719**-based DSC (PCE = 7.69%). A comparison is also made between **32** and the thiophene congener (PCE = 6.09%), suggesting the superiority of furan.

To develop and evaluate the potential of pyrroles-based sensitizers, Lin, Hsu and co-workers reported a series of organic dyes with pyrrole in the spacer.[41] Among these dyes, **34** and **35** exhibited PCEs of 4.77% and 4.79%, respectively. An advantage of the pyrrole moieties in the spacer is better charge separation in the excited states, arising from less interaction with its neighboring aromatic units. Li and coworkers developed a series of "H" type dye sensitizers with pyrrole as the conjugated bridge.[42] Two *N*-arylpyrrole-based organic dye moieties were linked through various aromatic rings. The solar cell based on dye **36** with carbazole as the isolation group exhibited 5.22% conversion efficiency under AM 1.5 irradiation (100 mW cm^{-2}). Moreover, coadsorption of CDCA did not improve the conversion efficiency of the devices, indicating that the "H" type dyes nearly did not aggregate on the TiO_2 surface.

Besides the electron-rich moieties (benzene, thiophene, fluorene, furan and pyrrole) mentioned above, electron-deficient blocks were also tested as effective fragments for organic dyes (Fig. 10).[43–52] Benzothiadiazole or benzoselenadiazole fragments were first exploited for DSCs by Lin, Ho and co-workers.[43] The lower extinction coefficient of **38** compared to the benzothiadiazole counterpart (**37**) was attributed to the larger size and smaller electronegativity of Se when compared to S, which lead to less electron density on Se and thus diminished aromaticity for the benzoselenadiazole. Despite the moderate PCEs of **37** and **38** (3.77 and 2.91%, respectively; **N3**, 5.3%), this design opened up the possibility of preparing new dye molecules for DSCs utilizing low band gap building blocks. Later, they further developed the benzothiadiazole unit by the introduction of alkoxy chains.[44] Dye **39**, containing a 5,6-bis-hexyloxy-benzo[2,1,3]thiadiazole entity in the conjugated spacer, gave a PCE of 6.72%, reaching 92% of the standard **N719** device.

Recently, the design of a conjugated bridge using low band gap building blocks plus long alkyl chains has become popular. Clearly, the low band gap building blocks could extend the spectral response region. On the other side, the introduction of alkyl chains would not only make the dyes more soluble and reduce aggregation in devices, but also suppress charge recombination in DSCs.

Dye **40**, showing a wide coverage of the solar spectrum, was synthesized by Jiang, Pei and co-workers.[45] The absorption onset of **40** red-shifted from about 710 nm in solution to about 800 nm in the solid state. The absorption features in thin films covered nearly the whole visible range, namely, from 300 nm to 800 nm. Such a broad absorption is greatly beneficial to the improvement of photocurrent density and power-conversion efficiency. The devices fabricated from **40** showed PCE as high as 6.04%, which is close to that of the classical dye **N3** under

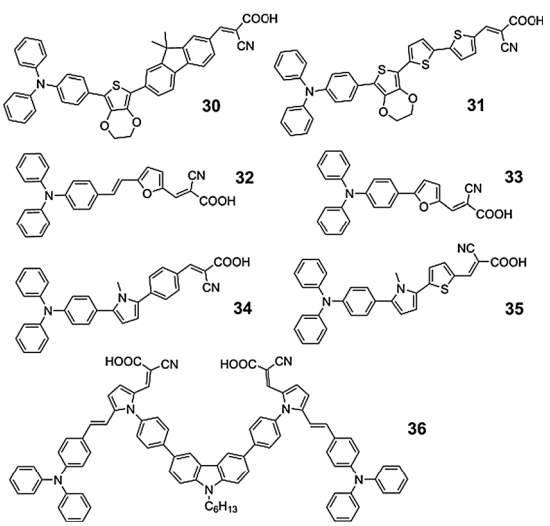

Fig. 9 Representative TPA dyes **30–36**.

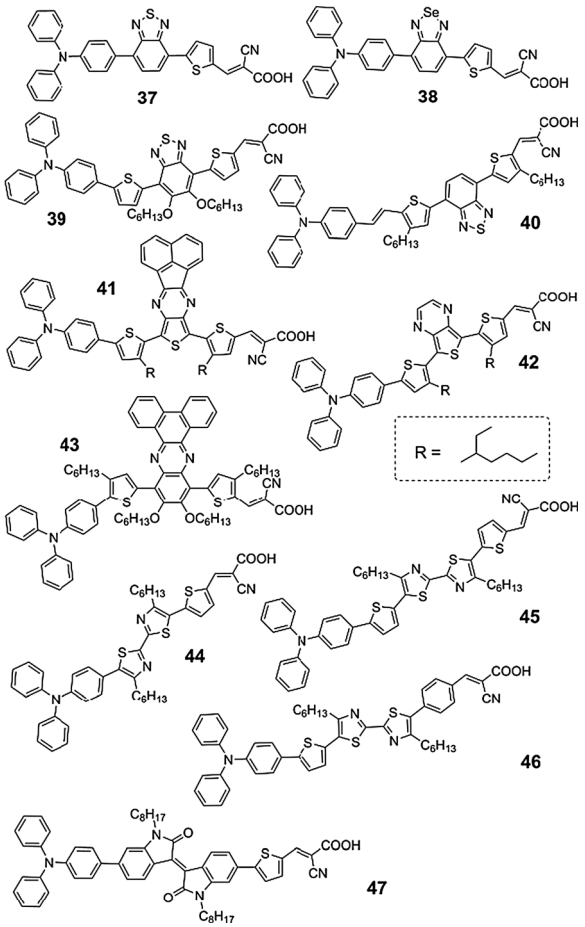

Fig. 10 Representative TPA dyes **37–47**.

the same conditions. A similar phenomenon was observed by Zhou and co-workers.[46] They introduced a thieno[3,4-*b*]pyrazine derivative unit into the conjugated backbone of **41** and **42** to tune the absorption spectra. The extended conjugation of the additional acceptor from thieno[3,4-*b*]pyrazine (**42**, λ_{max} = 596 nm) to acenaphtho[1,2-*b*]thieno-[3,4-*e*]pyrazine (**41**, λ_{max} = 625 nm) bathochromically shifted the absorption peak significantly. They compared the absorption spectra of the terthiophene based dyes and proposed that increasing the thiophene number is not an effective way to bathochromically shift the maximum absorption of the sensitizers significantly (*e.g.* λ_{max} > 600 nm). It is impressive that the IPCE onsets are located at around 900 nm for the two dyes, which is comparable to that for the black dye. However, **41** and **42** exhibit low V_{OC} values (below 500 mV), which partially compensate for the positive effect of the near infrared (NIR) IPCE response, resulting in moderate PCEs of 5.3 and 3.66%, respectively.

Shi *et al.* developed TPA dyes containing an 11,12-bis(hexyloxy)dibenzo[*a*,*c*]phenazine (BPz) unit. They demonstrated that the intermolecular aggregations can be suppressed in a large degree by the addition of the BPz unit in the π-conjugated spacer, which would avoid the unnecessary energy loss by the molecular interactions. Dye **43** showed a PCE of 5.3%.[47]

Hua, Tian and co-workers studied a series of TPA dyes containing bithiazole moieties.[48,49] Despite the long π-bridge of the dye, a remarkably high V_{OC} of 810 mV was achieved by **44**-sensitized solar cells with thick TiO_2 films (double layers: 10 μm + 4 μm). Under the same conditions, **45** and **46** showed high V_{OC} of 778 and 789 mV (**N719**, 672 mV), respectively. This feature can be attributed to the retarded charge recombination by two hexyl chains with substituted bithiazole. Compared with **46** (12.47 mA cm^{-2}), **45** (15.69 mA cm^{-2}) has an improved J_{SC} due to its higher molar extinction coefficient and broader photocurrent action spectra. These results indicated that thiophene is superior to benzene in terms of light harvesting and response of photocurrent, but inferior to the latter in terms of photovoltage. **44** displayed the best overall light-to-electricity conversion efficiency of 7.51% under AM 1.5 irradiation (100 mW cm^{-2}). The same group also reported a series of TPA dyes containing isoindigo as an auxiliary electron-withdrawing unit. Compared with **44** (λ_{max} = 457 nm), **47** (λ_{max} = 563 nm) exhibited a broad absorption in the near NIR region. However, the power conversion efficiency of **47** is limited by the low V_{OC} (559 mV).[50]

In summary, the incorporation of both electron-rich moieties and electron-deficient blocks into the π-bridge are effective ways to tune the performance of TPA dyes. However, the performance of this type of system is still behind the ruthenium dyes owing to lower J_{SC} and V_{OC}. To achieve high J_{SC}, improving the electron-donating ability of TPA and designing new push–pull systems for broader and higher IPCE response is necessary. Meanwhile, suppressing charge recombination and dye aggregation remain key factors for this issue, as these are intimately correlated with the ultimate power output of a DSC. This recognition has translated into massive efforts in designing new classes of substituted TPA dyes.

4.2 Substituted TPA dyes

Thanks to its starburst structure, TPA can be engineered to meet the requirements of ideal donors (with a strong electron-donating ability and contribution to suppressing charge recombination and dye aggregation). Up to now, a variety of 4-substituted TPA derivatives and 4,4′-disubstituted TPA derivatives have been explored and these have become classic classes of electron donors.[53–98]

To enhance the electron-donating ability of TPA, our group reported a family of TPA dyes (Fig. 11) with the introduction of electron-rich groups to an adjacent phenyl ring, which was proved to be an effective way to improve the dye performance.[15,53–60] For example, dye **49** (PCE = 5.8%), with a CH_2═CH– substituted TPA electron-donating group, exhibits a superior performance when related to the corresponding dye (**48**, PCE = 4.3%) without the CH_2═CH– substitution.[53] Later, diphenylvinylsubstituted TPA as the electron donor was employed, and dye **50** achieved a power conversion efficiency of 6.3% (AM 1.5 irradiation) and exhibited good stability under one sun irradiation for 20 days.[56] The all-solid-state solar cell with this electrolyte and the organic dye **53** shows a PCE of 2.70% and 4.12% under the illumination intensities of 100 and 10 mW cm^{-2}, respectively.[57]

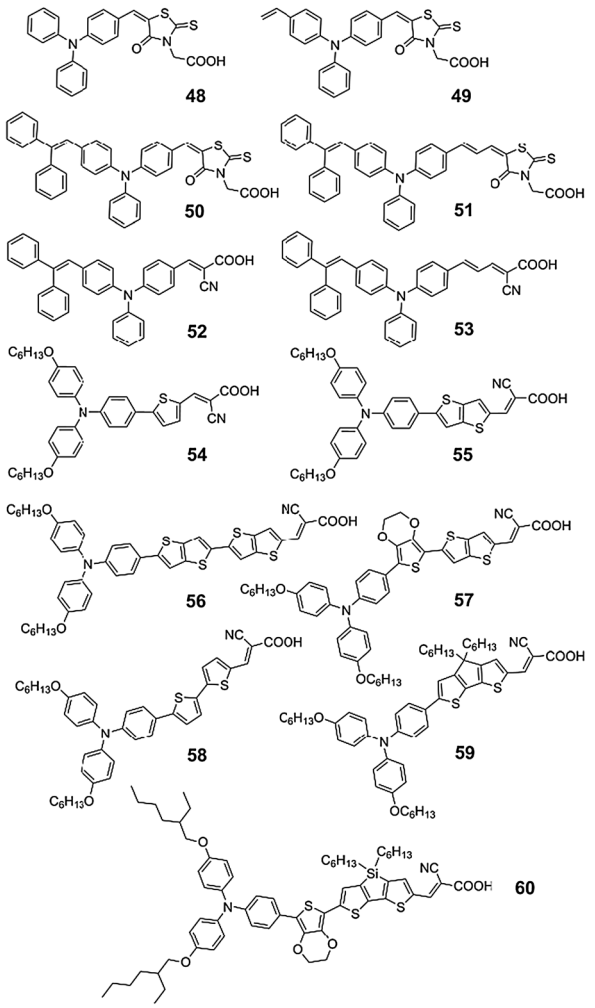

Fig. 11 Representative substituted TPA dyes **48–60**.

In our development of TPA-based organic sensitizers, we noticed an interesting trend in which sensitizers incorporating cyanoacrylic acid (CA) as the acceptor/anchoring group always gave higher V_{OC} values than the corresponding dyes bearing identical donors and π-bridges but a different acceptor of rhodanine-3-acetic acid (RA).[15] This phenomenon was also observed by other groups.[24,30,61] From analysis of the transient absorption traces in the NIR region, Wiberg *et al.* concluded that the RA dyes facilitate recombination by injecting electrons to short-lived surface trap states, suffering from their specific electronic structures.[61] Our theoretical investigation based on density functional theory (DFT) and time-dependent DFT (TDDFT) have shown that the cyanoacrylic acid anchor favors better photoelectrochemical properties of DSCs than those of the rhodanine-3-acetic acid anchor *via* providing more shift of the TiO_2 conduction band toward the vacuum energy levels and more favorable conjugation with titanium.[62] Moreover, we systematically investigated the relationship between the dye adsorption behavior and V_{OC} of DSCs based on four TPA-based organic sensitizers (**50**, 631 mV; **51**, 534 mV; **52**, 715 mV; **53**, 692 mV).[15] **52** and **53** with cyanoacetic acid as an anchoring

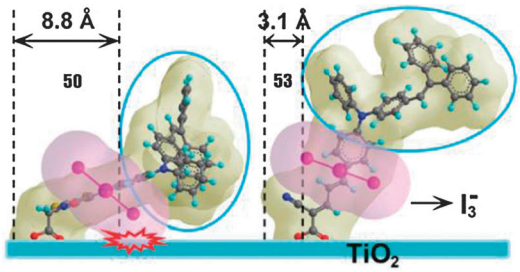

Fig. 12 Graphical illustration of the geometries of the adsorbed dyes and the dye–I_3^- interaction. Reproduced with permission from ref. 15. Copyright 2010, American Chemical Society.

group adopt a standing adsorption mode and exert a larger surface dipole potential on TiO_2 than their counterparts bearing rhodanine-3-acetic acid (**50** and **51**), which lie along the surface. As illustrated in Fig. 12, **50** exhibited a greater extent of charge recombination than **53** because of the low surface-blocking efficiency of the dye layer and the intimacy between the I_3^--bound dyes and the TiO_2, leading to lower V_{OC} values.[15] This work made an important proposal that dyes with a standing absorption mode should be a preferred choice in the future development of organic sensitizers.

Dihexyloxy-substituted TPA (DHO–TPA), a typical 4,4′-aryl-substituted TPA derivative, has been identified as a good donor in the construction of amphiphilic organic sensitizers. The dihexyloxy groups not only slow down the titania/electrolyte interface charge recombination kinetics, contributing to a high open-circuit photovoltage, but also provide strong electron-donating ability, enhancing the light harvesting capacity of the dyes. Remarkable progress has recently been made in the field of DHO–TPA organic dyes. Wang and co-workers reported about fifty DHO–TPA organic dyes,[63–72] holding the record of validated efficiency of 10.3%.[68] They focused on adjusting the conjugated bridge with different thiophene derivatives to increase the molar extinction coefficient, suppress dye aggregation on the semiconductor, and optimize the redox potential of the photosensitizer (Fig. 11).

Using the thienothiophene (TT) to replace the thiophene unit, **55** (PCE = 7.5%) showed an improved efficiency related to that of **54** (PCE = 6.88%).[64,65] With the motivation to further enhance the light-harvesting capacity and get an insight into the optoelectronic properties of bisthienothiophene, compound **56** (containing bisthienothiophene as the π conjugated unit) was synthesized, giving an efficiency of 8.0% measured under AM 1.5 irradiation (100 mW cm^{-2}).[66] In conjunction with a solvent-free ionic liquid electrolyte, the device based on **56** (PCE = 6.5%) showed an excellent stability under thermal and light-soaking dual stress. Along with the increase of the conjugation length, the charge-transfer transition absorption was not only bathochromic but also enhanced, leading to a high J_{SC} of 15.2 mA cm^{-2}. Nevertheless, the bisthienothiophene possessed by **56** (λ_{max} = 524 nm) dye shifts the absorption peak bathochromically only 8 nm compared to the thienophene of **55** (λ_{max} = 516 nm). In contrast, when a binary spacer of the orderly conjugated EDOT and thienothiophene was employed, the absorption peak of **57**

(λ_{max} = 552 nm) is red-shifted by 36 nm compared with that of **55**.[66] In a 7 + 5 μm double layer TiO_2 film, this dye exhibited an IPCE of greater than 90% in the range 440–590 nm, with the absorption onset at 800 nm. The TiO_2 electrode was stained by immersion into a dye solution containing 150 mM **57**, 300 mM tetrabutylammonium hydroxide, and 1 mM 3a,7a-dihydroxy-5b-cholic acid in a mixed solvent of acetonitrile, tetrahydrofuran and chlorobenzene (1 : 1 : 2 v/v/v) for 72 h. DSCs based on **57** and an iodine electrolyte consisting of 1.0 M 1,3-dimethylimidazolium iodide (DMII), 50 mM LiI, 30 mM I_2, 0.5 M *tert*-butylpyridine (TBP), and 0.1 M guanidinium thiocyanate (GNCS) in acetonitrile–valeronitrile (85 : 15 v/v) generated an impressive efficiency of 9.8%. It is noted that apart from a high J_{SC} (16.1 mA cm^{-2}) related to good light-harvesting, compound **57** exhibited a high V_{OC} (803 mV) and FF (0.738). Interestingly, they claimed that when other solvents are used in the **57** staining the cells present a much lower performance, mainly owing to fast charge recombination at the titania/electrolyte interface. Moreover, the stability and high efficiency of a solvent-free DSC based on **57** has been demonstrated. This finding proved that the exploration of fused ring building blocks to construct a wide-spectral response organic chromophore for DSCs is an effective strategy.

After that, they employed a 4,4-dihexyl-4*H*-cyclopenta-[2,1-*b*:3,4-*b*′]dithiophene (CPDT) segment as a conjugated spacer to construct the organic chromophore **59** for DSCs, exhibiting a high power conversion efficiency of 8.95% measured under irradiation of AM 1.5 irradiation (100 mW cm^{-2}).[67] **59** displayed an impressive maximum molar absorption coefficient of 62.7 × 10^3 M^{-1} cm^{-1} at 555 nm, which is about 2 times higher than **58** (33.8 × 10^3 M^{-1} cm^{-1} at 525 nm). Interestingly, experiments showed that the two side chains of CPDT themselves do not form an effective barrier to attenuate the interfacial tunneling electron transfer. They supposed that the two aliphatic chains tethered to the conjugated backbone of **59** through the tetrahedral sp^3 carbon endow more uncovered titania after dye-coating, which, however, could subsequently interact with TBP and GNCS very efficiently. The resultant compact layer coassembled with **59** and the electrolyte components (mainly TBP and GNCS) on titania not only reduces the surface states of nanocrystals but also prolongs the electron lifetime considerably.

In 2010, the same group utilized a binary π-conjugated spacer of EDOT and dihexyl-substituted dithienosilole (DTS) to construct another promising sensitizer **60**, which is characteristic of an intramolecular charge-transfer band peaking at 584 nm measured in chloroform.[68] The IPCE exceeds 90% from 500 to 590 nm, reaching a maximum of 95% after coating the cells with an antireflection film. In comparison with the standard ruthenium sensitizer **Z907**, this metal-free chromophore **60** endowed a nanocrystalline titania film with an evident light-harvesting enhancement, leading to a remarkably high efficiency of 10.0–10.3% (J_{SC} = 17.94 mA cm^{-2}, V_{OC} = 770 mV, FF = 0.730) at the AM 1.5 irradiation (100 mW cm^{-2}) for DSCs, although a highly volatile iodine electrolyte was used. A solvent-free ionic liquid cell with **60** as the sensitizer showed an impressive efficiency of 8.9% under a low light intensity of

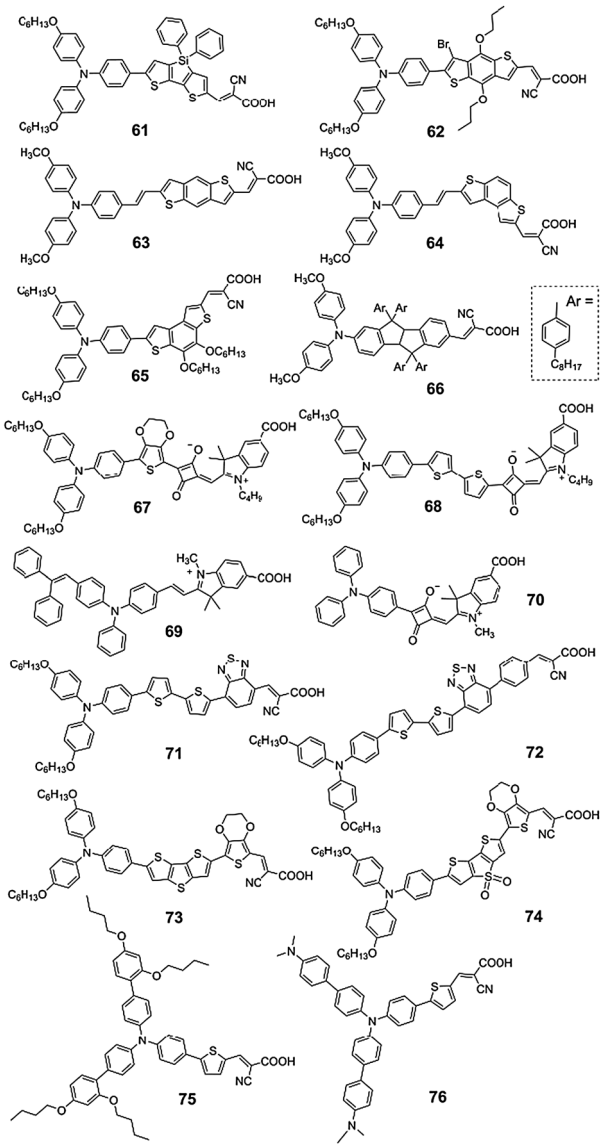

Fig. 13 Representative substituted TPA dyes **61–76**.

14.39 mW cm^{-2}, making it very favorable for the indoor application of flexible dye-sensitized solar cells.

Based on the DTS, Wong, Wu and co-workers designed and synthesized a DHO–TPA dye **61** containing coplanar diphenyl-substituted dithienosilole as the central linkage for high-performance DSCs (Fig. 13).[73] By incorporating the diphenyl-substituted DTS core, **61** exhibited the enhanced light-capturing abilities and suppressed dye aggregation. A solar-cell device based on the sensitizer **61** yielded a high overall conversion efficiency up to 7.6%, reaching ~96% of the ruthenium dye **N719**-based reference cell under the same conditions.

As mentioned above, exploring new fused ring building blocks for organic dyes has proved to be an effective strategy for enhancing the light-harvesting capacity, leading to impressive performances under AM 1.5 irradiation (100 mW cm^{-2}). Recently, our group developed new benzo[1,2-*b*:4,5-*b*′]-dithiophene (BDT)-containing organic dyes with single or binary π-conjugated

spacers.[74] The length of the π-conjugated spacers has a strong impact on the electro-optical properties of these dyes. The fabricated DSC from **62** (Fig. 13, PCE = 5.68%) exhibited high efficiency reaching ~73% of the standard cell using **N719** (PCE = 7.73%) as the sensitizer, indicating that the BDT unit is a promising candidate in organic sensitizers. Longhi *et al.* introduced two isomeric BDT as π-spacers for photosensitizers (**63** and **64**, Fig. 13). In particular, **63** showed a high PCE of 5.14%.[75]

Gao *et al.* reported a series of metal-free organic dyes exploiting different combinations of (hetero)cyclic linkers (benzene, thiophene, and thiazole) and bridges (CPDT and another isomer of BDT, benzo[1,2-*b*:4,3-*b*′]-dithiophene) as the central π-spacers.[76] They found that the absorption spectrum of the dyes containing CPDT were red-shifted compared with the dyes containing benzo[1,2-*b*:4,3-*b*′]-dithiophene. Such absorption characteristics indicate that the electron density on CPDT is richer than that of benzo[1,2-*b*:4,3-*b*′]-dithiophene. The performance of the dye **59** (Fig. 11, J_{SC} = 15.4 mA cm^{-2}, V_{OC} = 756 mV, FF = 0.76) cell surpassed that fabricated with dye **65** (Fig. 13, J_{SC} = 9.4 mA cm^{-2}, V_{OC} = 810 mV, FF = 0.74) under the same conditions.[76]

Zhu *et al.* demonstrated that a carbon-bridged phenylenevinylene (CPV)-linked dye serves as an efficient sensitizer (**66**, Fig. 13) for DSCs.[77] This robust and bulky linker helps to reduce the recombination, which resulted in the high V_{OC} values. The octyl side chains protruding laterally from the sensitizer hamper contact between the donor moiety and the TiO_2 surface and suppress the charge recombination to achieve high FF values. The cells show PCEs of up to 7.12%, and high V_{OC} reaching close to 0.8 V based on the iodide/triiodide electrolyte.

Aiming to improve the spectral response of organic dyes in the far-red and NIR regions, Wu and co-workers developed two DHO–TPA dyes,[78] **67** and **68** (Fig. 13), where the electron-rich EDOT or bithiophene conjugated fragment was used to link, unconventionally, a squaraine core and a hexyloxyphenyl amino group. The corresponding photovoltaic devices exhibited an attractively panchromatic response and also converted a portion of the NIR photons into electricity. The IPCE onset was red-shifted for both dyes to 950 nm. Unfortunately, moderate efficiencies (2.61% and 2.34%, respectively) were observed for **67** and **68**, which was primarily as a result of the worse V_{OC} values (422 and 432 mV, respectively). In fact, a survey of the literature also revealed that the efficiencies of DSCs based on ionic dyes fell well behind those based on nonionic ones, mainly because the V_{OC} values of DSCs based on the former dyes (300–600 mV) are generally lower than those based on the latter ones (600–800 mV).[79] As part of our systematic development of triphenylamine-based organic sensitizers, we prepared two ionic dyes (**69** and **70**, Fig. 13) and investigated the origin of such a V_{OC} disadvantage.[80]

We calculated the electrostatic potentials of **69** and **70**, which are plotted in Fig. 14.[80] In the case of **69**, the positive charge in the indolium unit could directly attract I_3^-, thus augmenting charge recombination. This feature should, at least in part, be responsible for the generally low V_{OC} values for ionic dyes because of the enhanced recombination reaction.

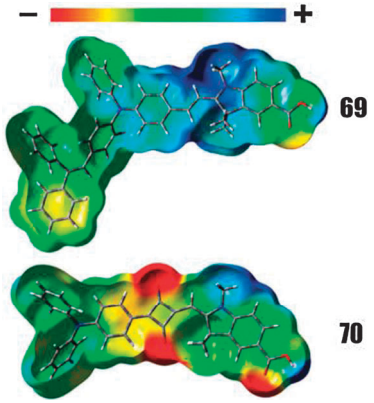

Fig. 14 Electrostatic potential plots of **69** and **70**. Reproduced with permission from ref. 80. Copyright 2010, American Chemical Society.

Interestingly, **70** has a negatively charged squaraine core in the π-bridge, which is usually immediately connected to the positive charge center. I_3^- would simultaneously feel the coulombic attraction from the indolium as well as the repulsion from the squaraine unit. In other words, the electrostatic interaction between **70** and I_3^- would be relatively weak. In spite of that, through photovoltaic measurements, an electrochemical impedance investigation, recombination reaction monitoring, electrostatic potential analysis, and dipole moment calculation, we concluded that the electronic distribution over the ionic dye molecules is intrinsically not ideal for the construction of efficient sensitizers, although the introduction of a squaraine unit in the dye backbone can, to some extent, alleviate such a situation. Our studies suggested that in the future design of NIR/panchromatic sensitizers, strongly electron-withdrawing nonionic (rather than ionic) moieties would be interesting candidates as building blocks. Nevertheless, this does not mean that ionic sensitizers such as squaraine dyes are not suitable for DSCs. The key issue is to make the most of the advantage of ionic sensitizers (*e.g.* absorption in the NIR region) but avoid their V_{OC} defects. One effective approach is to employ ionic sensitizers together with nonionic sensitizers in cosensitized solar cells.[81,82] More importantly, a panchromatic response in the visible region can be realized by DSCs based on the co-sensitization of organic dyes.

For the purpose of extending the absorption range to enhance the photocurrent response, Bäuerle and co-workers prepared two DHO–TPA dyes (**71** and **72**, Fig. 13) by implementing the electron-deficient benzothiadiazole unit into the bridging framework of D–π–A molecules.[83] They found that a subtle structural change in the sensitizer induced a significant influence on the DSCs performance. The incorporation of a BTDA unit close to the anchoring acceptor group in **71** (λ_{max} = 570 nm) led to a bathochromic shift of the CT bands in the UV-vis spectra in comparison to **72** (λ_{max} = 515 nm), in which the two acceptor units are decoupled by a phenyl ring. However, the efficiency of **72** (PCE = 8.21%) was raised by a factor of 6.5 compared to **71** (PCE = 1.24%). Photophysical investigations revealed that the insertion of the phenyl ring blocks the back electron transfer of the charge

separated state. This slows down the recombination processes by over 5 times, while maintaining efficient electron injection from the excited dye into the TiO_2-photoanode.

Recently, we obtained a sensitizer with strongly electron-withdrawing nonionic moieties by modifying DTT, namely, dithieno[3,2-*b*:2′,3′-*d*]thiophene-4,4-dioxide (DTTO).[84] Two push–pull organic dyes (**73** and **74**, Fig. 13) incorporating DTT and DTTO as units of binary spacers have been synthesized and used as sensitizers for DSCs. Compared to the DTT counterpart, the introduction of DTTO into the binary spacer is advantageous to the light harvesting in terms of both the maximum absorption (red-shifted 17 nm) and the molar extinction coefficients. Importantly, this bridge alteration not only evokes an enhancement of J_{SC} but concomitantly prompts a V_{OC} improvement, leading to a higher conversion efficiency (**73**, PCE = 4.18%; **74**, PCE = 5.19%). The results revealed that the electron-deficient fused thiophene is a promising candidate for contrasting efficient organic dyes.

From the structure–function relationships point of view, the dihexyloxy-substitution on the TPA is undoubtedly successful. To improve the efficiency of DSCs based on DHO–TPA dyes further, a remarkable increase in the V_{OC} of these cells in combination with iodine-free redox couples is necessary, which will be discussed in Section 11.

As a result of the strategic structural modification of organic sensitizers, a new family of interesting substituted triphenylamine dyes was reported by Sun, Hagfeldt and co-workers.[85–87] As shown in Fig. 13, the TPA donor was functionalized at the adjacent phenyl rings of the TPA core with either butoxyl groups (**75**) or short dimethylamine groups (**76**). Despite the red-shift (37 nm) in the absorption spectrum, the **76** (PCE = 4.83%) dye showed a comparatively low performance related to **75** (PCE = 6.0%).[85] The prominent feature of **75** is the free rotation of the phenyl rings containing four long butoxyl chains in *ortho* and *para* positions, which are connected to the TPA core by single bonds. They proposed that the protection by the butoxyl chains produces surface blocking through steric hindrance, preventing electrons in TiO_2 from recombining with the redox species and yielding a high V_{OC}, which is the essential reason for higher DSCs performance based on the **75** sensitizer.[86] Moreover, the protection by the butoxyl chains was proven to be more efficient as compared to the co-adsorption of CDCA under the examined conditions.

Tian and co-workers developed several starburst triarylamine based dyes with a D–D–π–A structure (Fig. 15).[88–90] The introduction of a starburst triarylamine group to form the D–D–π–A configuration brought about superior performance over the simple D–π–A configuration, in terms of bathochromically extended absorption spectra, enhanced molar extinction coefficients and better thermo-stability. Dye **79** has a conversion efficiency as high as 6.02% (V_{OC} = 0.63 V, J_{SC} = 13.8 mA cm^{-2}; FF = 0.69) under 1 sun illumination.[88] It is noted that dye **80** showed a good efficiency in quasi-solid-state devices, which was performed over 1200 h in full sunlight at 50 °C.[89] This result means that carbazole is a photostable hole-transporting moiety for use in dye-sensitized solar cells. Recently, Jia, Lin and co-workers demonstrated the possibility of phenothiazine units as antennas in D–D–π–A dyes.[91,92] Under the same conditions, an increase of about 39% was obtained from **82** (PCE = 4.54%) to **81** (PCE = 3.26%).[91]

Considering that heterocyclic groups with lone pair electrons may effectively delocalize the positive charges after the photo-oxidation of dyes, Zhang *et al.* predicted that using suitable heterocyclic groups to modify the structures of triarylamine units may improve their electron-donating ability (Fig. 15). They demonstrated that adopting heterocyclic (2-thienyl, **83**; 1-pyrazolyl groups, **84**) substituted triarylamine units as the electronic donor moieties led to the improved performance of dyes.[93] The PCE of **83** and **84** are 5.2% and 4.9%, respectively.

Shi and co-workers incorporated the tetraphenylethylene (TPE) units as antennas in D–D–π–A dyes. The TPE moieties were employed to suppress charge recombination and aggregation. DSCs based on **85** (Fig. 15) with 10 mm CDCA showed a high PCE of 6.77% (J_{SC} = 14.69 mA cm^{-2}, V_{OC} = 740 mV, FF = 0.62).[94] Unlike the D–D–π–A dyes, reports on the A–D–A type of substituted TPA dyes are limited. Singh *et al.* synthesized dye **86** (Fig. 15), which contains TPA as an electron donor and both cyanovinylene 4-nitrophenyl and carboxylic (anchoring) units as electron acceptors. The PCE of **86** with DCA addition is 4.4%.[95]

Further tuning the structure of the substitutes to construct new D–D–π–A or A–D–A dyes could lead to even better cell performance in the future.

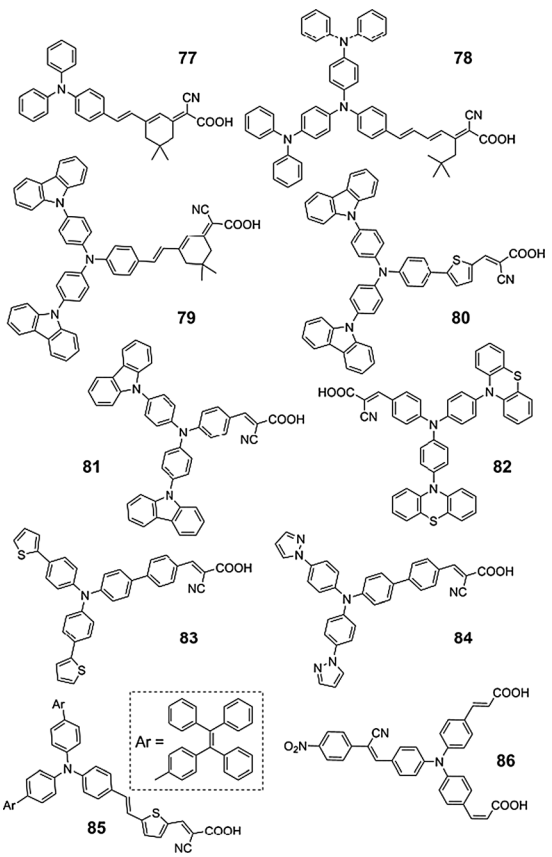

Fig. 15 Representative substituted TPA dyes **77–86**.

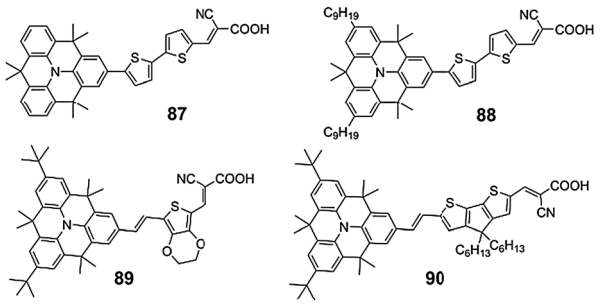

Fig. 16 Representative planar TPA dyes **87–90**.

4.3 Planar TPA dyes

Ko and co-workers developed a novel type of organic sensitizers incorporating a planar TPA unit (Fig. 16).[99] The planar donor units show evidence of intermolecular interactions on TiO_2 films, which provide a significantly red-shifted spectra and photovoltaic response. As a result, the dye **87** (J_{SC} = 15.2 mA cm^{-2}, V_{OC} = 720 mV, PCE = 7.8%) based DSC gave a higher J_{SC} compared to the TPA congener (dye **21**, J_{SC} = 13.0 mA cm^{-2}, V_{OC} = 660 mV, PCE = 6.0%) under the same conditions. Dye **88** achieved over 8.71% power conversion efficiency, indicating that incorporating a planar amine with bulky substituents is effective for increasing the life of the charge-separated state and inhibiting the dye aggregation.

After that, Cai *et al.* proposed planar TPA dyes (**89** and **90**) containing a bridged triphenylamine with *t*-butyl substituents as donors.[100] Planarization of the donor and the use of an alkene linkage have proven extremely powerful in extending the red light response of the sensitizer, leading to a significant enhancement in J_{SC} of the DSCs. A high efficiency of 7.51% (J_{SC} = 15.4 mA cm^{-2}, V_{OC} = 651 mV, FF = 0.75) was obtained with DSCs based on **89**. The PCE and J_{SC} of **90** were improved to 8.0% and 16.1 mA cm^{-2}, respectively, with the spacer alteration from EDOT to CPDT.

4.4 Branched TPA dyes

Chemists had placed a lot of hope on branched TPA dyes (Fig. 17, **91–103** and Fig. 18, **104–111**) because of the antenna effect of branches. To avoid aggregation of the organic dyes and recombination, Sun, Hagfeldt, Nazeeruddin and co-workers synthesized branched TPA dyes with two arylamine moieties at the donor part.[101] The disubstituted donor moieties in **92** not only evoked an enhanced higher extinction coefficient, but also prevented the triiodide in the electrolyte from recombining with injected electrons in the TiO_2 conduction band, leading to an increased V_{OC} when compared to the **91** sensitizer (**91**, V_{OC} = 694 mV; **92**, V_{OC} = 744 mV). **92**-sensitized solar cells yielded a PCE of 7.20% under AM 1.5 irradiation (100 mW cm^{-2}). For thin-film solid state solar cells based on these organic dyes, **92** showed a PCE of 3.25%. In the meantime, Lin, Ho, Chow and co-workers reported a new class of organic dyes featuring a dendritic structure at the donor part (**95–97**). Similar features as mentioned above were observed for these dyes when compared to **93** and **94**.[102]

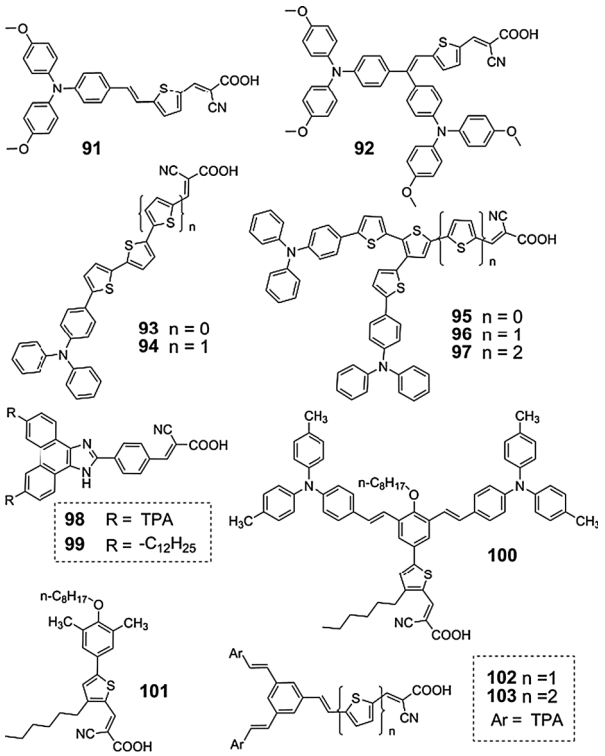

Fig. 17 Representative branched TPA dyes **91–103**.

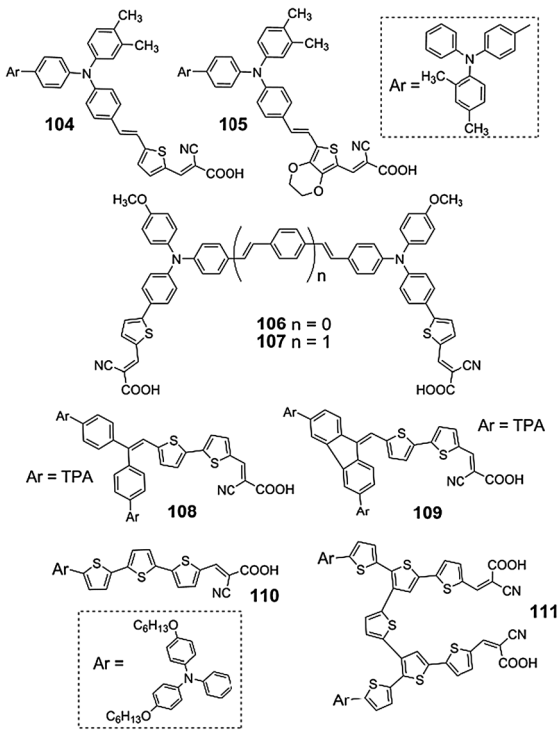

Fig. 18 Representative branched TPA dyes **104–111**.

In fact, when compared to those of linear TPA dyes with one arylamine moiety, the advantage of the branched TPA dyes with two arylamine moieties is not obvious in terms of the PCE values.

For example, the PCE of **91** is 6.9%, which is comparable to that of **92**. However, when two arylamine moieties are replaced by two alkyl chains, the PCE advantage of branched TPA dyes is clear. For instance, **98** (PCE = 4.68%) and **100** (PCE = 5.13%) achieved better photovoltaic performances over **99** (PCE = 4.01%) and **101** (PCE = 2.52%), respectively.[103,104] This was ascribed to the effectively retarded charge recombination between the electrons at the TiO_2 and the oxidized dyes by incorporation of the dendritic structure.

Chang *et al.*[105] and Li *et al.*[106] reported the influence of the π-bridge on the performance of branched TPA dyes. Between dyes **102** and **103** that were tested, a better PCE was obtained with **103** (PCE = 5.67%) because of both broader and stronger light absorption from the sensitizers.[105] **105**, bearing EDOT as an electron linker, showed a significant red shift in the long-wavelength band compared with that of dye **104**, resulting in an increase of J_{SC} and, hence, higher efficiency (PCE = 5.63%).[106]

Abbotto *et al.* introduced a novel design based on tri-branched organic sensitizers (**106** and **107**), carrying two donors, two acceptors, three π spacers, and two anchoring points.[107] This approach led to significantly different optical properties and enhanced stability with respect to the related di- and monobranched dyes and yielded PCE of up to 5.05% (**106**).

Han and co-workers reported an aggregation-free branch-type organic dye, **108**, for DSCs, which was developed by means of a twisting π-conjugation strategy.[108] In comparison with the analogue planar dye **109**, the twisting dye showed excellent potential as a new aggregation-free organic dye for DSCs. It produced the higher PCE of 5.35% with an IPCE maximum of about 80%, and the photovoltaic performance was almost unchanged by co-adsorption with DCA.

Wang and co-workers obtained a thiophene bridged double D–π–A dye **111** (J_{SC} = 11.2 mA cm^{-2}, V_{OC} = 770 mV, PCE = 6.6%), which has a much stronger π–π* electron transition band than its monobranched analogue dye **110** (J_{SC} = 7.1 mA cm^{-2}, V_{OC} = 670 mV, PCE = 3.4%).[109] The advantage of the cross structure of **111** includes: (i) reducing intermolecular interaction, which is thus favorable for electron injection; (ii) blocking triiodides approaching the TiO_2 surface, which means the electron lifetime is enhanced remarkably at the same charge density. As a consequence, the PCE of **111** is enhanced about 2-fold.

Although these branch-type organic dyes were less efficient than TPA or substituted TPA dyes, rational design of the molecular structure could trigger the development of optimized systems through the incorporation of appropriate new branches.

5. Triarylamine dyes

5.1 Fluorene based triarylamine dyes

The fluorene based triarylamine dyes (Fig. 19, **112–122**) were developed as photosensitizers by Ko and co-workers for the first time.[110–122] The tailored dialkylfluoreneaniline moieties in dyes ensure greater resistance to degradation when exposed to light and high temperatures, as compared to simple arylamines. In addition, the nonplanar structure of the dialkylfluoreneaniline suppressed aggregation, disfavoring molecular stacking.[110]

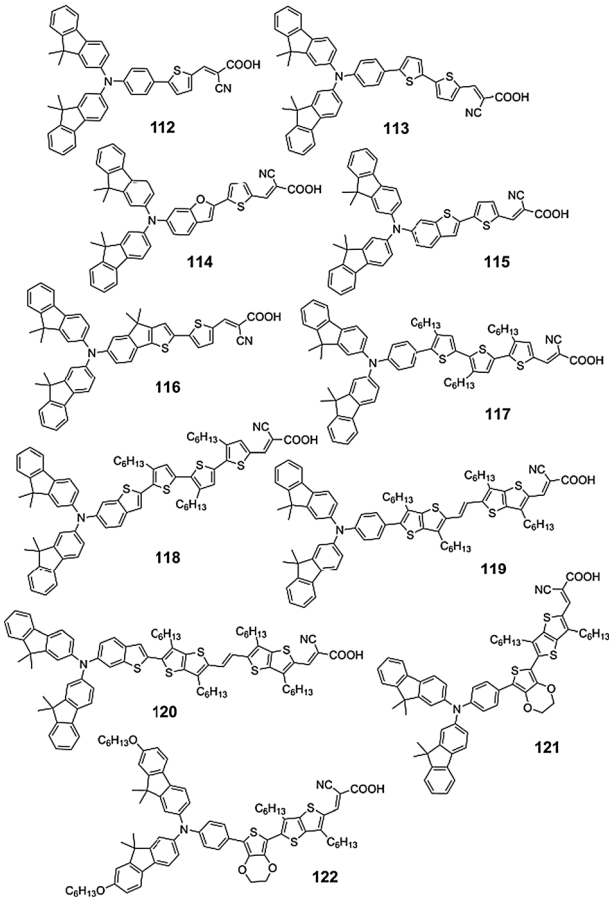

Fig. 19 Representative fluorene based TPA dyes **112–122**.

In an attempt to increase the molar extinction coefficient of the dye, in 2006, dyes **112** and **113** with bridging thiophene units were reported.[110] The IPCE spectrum of **113** is red-shifted by about 30 nm compared with that of **112** as a result of extended π-conjugation, which contributed to the high J_{SC} of **113** (14.0 mA cm^{-2}). Under AM 1.5 irradiation (100 mW cm^{-2}), dyes **112** and **113** gave efficiencies of 7.2% and 8.0%, respectively. Inspired by the success of these two dyes, great efforts in structural modification of the π-bridge have been made to obtain red-shifted absorption spectra and increase the extinction coefficient. A representative example was the introduction of a fused-heterocyclic ring spacer such as [bis(9,9-dimethylfluoren-2-yl)amino]benzo[*b*]furan[111] and [bis(9,9-dimethylfluoren-2-yl)amino]benzo[*b*]thiophene[112] in **114** and **115**, respectively. The maximum absorption spectrum of **114** and **115** in ethanol are 463 and 456 nm, respectively, which is red shifted related to that of **112** (λ_{max} = 436 nm). This structure design can also be found in **118**[113] and **120**,[114] which is beneficial to the light harvesting of dyes and hence the efficiency. Typically, the photosensitizer transformation from **117** to **118** has caused a PCE enhancement of 1.2%.

Recently, they introduced 4,4-dimethyl-4*H*-indeno[1,2-*b*]thiophene, in which a 2-phenylthiophene was bridged by a dimethylmethylene at the 2′,3-position,[115] showing enlargement of the π-conjugation of the indeno[1,2-*b*]thiophene unit because the methylene bridge renders the indeno[1,2-*b*]thiophene coplanar.

The IPCE of **116** exceeded 70% in a broad spectrum range from 420 to 620 nm, reaching a maximum of 86%. A big J_{SC} enhancement of **116** relative to that of **113** was observed owing to the high molar extinction coefficient and the red shift in the absorption spectrum of **116** relative to **113**. Of particular importance is the 40 mV increase in the V_{OC} of the **116** cell, which was regarded as the result of an upward shift of the TiO_2 band edge. Consequently, the device based on the sensitizer **116** gave an overall conversion efficiency of 8.2%.

To enhance the interface and the tolerance towards water in the electrolytes, a successful approach was introduced in **117** and **118** by incorporating thiophene units with aliphatic chains as the π-bridge.[113] Under AM 1.5 irradiation (100 mW cm^{-2}), the **118**-based DSC exhibited a J_{SC} of 17.45 mA cm^{-2}, a V_{OC} of 0.664 V, and a FF of 0.742, which corresponds to a PCE of 8.60%. Using solvent-free ionic-liquid electrolytes, the **118** sensitizer yielded a high conversion efficiency of 7%. Particularly, the long term stability of the device is remarkable because the initial efficiency of 6.82% was slightly increased to 7.03% during the 1000 h light soaking test under light soaking at 60 °C. The enhanced stability of the two dyes can be attributed to the bis-dimethylfluorenyl-amino moiety coupled to the substituted hexyl chains, which prevents water-induced dye desorption from the TiO_2 surface.

Although dye **118** afforded a high PCE value, the light harvesting ability of **118** is not ideal (*e.g.* λ_{max} = 430 nm). Dyes **119** and **120** consisting of a dimethylfluorenylamino-appended thienothiophene-vinylene-thienothiophene unit with aliphatic chains to maintain the planar geometry of the conjugated linker were synthesized.[114] This type of structure not only increased the light harvesting ability of the sensitizer by extending the π-conjugation of the bridging linker (**119**, λ_{max} = 480 nm; **120**, λ_{max} = 490 nm), but also augmented its hydrophobicity, increasing the stability under long-term light soaking and thermal stress. Under AM 1.5 irradiation (100 mW cm^{-2}), the **120**-sensitized cell gave a J_{SC} of 17.61 mA cm^{-2}, a V_{OC} of 0.71 V, and a FF of 0.72, corresponding to a PCE of 9.1%. A **120**-based solar cell fabricated with a solvent free ionic liquid electrolyte displayed a high conversion efficiency of 7.9% and showed excellent stability under light soaking at 60 °C for 1000 h.

Structural modification of dye **121** was performed through introducing hexyloxy chains into fluorene,[116] yielding dye **122**. The **122** (λ_{max} = 466 nm) sensitizer incorporating the hexyloxy unit exhibited a red-shifted absorption relative to its counterpart **121** (λ_{max} = 450 nm) containing non-substituted fluorenyl. In particular, incorporating hexyloxy also minimized charge recombination, realizing a significant increase in V_{OC} by 130 mV. Consequently, the power conversion efficiency of **122** (PCE = 8.70%) is higher than that of **121** (PCE = 5.43%).

Wang and co-workers reported a series of bisfluorenylaniline based dyes (**123–126**, Fig. 20) by employing dithienothiophene, thienothiophene, and EDOT as the conjugation bridge and volatile acetonitrile based electrolytes, showing efficiencies in the range of 7.8–8.3%.[123–125] In combination with a solvent-free ionic liquid electrolyte, these dyes exhibited excellent stabilities during long-term accelerated tests under light-soaking and thermal dual stress.

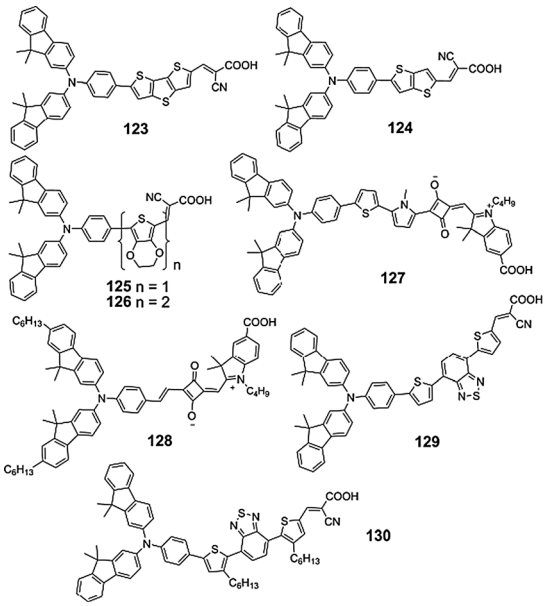

Fig. 20 Representative fluorene based TPA dyes **123–130**.

To obtain panchromatic fluorene based triarylamine dyes, **127** and **128** were synthesized, in which the unsymmetrical squaraine unit was incorporated as the conjugation bridge.[126,127] Both dyes showed a broad absorption that extended throughout the visible and nearinfrared region. Unfortunately, cells based on these dyes suffered from low V_{OC} values, and therefore exhibited moderate efficiencies (5.20–6.29%) relative to the aforementioned fluorene based triarylamine dyes. In contrast, the introduction of low-band gap chromophores such as the benzothiadiazole unit in the bridging framework seems to be a good choice. With this molecular design, power conversion efficiencies of 7.51% and 8.19% were achieved with **129**- and **130**-based DSCs, respectively.[128]

5.2 Naphthalene based triarylamine dyes

Chow and co-workers showed a series of dipolar compounds containing *N*,*N*-diphenylnaphthalen-1-amine as an electron donor (Fig. 21, **131–146**). The performance of the *N*,*N*-diphenylnaphthalen-1-amine based dyes, in general, was slightly better than that of the TPA type. For example, DSCs based on dye **131** gave 7.08% efficiency, and dye **132** showed 5.25% efficiency under the same measurement conditions.[129] This was ascribed partly to the higher absorptivity of the former compounds, and partly to a better resonance effect provided by the naphthalene moiety. Moreover, the larger size of the naphthalene group may also effectively hinder self-aggregation of the dyes on the TiO_2 surface. Similar results were observed by Thomas and co-workers. Four examples of these dyes are **133–136**.[130,131] They proposed that the one containing the naphthylphenylamine segment showed better device characteristics, attributable to the higher HOMO energy level, which probably facilitates the regeneration of the dye and effective suppression of the back reaction of the injected electrons with the I_3^- in the electrolyte.

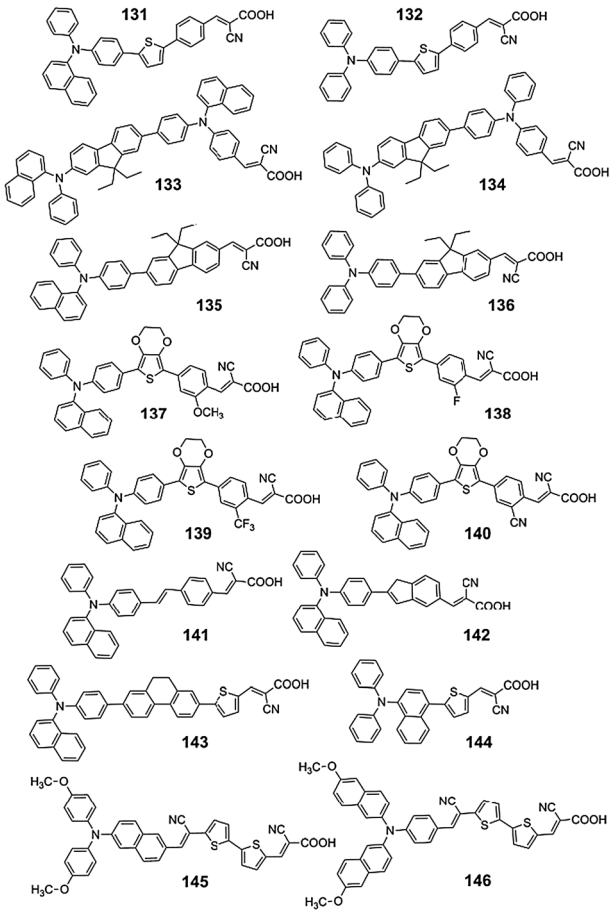

Fig. 21 Representative naphthalene based TPA dyes **131–146**.

To further improve the performance and tune the absorption spectra of the naphthalene based triarylamine dyes, Chow and co-workers investigated the effects of substituents on the phenyl group *ortho* to the cyanoacrylate acceptor of the dyes **137–140**.[132] They found that the presence of an electron-withdrawing group (–F, $–CF_3$ and –CN) located on the acceptor side can stabilize the charge-separated excited state and thus reduce the rate of charge recombination. Such an effect can be evidenced by the high V_{OC} (around 690 mV) values of both compounds **138** and **139**, whilst an electron-donating group ($–OCH_3$) may improve the charge injection efficiency toward the TiO_2 conducting electrode. The compound **137** thus exhibited the highest J_{SC} (17.04 mA cm^{-2}) value of all. An exception was found for compound **140**, which exhibited a low absorption on the CT transition and a small value of J_{SC} (8.32 mA cm^{-2}). The best performance was observed for the device made with **139**, which displayed a J_{SC} value of 15.16 mA cm^{-2}, a V_{OC} value of 0.68 V, and a FF value of 0.68. The PCE was estimated to be 7.0%.

The same group also developed several novel naphthalene based TPA dyes through the structural modification of a spacer, adopting a planarity strategy.[82,133,134] Dye **142** contains a 2-phenylindene moiety with the central double bond locked in *transoid* geometry.[133] The performance of **142** (PCE = 5.27%) behaved better than **141** (PCE = 4.46%), as a result of restricting the *trans* → *cis* isomerization of the C=C bond as a major channel of non-radiative decay. Dye **143**, containing a 9,10-dihydrophenanthrene entity in the conjugated spacer, yielded a more planar configuration, which allows better electronic communication between the arylamine and electron excessive heteroaromatic ring.[82] Consequently, this exhibited a better J_{SC} than its biphenyl counterpart. In particular, dye **143** was used in combination with a squaraine dye for cosensitized DSCs, yielding a high efficiency record of 8.14% among cosensitized systems with all metal-free sensitizers.[82]

Olivier *et al.* reported a series of organic "push–pull" dyes that contain naphthyl units at various positions.[135] The naphthyl unit attached to the bi-thiophenyl *p* conjugated spacer (**145**) achieved a cell performance with a PCE of 6.6%. Nevertheless, the **146** dye containing naphthyl groups at terminal positions showed a lower V_{OC}, FF, and therefore PCE value (PCE = 6.2%). Interestingly, in recent work by Lin, Yao and co-workers, a contrary result was reported. That is, dye **144** containing a naphtha-1,4-diyl unit in the conjugated bridge was inferior to dye **15** containing a phenyl unit in the conjugated bridge.[136] This result highlighted the importance of the molecular engineering of the sensitizer.

5.3 Truxene based triarylamine dyes

Starburst truxene, which is recognized as a potential starting material for organic semiconductors, liquid crystalline compounds, and fullerenes,[137] has attracted increasing interest for the design of photosenzitizers because of the prominent advantages of a bulky rigid conjugation structure, the facile introduction of alkyl chains, and outstanding thermal stability.[138] Truxene based triarylamine dyes have now stood out as a new class of attractive organic dyes. Representative dyes (**147–158**) are shown in Fig. 22.

Originally, Tian and co-workers reported three truxene-based dyes with 2-cyanoacrylic acid as the acceptor and starburst triarylamine as the donor (**147**, **148**, and **149**).[139] It was found that the π–π aggregation is significantly reduced by the addition of long alkyl substituents on the middle of the starburst shaped sensitizers. Moreover, a compact sensitizer layer was molecular interfacially engineered on the TiO_2 surface. As a result, the approach of the electrolyte to the TiO_2 surface is blocked significantly by the compact sensitizer layer formed, and the charge recombination in the DSCs is proved to be prohibited effectively. A tremendously improved V_{OC} was observed for the dye **148**- and **149**-sensitized solar cells, with comparable or higher V_{OC} values than **N719** under the same conditions (**148**, 731 mV; **149**, 752 mV; **N719**, 728 mV). Compared to the hexyl counterpart (**148**), a V_{OC} attenuation of 42 mV (689 *vs.* 731 mV) can be noted upon the substitution with the ethyl group (**147**), highlighting that the aryl chains need to be sufficiently long to allow a more compact sensitizer blocking wall on the TiO_2 surface. Unfortunately, the relatively low J_{SC} (6.86–7.89 mA cm^{-2}) precluded high PCE values (3.61–4.27%). The photocurrent intensity of these dyes was limited by their narrow IPCE conversion region, which was mainly due to their narrower absorption profile.

Considering that the *ortho–para*-branched isotruxene core allows strong electronic couplings among the donors and the

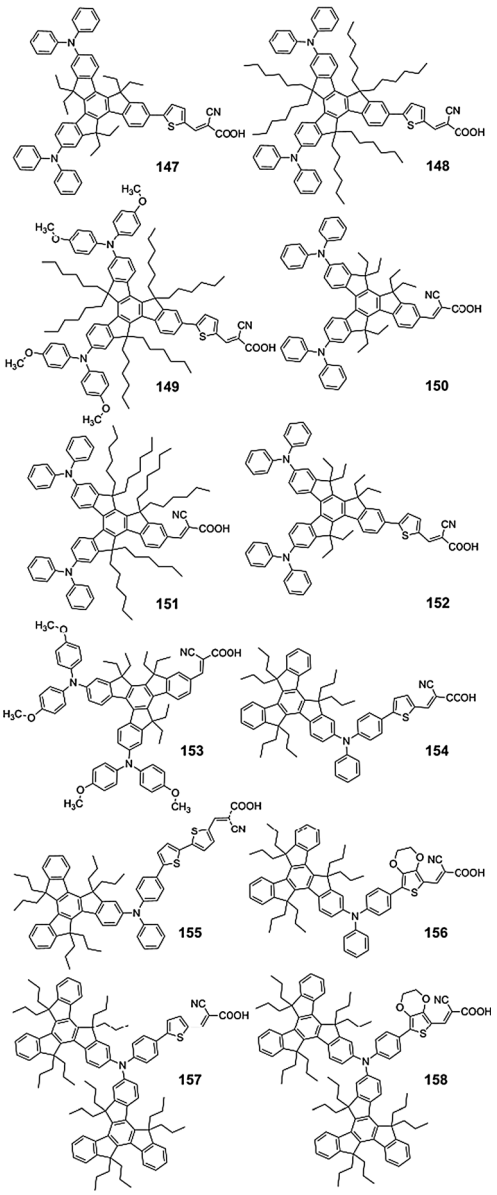

Fig. 22 Representative truxene based TPA dyes **147–158**.

acceptor, leading to red-shifted absorption profiles with significant charge-transfer character, a series of isotruxene dyes (**150** to **153**) were designed by Lin, Yang and co-workers.[140] The DSCs fabricated with the coneshaped organic dyes exhibited high V_{OC} (0.67–0.76 V) and FF (0.67–0.72) with a PCE up to 5.45%, which is 80% of PCE for the ruthenium dye **N719**-based standard cell fabricated and measured under the same conditions.

Both truxene- and isotruxene-based dyes have V_{OC} and FF comparable or superior to **N719**, but their J_{SC} are unsatisfactory. Overall, the PCE for truxene- and isotruxene-based dyes is lower than that for **N719**. Although the light harvesting in the region of 550–600 nm for isotruxene-based dyes (*ca.* 40%) is more efficient than that for truxene- based dyes (*ca.* 10%) in terms of the IPCE profiles, it is still valuable to note that the use of isotruxene did not fundamentally solve the light harvesting problem.

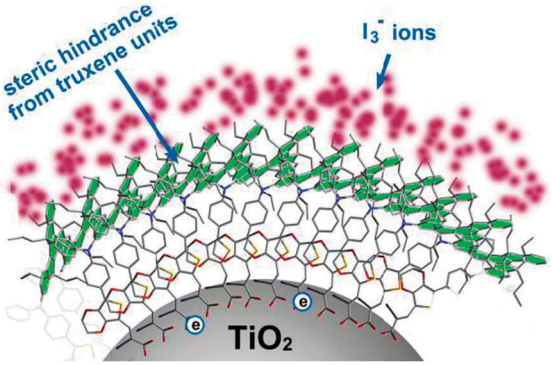

Fig. 23 Schematic representation of the bulky structure of truxene units, which block the I_3^- ions approaching the TiO_2 surface. Reprinted with permission from ref. 141. Copyright 2011, Elsevier.

Our group developed a new kind of truxene-based dye (**154–156**) with six propyl chains attached to truxene.[141] The noteworthy feature of these dyes, different from dyes **147–153**, is that the functionalized-truxene unit acts as the electron donor moiety but not the linker. This slight structure modification not only significantly red-shifted the absorption spectra of the dyes but also induced a high-absorption coefficient. For example, the λ_{max} of **154** (λ_{max} = 486 nm, ε = 65 000 M^{-1} cm^{-1}) in CH_2Cl_2 showed a 66 nm red shift in the visible absorption band compared with that of **148** (λ_{max} = 420 nm, ε = 24 600 M^{-1} cm^{-1}), which contributed to the higher J_{SC} (9.8 mA cm^{-2}) of **154**. The power conversion efficiencies for **154** and **155** are 4.92% and 5.26%, respectively. **156**, bearing EDOT as the electron linker, gave a J_{SC} of 11.5 mA cm^{-2}, a V_{OC} of 772 mV, and a FF of 0.68, corresponding to a PCE of 6.04%. As shown in Fig. 23, the bulky structure of the propyl-functionalized truxene unit blocks the I_3^- or cation approaching the TiO_2 surface, decreases the I_3^- concentration at the vicinity of the TiO_2, and increases the electron lifetimes. Respectable high V_{OC} values (745–772 mV) in DSCs based on the three dyes are thus achieved. Following this work, we investigated the performance of dyes **157** and **158** containing bis-hexapropyltruxeneamino.[142] The nonplanar structure of bis-hexapropyltruxeneamino is introduced for the suppression of dye aggregation. With CDCA addition (3 mM), the DSCs based on the two dyes afforded a slight increase in power conversion efficiency, indicating that the aggregation of the two dyes on the TiO_2 surface was not obvious. As expected, the two dyes located well above the TiO_2 surface, resulting in a good blocking effect and hence high V_{OC} values (754–765 mV). DSCs based on **158** showed a J_{SC} of 11.8 mA cm^{-2}, a V_{OC} of 772 mV and a FF of 0.68, yielding a PCE of 6.18%.

Though the power conversion efficiency from truxene based triarylamine dyes is moderate at the current stage, there is much room left for further enhancement by increasing the light harvesting ability to improve the J_{SC}.

6. Indoline dyes

Indoline dyes[143–162] were first reported by Horiuchi and Uchida (**159–165**, Fig. 24). A PCE of 6.1% was achieved with **159** (λ_{max} = 494 nm, ε = 61 000 M^{-1} cm^{-1}) employing an electrolyte of 0.1 M

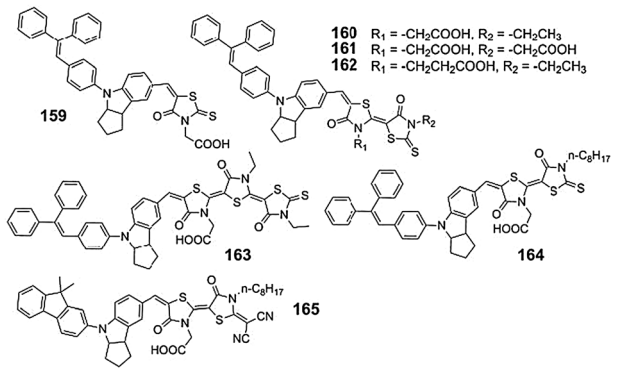

Fig. 24 Representative indoline dyes **159–165**.

LiI, 0.05 M I_2, 0.5 M 1,3-dimethyl-3-imidazolinium iodide in 3-methoxypropionitrile, compared to 6.3% for the **N3** dye under the same experimental conditions.[143] In addition to high efficiency, this dye was observed to be stable to redox process by cyclic voltammogram (CV) tests. They found that the molecular design of the rhodanine ring contributed to the red shift in the absorption spectrum and the enhanced performance. To further improve the DSC performance, a series of novel indoline dyes containing two or three rhodanine frameworks were therefore designed and synthesized (**160–163**).[144,145]

The light absorption spectra of **160**, **161**, and **162** in *tert*-butyl alcohol/acetonitrile (1 : 1) revealed peaks at 526, 532 and 532 nm, respectively. **163** has a slightly red-shifted absorption spectra peak in comparison to **160–162** since it has three rhodanine rings. A high J_{SC} of 18.75 mA cm^{-2} was achieved with **160** by employing an iodine electrolyte (0.1 M LiI, 0.05 M I_2, and 0.6 M DMPII in 3-methoxypropionitrile) without TBP addition. This high photocurrent was also attributed to the high absorption coefficient of the **160** dye (ε = 68 700 M^{-1} cm^{-1}) that is five times higher than that of the conventional high-efficiency Ru dye (**N719**, ε = 13 900 M^{-1} cm^{-1} at 541 nm). Unfortunately, the **160**-sensitized cell exhibited low V_{OC} (645 mV) and FF (0.538). To alleviate this problem, 1 mM CDCA was used as a coadsorbent and a 0.05 M concentration of TBP was added to the electrolyte for optimizing the electrolyte composition. As a result, **160** generated an improved PCE of 8.0%, mainly benefiting from a significant improvement of V_{OC} (693 mV) and FF (0.624).[144] Later, Grätzel and co-workers scrutinized the effect of the film thickness of nanocrystalline TiO_2 films on the photovoltaic performance of the **160**-sensitized cell employing acetonitrile- and ionic-liquid-based electrolytes. The optimized thickness of the **160**-sensitized nanocrystalline TiO_2 layers for the acetonitrile- and ionic-liquid-based electrolytes were 6.3 and 12.6 μm, respectively, with conversion efficiencies of 6.67 and 9.03%, respectively.[145]

In order to control the aggregation between indoline dye molecules, dye **164** was designed by elongating the end alkyl chains on the rhodanine ring of **160** for use in DSC. It was significant that the combination of CDCA and the *n*-octyl chain (**164**) improved the V_{OC} up to 717 mV, leading to a progressive PCE of 9.52%,[146] which is the highest efficiency obtained so far among DSCs based on an indoline dye under AM 1.5 radiation (100 mW cm^{-2}). This dye gave a 7.2% conversion efficiency using an ionic–liquid electrolyte.[147]

Recently, Matsui's group reported a novel idoline dye (**165**, PCE = 5.55%) for a zinc oxide dye-sensitized solar cell, having a dimethylfluorene-substituted indoline donor and a dicyanovinylidene-introduced rhodanine acceptor, which gave a higher efficiency than **164** (PCE = 4.92%).[148] This result was attributed to the bathochromic shift (567 nm *vs.* 554 nm in chloroform) based on the introduction of the electron- withdrawing dicyanovinylidene moiety into the terminal rhodanine ring and the reduced aggregate formation from the dimethylfluorenyl group.

Unfortunately, these indoline derivatives containing rhodanine-3-acetic acid as the acceptor and anchoring unit have been pointed out to maintain short-term stability as a result of desorption. To avoid this problem, Tian, Wang, Zhu and co-workers developed a series of D–A–π–A organic sensitizers (Fig. 25, **166–182**),[150–156] and a remarkable progress has been made on the utilization of low bandgap and strong electron-withdrawing units for indoline dye-based DSCs. They proposed several favorable characteristics of this type of dyes in the areas of light-harvesting and efficiency: (i) optimized energy levels, resulting in a large responsive range of wavelengths into the NIR region; (ii) a very small blue-shift in the absorption peak on thin TiO_2 films with respect to that in solution; (iii) an improvement in the electron distribution of the donor unit to distinctly

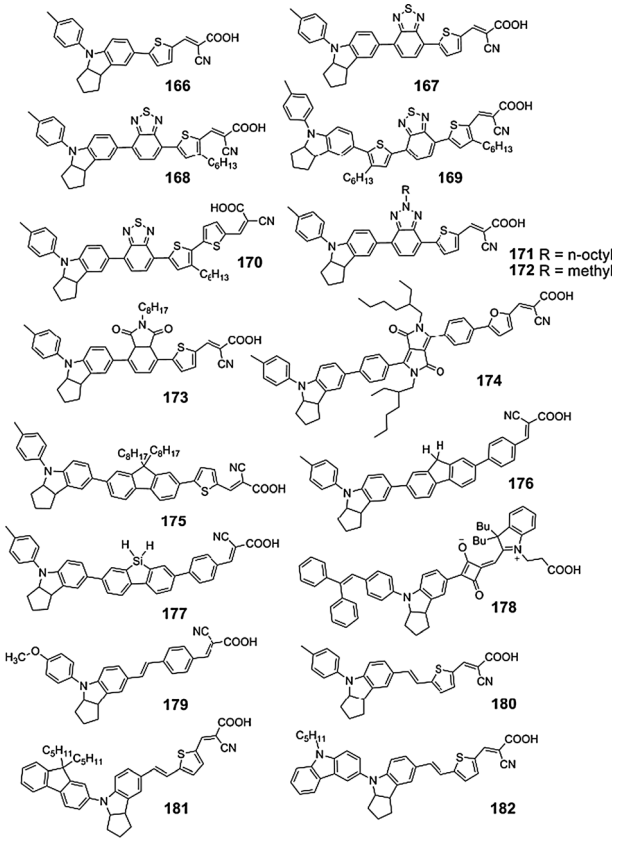

Fig. 25 Representative indoline dyes **166–182**.

increase the photo-stability of the synthetic intermediates and final sensitizers.[150] For example, the maximum absorption peak of **167** (λ_{max} = 533 nm, ε = 16 700 M^{-1} cm^{-1}) is red-shifted by about 47 nm compared with that of **166** (λ_{max} = 486 nm, ε = 21 000 M^{-1} cm^{-1}) as a result of the introduction of a benzothiadiazole unit into the molecular frame, which distinctly decreased the bandgap between the HOMO and the LUMO. Simultaneously, the IPCE of **167** showed a high plateau at the visible region until 720 nm, extending the onset to the NIR region at about 850 nm. They found that **167** co-adsorption with DCA evoked a remarkable enhancement of the J_{SC} (from 12.9 to 17.7 mA cm^{-2}), which was attributed to the break-up of dye aggregates upon co-adsorption. Finally, a **167**-based DSC with a volatile electrolyte yielded an overall conversion efficiency of 8.7%. Importantly, **167** with an ionic-liquid electrolyte showed good stability with the overall efficiency remaining at 94% of the initial value after 1000 h of visible-light soaking.[150]

To alleviate the dye aggregation on the TiO_2 film and charge-recombination in the DSC, they further developed coadsorbent-free **167**-like D–A–π–A sensitizers (**168** and **169**) *via* attaching alkyl chains.[151] The attached *n*-hexyl chains in both dyes are effective to suppress the charge recombination, resulting in a decreased dark current and enhanced V_{OC}. Without DCA coadsorption, the power-conversion efficiency of **168** (PCE = 7.76%, J_{SC} = 15.0 mA cm^{-2}, V_{OC} = 672 mV, FF = 0.77) on a 16 μm thick TiO_2 film device is 45% higher than that of **167** (PCE = 5.31%, J_{SC} = 12.9 mA cm^{-2}, V_{OC} = 604 mV, FF = 0.68) under the same conditions. In contrast, the additional *n*-hexylthiophene in **169** extends the photoresponse to a panchromatic spectrum but causes a low IPCE. Following this work, a more efficient dye, **170**, was obtained.[152] This dye showed a strong anti-aggregation ability, and always exhibited a high performance regardless of the coadsorbent and dye bath solvent. Without DCA coadsorption, the power-conversion efficiency of **170** (PCE = 8.15%, J_{SC} = 16.99 mA cm^{-2}, V_{OC} = 689 mV, FF = 0.71) on a 8 + 5 μm double layer TiO_2 film device is 12.8% higher than that of **167** (PCE = 7.22%, J_{SC} = 16.25 mA cm^{-2}, V_{OC} = 618 mV, FF = 0.72) under the same conditions. Following coadsorption with 20 mM CDCA, the photovoltaic performance of the **170** device was further improved, reaching 9.04% with a high J_{SC} of 18.00 mA cm^{-2} and V_{OC} of 696 mV. Moreover, the **170**-based DSC device with an ionic liquid redox electrolyte was stable under AM 1.5 irradiation (100 mW cm^{-2}) for at least 500 h.

Apart from the benzothiadiazole, other electron-withdrawing units such as benzotriazole, phthalimide and diketopyrrolopyrrole have also been incorporated into the D–A–π–A configuration to design indoline sensitizers. The advantages of the benzotriazole[153] unit as the conjugation bridge in **171** and **172** include: (i) the strong electron-withdrawing properties of benzotriazole to essentially facilitate the electron transfer from the donor to the acceptor/anchor; (ii) a facile structural modification on the 2-position in the benzotriazole unit to tailor their solar cell performance; (iii) the absence of a sulfur site in benzotriazole, which is prone to form dye–iodine complexes that are available for serious charge recombination, being probably favorable for high V_{OC};[154] and (iv) the nitrogen-containing heterocyclic group of benzotriazole is expected to improve V_{OC}. Replacing the methyl group (**172**) with an octyl group (**171**) brings about significant changes in the DSCs performance. The octyl group suppressed the charge recombination rate constant by 4-fold as compared to the methyl group. As a result, without any coadsorption, the **171**-based DSC achieved a PCE of 8.02% with a significant improvement of V_{OC} by 100 mV with respect to **172**. Note that, because of the incorporation of the benzotriazole unit into the dye skeleton, a V_{OC} as high as 780 mV was obtained. Obviously, the benzotriazole is superior to benzothiadiazole in terms of the V_{OC} performance. Interestingly, the absorption spectra of dyes **171** and **172** displayed maximum absorption wavelengths at 495 and 496 nm in CH_2Cl_2 solution, respectively, which is clearly blue shifted related to that of **167** (λ_{max} = 533 nm) in $CHCl_3$: CH_3OH = 4 : 1, even not considering the solution effect (usually, CH_3OH leads to a blue shift of λ_{max} compared to CH_2Cl_2 or $CHCl_3$). In view of this, benzothiadiazole is preferred for light harvesting in D–A–π–A sensitizers.

With a very similar D–A–π–A feature but changing the additional acceptor from a benzotriazole (**171**) to a phthalimide (**173**) unit, the photovoltaic efficiency based on **173** was only 5.11% (J_{SC} = 10.06 mA cm^{-2}, V_{OC} = 748 mV, FF = 0.68), it decreased by 39% mainly due to its lower photocurrent.[155] The twist conformation formed between phthalimide and its neighboring groups in **173** not only led to a significant hypsochromic shift in the absorption spectra of **173** (λ_{max} = 442 nm in CH_2Cl_2) but also broke the molecular conjugation, which is unfavorable to the charge migration from donor to acceptor. In contrast, dye **174**, incorporating a diketopyrrolopyrrole unit with a branched alkyl chain as the additional acceptor and furan as the linker, showed a high conversion efficiency of 7.43% (AM 1.5, 100 mW cm^{-2}) with a J_{SC} of 13.40 mA cm^{-2}, a V_{OC} of 760 mV, a FF of 0.73 and an excellent stability.[156] A broad IPCE response from 350 to 625 nm with a maximum value of 80% in the plateau region accounts for the increased J_{SC} related to **173**.

According to the results from **168–174**, it can be found that the strategy of introducing alkyl chains to indoline dyes is quite successful in achieving high V_{OC} values. Another approach to obtain this effect is to introduce conjugation bridges such as fluorene and dibenzosilole units.[157,158] The V_{OC} values of dyes **175–177** are in the range of 727–772 mV. The dibenzosilole-containing dye (**177** PCE = 4.64%) showed a higher PCE compared to the fluorine-based dye **176** (PCE = 2.88%). DFT calculations showed that the torsion angle across the biphenyl linkage in **177** is smaller than that in the silicon-free dye (**176**), which contributed to better charge separation and enhancements in the total efficiency of **177**.[158]

Funabiki *et al.* designed NIR-absorbing indoline dyes containing asymmetric squaraine for DSCs with Pt-free electrodes.[159] Dye **178**, without the introduction of linker groups such as phenyl, thienyl or pyrrole groups, was quite efficiently sensitized on TiO_2 with the long-wavelength visible and NIR region (up to 800 nm) of the spectrum. Like other squaraine dyes discussed above, this dye also suffers from the drawback of low ionic moiety, resulting in a low V_{OC} of 480 mV.

Besides the works dealing with spacers, other fundamental research of indoline dyes focuses on further increasing the electron-donating ability of the donor part to optimize the light harvesting capability. Successful results have been achieved by introducing second donors (*i.e.* 4-methoxyphenyl, 4-methylphenyl, fluorene and carbazole) into the indoline group to form a donor–donor structure, which allowed connection with the π-linker and acceptor to form a D–D–π–A system. Akhtaruzzaman *et al.* reported dye **179**, bearing a phenylenevinylene-conjugated system and a 4-methoxyphenyl substituted indoline donor.[160] Furthermore, the DSC based on **179** showed panchromatic TiO_2 sensitization (the onset of the IPCE spectra is close to 800 nm) with a high overall conversion efficiency of 6.2% under AM 1.5 illumination (100 mW cm^{-2}).

Liu *et al.* reported three D–D–π–A indoline dyes **180**, **181** and **182** by the introduction of 4-methylphenyl, fluorene and carbazole as the second donors, respectively.[161] They found that the introduction of an additional donor (D–D moiety) with a large π conjugation into the indoline unit is helpful to both red-shifting in the absorption spectra and enhancing the molar extinction coefficient. For example, compared with the **180** dye containing a 4-methylphenyl group, the λ_{max} of **181** and **182** was red-shifted by about 13 and 32 nm, respectively. Moreover, there is around a 25% enhancement in the molar extinction coefficient with respect to **180**. Particularly, the IPCE action spectrum of **182** keeps an extraordinarily high plateau in the visible region till around 700 nm, and the onset wavelength extends from 780 to about 860 nm in NIR region along with the increase of the electron-donating ability of the donor. Upon coadsorption with DCA (30 mM), **182** achieved a performance with a J_{SC} of 18.53 mA cm^{-2}, a V_{OC} of 649 mV, and a FF of 0.71, corresponding to a PCE of 8.49%.

An obvious advantage of the indoline dyes is their impressive J_{SC}. However, their V_{OC} values are just comparable to or lower than those of substituted TPA dyes, which limits their improvement in efficiency. Further works should focus on how to improve the V_{OC} values.

7. *N,N*-dialkylaniline dyes

The *N*,*N*-dialkylaniline (DMA) moieties were used as donors for organic dyes because of their simpler structures and stronger electron-donating ability than the coumarin moiety. Representative dyes (**183–192**) are shown in Fig. 26. Arakawa, Hara, and co-workers developed a series of *N*,*N*-dialkylaniline dyes (**183–186**) by employing oligoene or thienyl as the π-bridge and cyanoacrylic acid as the electron acceptor.[163,164] **185** showed a maximum PCE of 6.8% under AM 1.5 irradiation (100 mW cm^{-2}) with J_{SC} = 12.9 mA cm^{-2}, V_{OC} = 710 mV, and FF = 0.74. After that, Yanagida and co-workers also demonstrated the high performance of *N*,*N*-dialkylaniline dyes as photosensitizers in DSCs.[21] In 2006, Yang's group developed two *N*,*N*-dialkylaniline dyes featuring thienothiophene- and thiophene-bridging structures (**187** and **188**, respectively).[165] A PCE of 6.23% was achieved from the DSC based on dye **187** (J_{SC} = 15.23 mA cm^{-2}; V_{OC} = 560 mV; FF = 0.73). Despite the larger π-conjugation system, **188** gave much lower PCE (3.87%) compared to **187**.

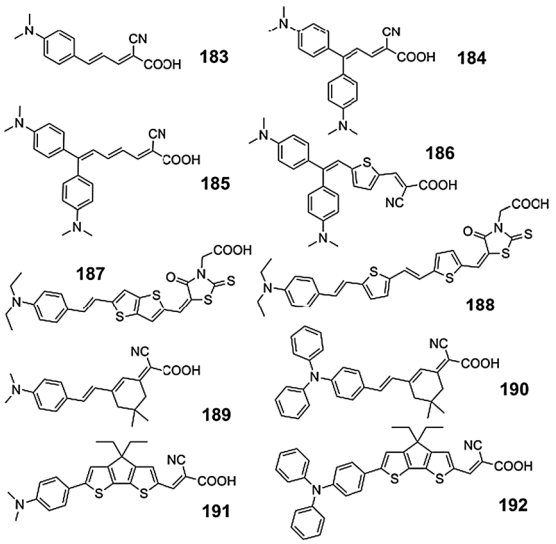

Fig. 26 Representative *N*,*N*-dialkylaniline dyes **183–192**.

To further understand the role of the *N*,*N*-dialkylaniline as donors, several groups compared the performance of DSCs sensitized with *N*,*N*-dialkylaniline dyes and triphenylamine dyes (*e.g.* **189** *vs.* **190**;[20] **191** *vs.* **192**[166]). Clearly, the *N*,*N*-dimethylaniline are superior to the TPA in terms of the light harvesting. For example, **189** and **191** showed a shift of the absorption peak bathochromically 14 and 30 nm compared to **190** and **192**, respectively. However, this light harvesting advantage did not always result in a higher efficiency because the steric hindrance of the *N*,*N*-dimethylaniline is not enough for the retardation of the charge recombination. In addition, studies also suggested that the electron-donating ability of *N*,*N*-dialkylaniline is inferior to that of indoline, which limited the J_{SC} of this type of dyes. Further tuning the structure of the *N*,*N*-dialkylaniline dyes should focus on these two issues.

8. Tetrahydroquinoline dyes

Like DMA moieties, tetrahydroquinoline was used as a donor due to its prominent electron-donating ability. Yang, Sun and co-workers have reported new tetrahydroquinoline dyes (**193–196**, as shown in Fig. 27) containing different lengths of thiophene-containing conjugation moieties (thienyl, thienylvinyl, and dithieno[3,2-*b*;2′,3′-*d*]thienyl) as electron spacers.[167] The bathochromic shift and increase of the molar extinction coefficient of the absorption spectrum are achieved by the introduction of more thiophene units. The elimination of the C=C bond and adoption of suitable electron spacers in dye structures are useful for getting higher PCE values of DSCs based on these dyes. A maximum PCE value of 4.53% is achieved under simulated AM 1.5 irradiation (100 mW cm^{-2}) with a DSC based on the **194** dye (V_{OC} = 597 mV, J_{SC} = 12.00 mA cm^{-2}, FF = 0.63).

Aiming to tune the HOMO–LUMO level (absorption spectra) in an easier way by modifying the structure of the acceptor units, Yang, Hagfeldt, Sun and co-workers proposed a new strategy for the design of organic dyes, in which the anchoring

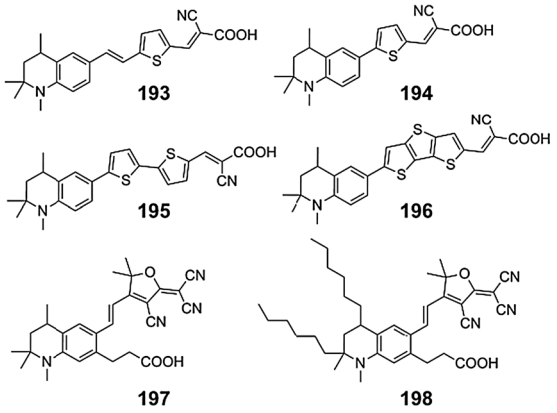

Fig. 27 Representative tetrahydroquinoline dyes **193–198**.

group is separated from the acceptor groups of the dyes.[168] By using this strategy, a new class of D–π–A organic dyes for sensitization in the NIR region was successfully synthesized. The **197** dye gave a maximum IPCE value of 86% at 660 nm and overall 3.7% solar energy to electricity conversion efficiency.[168] Unfortunately, this dye suffers from a strong tendency to aggregate on TiO_2. To alleviate this problem, **198** with flexible long carbon chains was introduced, leading to higher J_{SC} and V_{OC} values and an improved PCE of 5.1%.[169]

9. Phenothiazine and phenoxazine dyes

Phenothiazine (PTZ) and phenoxazine (POZ) are well-known heterocyclic compounds with electron-rich sulfur–oxygen and nitrogen heteroatoms.[170] Organic sensitizers containing phenothiazine or phenoxazine[171–187] (**199–210** shown in Fig. 28 and **211–231** shown in Fig. 29) have recently attracted considerable research interests on account of their unique excellent hole-transporting ability, rigid structure and large π conjugated system.

In 2007, Yang, Hagfeldt, Sun and co-workers reported organic dyes based on the phenothiazine chromophore (**199** and **200**), which are simple in structure and easy to synthesize.[171] Dye **199** (PCE = 5.5%), containing a cyanoacrylic anchor group, has a much better DSC performance than dye **200** (PCE = 1.9%), containing a rhodanine-3-acetic acid group, owing to a better orbital overlap (LUMO) with the TiO_2 conduction band. To obtain a panchromatic metal-free dye, they employed phenoxazine (donor), thiophene (π-bridge) and co-rodanmine (acceptor) to construct a D–π–A "black dye" **201**.[172] When the dye was fabricated to DSCs, a broader IPCE spectrum over the whole visible range of solar spectrum extending into the NIR region up to 920 nm was obtained. However, the **201** dye did not obtain a higher PCE value than 3.0%, mainly owing to poor V_{OC} (390 mV). Recently, Meyer *et al.* reported a series of new phenothiazinyl rhodanylidene acetic acid merocyanine dyes.[173] The V_{OC} was largely increased due to the introduction of a phenothiazine and decyltetradecyl substituent at the 7-position and 10-position of the PTZ, respectively. **202** displayed a high V_{OC} of 698 mV.

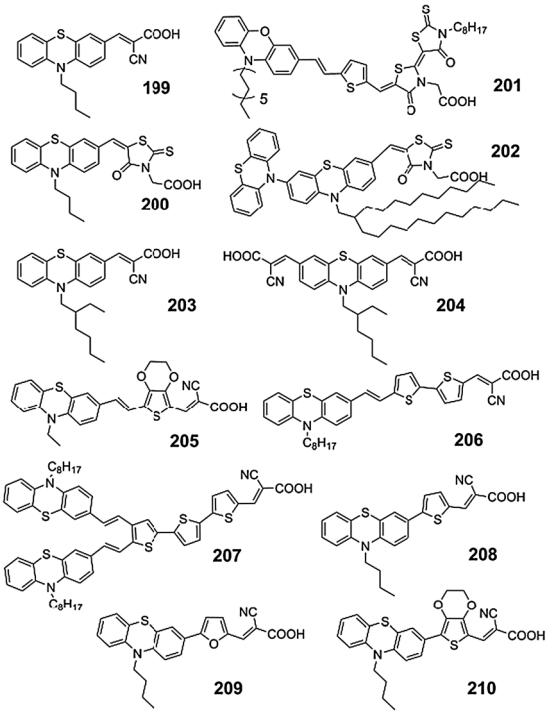

Fig. 28 Representative PTZ dyes **199–210**.

After that, Park *et al.* also found the adverse effects of the rodanmine ring as an acceptor for PTZ dyes. In addition, their results suggested that the dyes with double electron acceptor moieties are promising for getting higher PCE in DSCs. The DSC based on **204** showed a better efficiency (6.8%) than that based on **203** (5.6%).[174]

Further progresses in efficiency performance were obtained by the introduction of five-membered heteroaromatic linkers (such as EDOT, thiophene and furan). A solar cell employing the **205** dye was fabricated and the photovoltaic performance showed a J_{SC} of 15.18 mA cm^{-2}, a V_{OC} of 645 mV, and a FF of 0.69, corresponding to an overall conversion efficiency of 6.72% under 100 mW cm^{-2} irradiation.[175] Xie *et al.* found that dye **207** (PCE = 2.8%), containing an additional donor moiety, deteriorated the performance of the DSCs because of serious dye aggregation.[176] In contrast, the DSC sensitized by the **206** dye achieved a promising conversion efficiency of 6.17% under AM 1.5 illumination (100 mW cm^{-2}). To study the effect of conjugated linkers on device performance, Kim *et al.* synthesized a group of PTZ derivatives with various conjugated linkers (**208**, **209** and **210**).[177] Interestingly, they found that the torsion angles arising from the butterfly conformations of PTZ were closely correlated with the V_{OC} values. The PTZ-torsion angles of the dyes were ranked: **208** (26.53°) < **210** (26.61°) < **209** (42.65°), which is consistent with the sequence of V_{OC} values (**208**, 724.5 mV; **210**, 745.7 mV; **209**, 771.7 mV) in the devices fabricated with CDCA (10 mM). They proposed that an increased torsion angle could reduce molecular aggregation through steric hindrance and improve the V_{OC}. Moreover, lower resonance energy of the furan linker (16 kcal mol^{-1}) was thought to be favorable for high J_{SC}. Thus, the highest solar

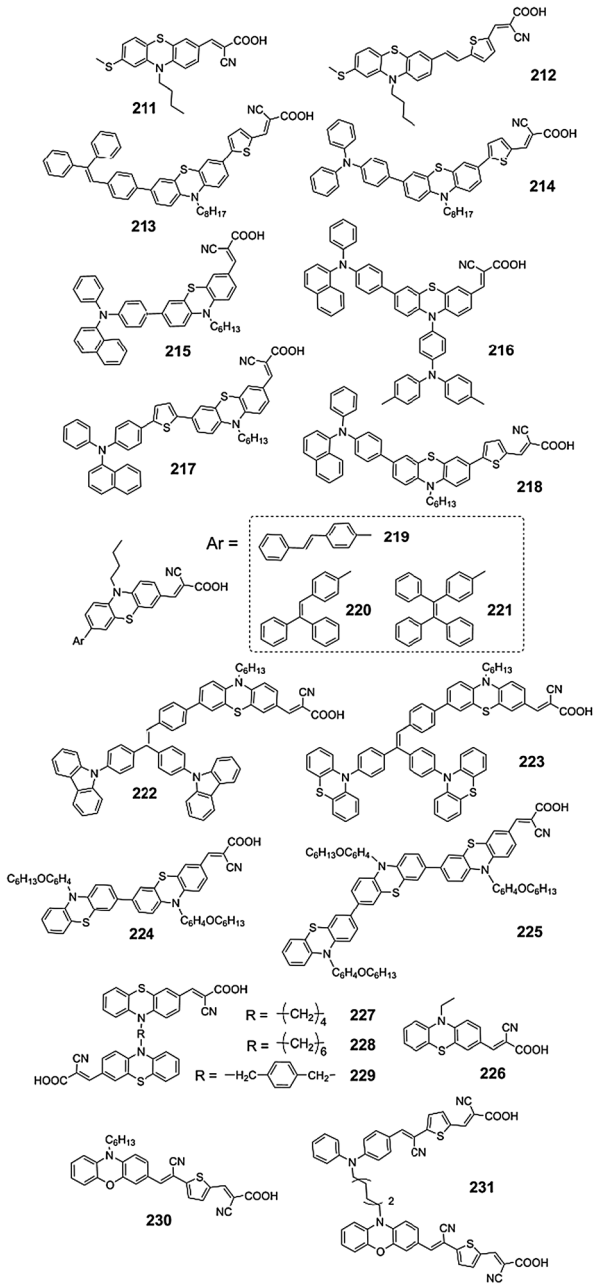

Fig. 29 Representative PTZ dyes **211–231**.

energy-to-electricity conversion efficiency was achieved by a cell fabricated with **209** (PCE = 6.58%, J_{SC} = 12.18 mA cm^{-2}, V_{OC} = 771.7 mV, FF = 70.02%).

The D–D–π–A types of triphenylamine dyes and indoline dyes as discussed in the former sections have shown superior performance over the corresponding dyes with simple D–π–A configuration. PTZ dyes with a D–D–π–A configuration were also developed. **211** and **212** (Fig. 29), containing electron-rich 10-butyl-(2-methylthio)-10*H*-phenothiazine as a donor and cyanoacrylic acid as an acceptor, were synthesized by Grätzel's group.[178] Extending the π-conjugated linker by the introduction of a vinyl thiophene group has helped to vastly enhance the optical properties of the resulting compound. The bathochromic shift of the absorption peak exhibited by **212** (λ_{max} = 478 nm) in the solution is 27 nm, and the onset of the absorption has been pushed much further. The cell sensitized with this dye has a greatly improved IPCE, which in turn translated to an enhanced photocurrent (J_{SC} = 15.2 mA cm^{-2}). The PCE of the device based on **212** under standard AM 1.5 irradiation (100 mW cm^{-2}) conditions reached 7.3% with a volatile electrolyte.

Hua, Tian and co-workers found that the introduction of a triphenylamine group as the electron-donor brought about improved photovoltaic performance in comparison with 1,1,2-triphenylethene for phenothiazine dyes.[179] A PCE of 4.41% (J_{SC} = 10.84 mA cm^{-2}, V_{OC} = 592 mV, FF = 0.69) under AM 1.5 irradiation (100 mW cm^{-2}) with a DSC based on **214** was obtained. The long-term stability of the DSCs with **213** and **214** under 1000 h light-soaking was demonstrated.

In a study of PTZ dyes, Chow and co-workers investigated the effects of hexyl and triphenylamino groups at the N(10) of PTZ.[180] **215**, containing a hexyl substituent (PCE = 5.6%, J_{SC} = 13.66 mA cm^{-2}) at the N(10), performs better than **216**, possessing a TPA substituent (PCE = 5.22%, J_{SC} = 11.65 mA cm^{-2}). To examine the influence of a thiophenylene group at different positions, **217** and **218** were synthesized. **217**, with thiophenylene at the C(7) position, displayed a J_{SC} of 14.42 mA cm^{-2}, a V_{OC} of 690 mV, and a FF of 0.63, corresponding to a PCE of 6.22%. In contrast, inserting a thiophene between the phenothiazine and the cyanoacrylate anchoring group reduced the loading amount of the dyes, as well as the morphology of the films. Thus, both J_{SC} (5.99 mA cm^{-2}) and V_{OC} (570 mV) of **218** decreased.

Chi, Kuang and co-workers observed that phenothiazine dyes with end-capped structures that are slightly different from diphenylethylene to tetraphenylethylene (**219–221**) can increase the PCE and V_{OC} values.[181] The introduction of twisted structures with increasing sizes onto the end of the organic dyes was thought to reduce more effectively the recombination of injected electrons at the interface or in the electrolyte. For this reason, the electron lifetime and V_{OC} in the DSCs increased in the following order: **219** (759 mV), **220** (789 mV), **221** (804 mV). By comparison, the performance efficiencies of the DSCs based on **219** (PCE = 5.84%), **220** (PCE = 6.29%), and **221** (PCE = 5.76%) were better than those of their parent-compound-sensitized counterpart **199** (V_{OC} = 712 mV, PCE = 5.5%), suggesting that the introduction of phenylethylene groups can increase the performance of the DSCs. Further modifications of **220** have been performed through the introduction of the triphenylethylene carbazole (**222**) and triphenylethylene phenothiazine (**223**) units.[182] Afterwards, **223**, containing a more twisted triphenylethylene phenothiazine unit, achieved a further increase in performance of the DSC (PCE = 6.55%, J_{SC} = 12.18 mA cm^{-2}, V_{OC} = 826 mV, and FF = 0.64). These results were ascribed to the increase of the twisted non-planar structure in the organic dyes.

Chang *et al.* have prepared and tested a series of organic dyes containing oligo-phenothiazine.[183] They found that the phenothiazine moiety functions both as an electron donor and as a π-bridge. The performance of the dimer system, *i.e.*, **224**, was better than the trimers (**225**). The high V_{OC} values reached a

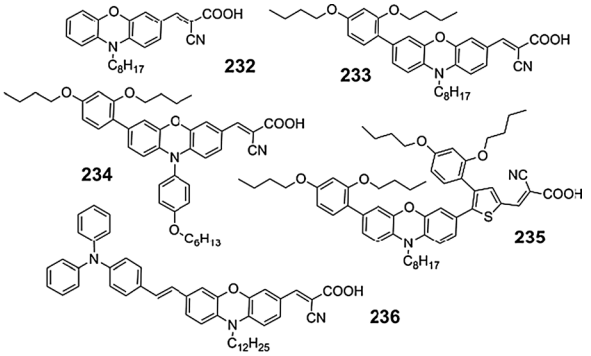

Fig. 30 Representative POZ dyes **232–236**.

level of >0.83 V, and a conversion efficiency of 7.78% was obtained in **224** (J_{SC} = 14.3 mA cm^{-2}, V_{OC} = 830 mV, FF = 0.65).

Cao *et al.* developed a novel class of PTZ dyes (**227–229**) that contained double D–A branches.[184] They considered that more light-harvesting units are preferred for light harvesting and high efficiency. In fact, the molar extinction coefficients of these double D–A branched dyes (DBD) are nearly twice as high as that of **226** because of the two donor–acceptor units of DBD. Importantly, the number of light-harvesting units adsorbed on TiO_2 for DBD is higher than that of **226.** Thus, the J_{SC} and PCE of the DSCs (J_{SC} = 6.98–8.27 mA cm^{-2}, PCE = 3.56–4.22%) were effectively enhanced in comparison with the corresponding single D–A PTZ dye **226** (J_{SC} = 6.13 mA cm^{-2}, PCE = 2.91%). Based on this finding, they synthesized a POZ dye (**231**) containing two asymmetric D–π–A chains.[185] An improved PCE of 6.06% was obtained for the **231**-sensitized solar cells as a result of its longer electron lifetime and higher IPCE related to **230**.

Recent developments of POZ dyes (Fig. 30, **232–236**) have been highlighted by Sun and co-workers.[186–188] A comparison between POZ- and PTZ-based sensitizers showed that the POZ-based dye **232** gave an efficiency of 6.7% and the structurally similar PTZ-based **199** showed an efficiency of 5.5% under similar conditions.[186] Due to the electron-donating properties, the introduction of a 2,4-dibutoxyphenyl substituent at the 7-position of the POZ (**233**, **234**) lifts both the HOMO and LUMO energy levels of the dyes relative to unsubstituted **232** (λ_{max} = 448 nm). The shift is larger for the HOMO, which resulted in a red shifted absorption due to the smaller energy-level gap. At the same time, the extinction coefficient was also enhanced. The J_{SC} of the DSCs based on **233** was therefore increased greatly due to the advantageous absorption properties compared to **232.** The V_{OC} of the **233**-based DSCs (780 mV) is slightly higher than those based on **232** (760 mV) because of the enhanced surface protection caused by the presence of a large substituent at the end of the molecule.

In the case of **234**, an interesting molecular configuration was presented by DFT study. The hexyloxy-substituted benzene ring at the N(10) is almost perpendicular to the POZ core, which leads to poor orbital overlap and inefficient conjugation. Not surprisingly, the absorption spectrum of **234** (λ_{max} = 500 nm) is slightly blue shifted compared to **232** (λ_{max} = 506 nm). In addition, the presence of the relatively large hexyloxy-phenyl unit decreased the dye loading on the TiO_2 surface. These two factors contributed to the relatively lower J_{SC} (13.09 mA cm^{-2}) of **234**. Despite that, **234** achieved an efficiency of 7.4% under 100 mW cm^{-2} light illumination because of its higher V_{OC} (800 mV) and FF (0.7). This result suggested that bulky substituents attached to the end or the middle of a molecule are necessary for the suppression of the charge recombination. Dye **235** (V_{OC} = 800 mV), showing a PCE of 7.0% under the same conditions, proved this strategy.[187] Apart from the 2,4-dibutoxyphenyl, TPA was also demonstrated as an appropriate energy antenna for constructing the POZ dyes. Under the optimized fabrication conditions, **236** achieved a PCE of 7.7%, with J_{SC} = 14.7 mA cm^{-2}, V_{OC} = 733 mV and FF = 0.71.[188] Note that, Sun and co-workers claimed that **236** is inferior to **234** in terms of PCE because the former showed a 7.3% efficiency under the same working conditions as for the latter.[186]

Therefore, structural modification of PTZ or POZ dyes has been performed through introducing substituents at the N(10) and C(7) positions, and changing the π bridge. Further tuning the structure at different positions may lead to the synthesis of interesting photosenzitizers.

10. Carbazole dyes

Based on the concept of the interface engineering of a dye-adsorbed TiO_2 surface, Koumura, Hara and co-workers reported efficient carbazole sensitizers with *n*-hexyl-substituted oligothiophenes as a π-conjugated system (**237–246**, Fig. 31).[189–194] They found that the photovoltaic performance of the DSCs markedly depended on the molecular structures of the dyes in terms of the number and position of *n*-hexyl chains and the number of thiophene moieties. Retardation of charge recombination caused by the existence of *n*-hexyl chains that are linked to the thiophene groups resulted in an increase in the electron lifetime. As a consequence, an improvement of V_{OC} and hence the PCE of the DSCs was achieved. For example, the V_{OC} for DSCs based on **237** (750 mV) and **238** (690 mV) were higher than that for **239** (670 mV) under the same conditions due to longer electron lifetimes.[189,190] However, a large amount and/or thick aggregate of adsorbed dyes decreased the FF and J_{SC} seriously because the dye layer suppressed the diffusion of redox species through the nanoporous TiO_2 electrode. Such a problem was solved by increasing the iodine content in the redox electrolyte. A DSC consisting of a **238** sensitized TiO_2 electrode (16 μm) produced a PCE of 7.6% (J_{SC} = 14.20 mA cm^{-2}, V_{OC} = 740 mV, FF = 0.72) with an electrolyte of 0.6 M DMPImI + 0.1 M LiI + 0.05 M I_2 + 0.5 M TBP in acetonitrile. The PCE dramatically went up to 8.3% (J_{SC} = 15.22 mA cm^{-2}, V_{OC} = 730 mV, FF = 0.75) when the iodine content was increased from 0.05 to 0.2 M.[190] The **238**-based DSCs showed a long-term stability under white-light irradiation at 80 °C under dark conditions.[191]

Following this work, they further synthesized hexyloxyphenyl substituted carbazole dyes (**240**, **241**) for DSCs and demonstrated that a hexyloxyphenyl substituent at the end of the dye increased the electron lifetime, and consequently gave a higher V_{OC}.[192] A better performance was observed for the device made with **240**

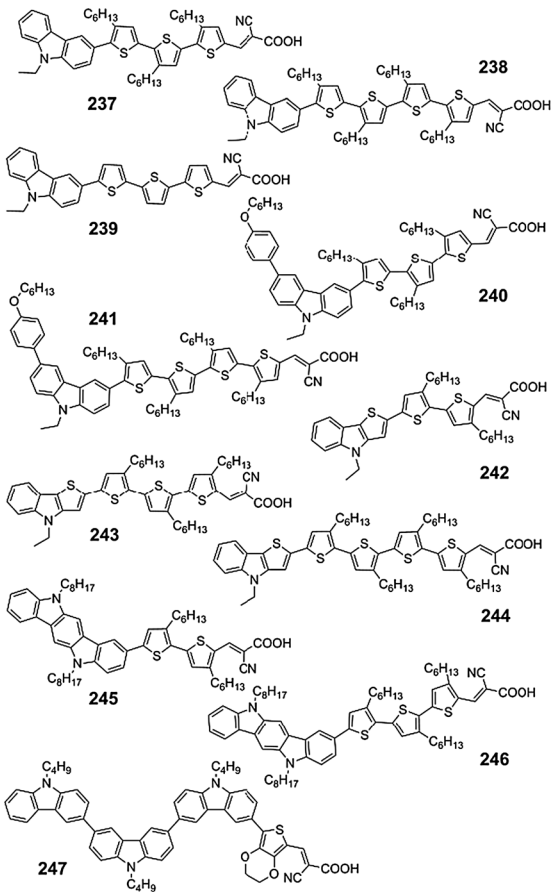

Fig. 31 Representative carbazole dyes **237–247**.

(PCE = 8.1%), which exhibited a J_{SC} value of 16 mA cm^{-2}, a V_{OC} value of 710 mV, and a FF value of 0.71. Later they reported a new class of thieno[3,2-*b*]indole-based organic dyes (**242–244**) with high molar extinction coefficient and long-term stability for DSCs application.[193] The ε at the maximum absorption of the three dyes in toluene ranged from 43 000 to 46 000 M^{-1} cm^{-1}, which is a little higher than those of carbazole dyes (42 100 M^{-1} cm^{-1} for **237** and 42 600 M^{-1} cm^{-1} for **238** in toluene). These dyes suffered from a shorter electron lifetime compared to conventional carbazole dyes, resulting in PCEs ranging from 7.3 to 7.8%. By using the 5,11-dioctylindolo[3,2-*b*]carbazole to replace the carbazole unit, other efficient organic dyes such as **245** and **246** were obtained, exhibiting PCEs of 7.3 and 6.7%, respectively, under AM 1.5 irradiation (100 mW cm^{-2}).[194]

Unlike dyes **237–246**, dye **247** inhibited dye aggregation and charge recombination in a different way.[195] Fang and co-workers proposed that the designed molecules have an interesting twisted structure and a zigzag-shape, in which the dihedral angles between two carbazole units were near 40°. The DSCs based on **247** showed a high V_{OC} (796 mV) and PCE (6.33%), indicating that a combination of alkyl side chains and a twisted linked backbone in a dye molecule is an effective way for the suppression of dye aggregation and charge recombination.

Attempts on structural optimization of carbazole-based dyes have also been made by replacing the alkyl chains with

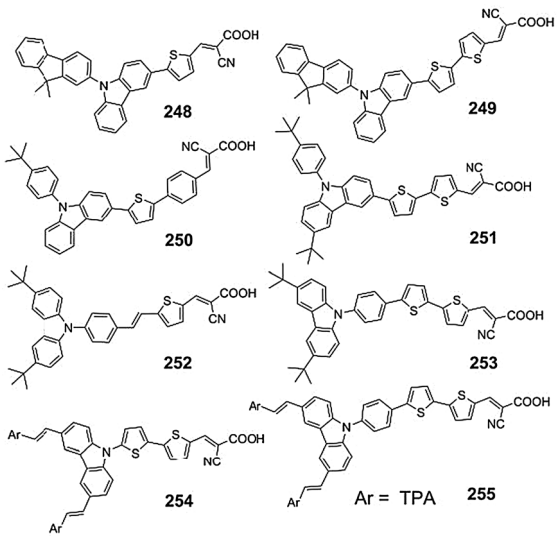

Fig. 32 Representative carbazole dyes **248–255**.

9,9-dimethylfluoren or *tert*-butylbenzene. PCEs ranging from 3.62 to 6.7% have been achieved with **248** to **251** (Fig. 32).[196–198] Dye **250**, containing a bulky tertbutylphenylene-substituted carbazole donor group, showed a PCE of 6.70%. Chow and co-workers proposed that the presence of a tertbutyl group not only enhanced the electron-donating ability of the donor, but also suppressed the intermolecular aggregation.[197]

Dyes **252–255** (Fig. 32) featuring 3,6-disubstituted carbazole were investigated by several groups.[199–201] **252** gave a PCE of 4.10% with an iodine electrolyte containing 0.6 M DMPII, 0.06 M LiI, 0.04 M I_2, and 0.4 M TBP in dried CH_3CN solutions. Surprisingly, a remarkably high V_{OC} (0.939 V) with a better PCE of 5.22% was achieved with a Br^-/Br_3^--containing electrolyte of 0.9 M 1,2-dimethyl-3-butylimidazolium bromide (DMBIBr), 0.08 M Br_2, and 0.5 M TBP electrolyte in dried CH_3CN solution.[199] Ko, Hong and co-workers found that the presence of a TPA unit in the **254** and **255** dyes as a donor increased not only the charge generation and injection but also the electron lifetime, improving V_{OC} and J_{SC}, and ultimately the PCE. Under AM 1.5 irradiation (100 mW cm^{-2}), a device using dye **255** exhibited a J_{SC} of 13.7 mA cm^{-2}, a V_{OC} of 680 mV, a FF of 0.70, and a calculated efficiency of 6.52%.[201] This performance is comparable to that of a reference cell based on **N719** (7.30%) under the same conditions. After 1000 hours of visible light soaking at 60 °C, the overall efficiency remained at 95% of the initial value.

11. Arylamine organic dyes for DSCs employing cobalt electrolytes

Arylamine organic dye-sensitized DSCs employing iodine electrolytes have reached power conversion efficiencies as high as 10–11%, comparable to those of Ru complexes. However, some disadvantages of the iodide/triiodide redox couple limited the performance of the DSCs with the following points. (i) The relatively high overpotential for dye regeneration has led

to a noticeable potential loss.[202] (ii) The halogen bonding between iodine and some electron-rich segments of dye molecules could cause a larger charge recombination rate at the titania/electrolyte interface.[203–205] (iii) Competitive light absorption by the triiodide has led to a light harvesting loss.[206,207] (iv) The large-scale manufacturing of DSCs remains a challenge due to the corrosiveness of the iodide/triiodide redox couple toward most metals and sealing materials.[208,209] To achieve a breakthrough in the development of highly efficient DSCs, alternative redox couples, including metal complexes, hole conductors, halogens and pseudohalogens and some redox active organic compounds have been explored for DSCs to avoid the problems mentioned above.[13] Researchers have made astonishing progress in this area in recent years, especially regarding polypyridyl cobalt redox shuttles. The following section summarizes recent progress in arylamine organic dyes for DCSs employing cobalt electrolytes.

An advantage of the cobalt electrolytes over the iodide/triiodide redox couple is that very high V_{OC} can be realized but without sacrificing short circuit photocurrent or fill factor. However, simply replacing the iodide/triiodide couple in the DSCs by cobalt redox couples may lead to poorly performing devices with low photovoltages and photocurrents,[207,210–212] which has been attributed to slow mass transport and increased recombination of the injected electrons with oxidized redox species in the electrolyte. To overcome the mass transport limitation associated with the polypyridyl cobalt redox shuttles, a relatively thin titania film is always needed. Additionally, to meet the requirements of effective light harvesting and retard the rate of interfacial back electron transfer from the conduction band of the nanocrystalline titanium dioxide film to the Co(III) ions, photosensitizers with high extinction coefficients, suitable electronic structures and steric properties are warranted.

Recent developments have been highlighted by several groups. Boschloo and co-workers found that the recombination and mass-transport limitations can be avoided by matching the properties of the dye and the cobalt redox mediator.[208,209] Recombination was reduced further by introducing insulating butoxyl chains on the substituted TPA-based dye **75** (Fig. 13) rather than on the cobalt redox mediator. This enables redox couples with higher diffusion coefficients and a more suitable redox potential to be used, simultaneously improving the photocurrent and photovoltage of the device. Optimization of DSCs sensitized with dye **75** in combination with tris(2,2′-bipyridyl)-cobalt(II/III) yielded solar cells with a PCE of 6.7% and V_{OC} of more than 0.9 V under AM 1.5 illumination (100 mW cm^{-2}).[208] Encouraged by the work done by Boschloo and co-workers, Wang and co-workers explored a series of DHO–TPA dyes (**256–268**, Fig. 33) for DSCs employing the cobalt redox shuttles.[18,213–218] Many encouraging results were presented, giving confidence that the cobalt DSCs can afford power conversion efficiencies comparable to those of the iodine DSCs. In a comparative study of the influences of arylamine electron donors on the optoelectronic features of thin-film DSCs employing a (Co(II/III)(phen)$_3$) (phen = 1,10-phenanthroline) redox electrolyte, they found that **256–258** based cells (7.6 to 8.4%) present lower PCE values than their **59** counterpart (9.3%), primarily owing to relatively low photocurrents.[213] Photovoltaic characterization evidently demonstrated the superiority of DHO–TPA over the other three electron donors (diphenothiazinyl- or di-*tert*-butylphenylsubstituted TPA and *N*-hexyl-carbazole) when applied in CPDT-cyanoacrylic acid organic dyes. Note that, high V_{OC} values (930–950 mV) were obtained by **59**-, **256**- and **257**-sensitized DSCs employing a cobalt electrolyte composed of 0.25 M [Co(II)(phen)$_3$](B(CN)$_4$)$_2$, 0.05 M [Co(III)(phen)$_3$](B(CN)$_4$)$_3$, 0.5 M TBP and 0.1 M lithiumbis(trifluoromethanesulfonyl)imide (LiTFSI) in acetonitrile. Comparisons of four DHO–TPA dyes (**259**, **260**, **59** and **261**) with the di(3-hexylthiophene), dihexyldithienosilole, CPDT and *N*-hexyl-dithienopyrrole linkers have revealed that dyes with rigidified dithiophene (**59**, **260**, **261**) presented notable red-shifts of the λ_{max} by 82–88 nm and over five times enhancement of the maximum molar visible absorption coefficient, leading to higher J_{SC} values.[214] Meanwhile, the rigidification of the conjugated dithiophene linkers generally diminished the V_{OC} in the range from 60 to 190 mV. For example, the dithienopyrrole dye (**261**) exhibited a 190 mV reduction in V_{OC} compared to its di(3-hexylthiophene) counterpart (**259**), which stems mainly from a remarkable downward displacement of the titania conduction band edge. Among the four dyes, **59** displayed a better cell efficiency, proving the superiority of CPDT as the conjugated spacer.

One of the most astounding findings in arylamine organic dye-sensitized DSCs employing cobalt electrolytes is the increment of the cell photovoltage concomitant with an extension of the π-conjugated linker in organic dyes, which is in prominent contrast to the traditional iodine electrolyte system. For example, along with an elongation of the π-conjugated linker from **262** to **263**, the V_{OC} in the case of the iodine electrolyte was actually decreased by 43 mV (795 mV *vs.* 752 mV), whilst that of the cobalt electrolyte was augmented by 22 mV (815 mV *vs.* 837 mV).[215] The dye–iodine interaction was thought to evoke a higher iodine concentration in the vicinity of titania anchored with the **263** dye, rationalizing its faster interfacial charge recombination kinetics. On the other side, the larger steric hindrance of the bulky cobalt(III) complex and the longer π-conjugated spacer contributed to slow the interception of photoinjected electrons with cobalt(III) ions. On the basis of this finding, dye **264** was synthesized, displaying a PCE of 9.4% in a cobalt cell measured at AM 1.5 irradiation (100 mW cm^{-2}).[216]

Through elongating the end or side alkyl chains of dye molecules, dyes **265–268** were obtained.[217] Upon alternation of the ethyl side chains with *n*-dodecyl, the corresponding **266** dye displayed a significantly enhanced V_{OC} of 930 mV, leading to a remarkably high PCE of 10.1%. A similar phenomenon was also perceived when the end alkyl chains are elongated. The **268** dye generated a cell efficiency of 10.1% with a J_{SC} of 14.55 mA cm^{-2}, a V_{OC} of 930 mV and a FF of 0.743, mainly benefiting from a significant improvement of V_{OC} by 100 mV with respect to the **267** dye bearing two ethyl end chains. This study revealed that either the end or the side alkyl chains of dye molecules play a pivotal role in the attenuation of interfacial charge recombination, which is one key photovoltage determinant.

Meanwhile, promising results have been reported by Nnazeeruddin and Grätzel.[219–221] Dye **269** (Fig. 33), containing

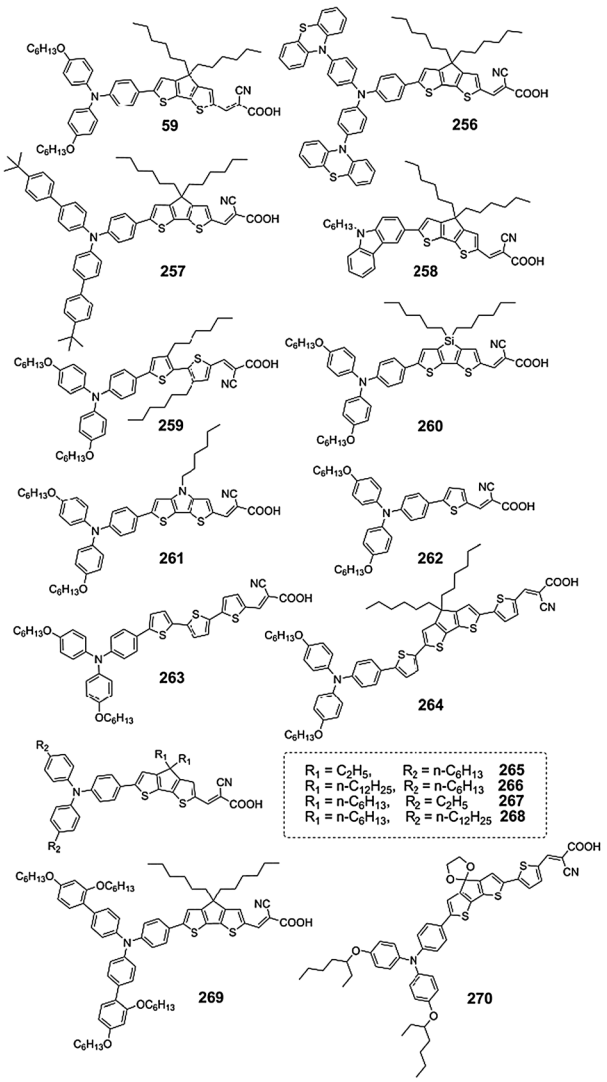

Fig. 33 Representative arylamine organic dyes **256–270** for DSCs employing cobalt electrolytes.

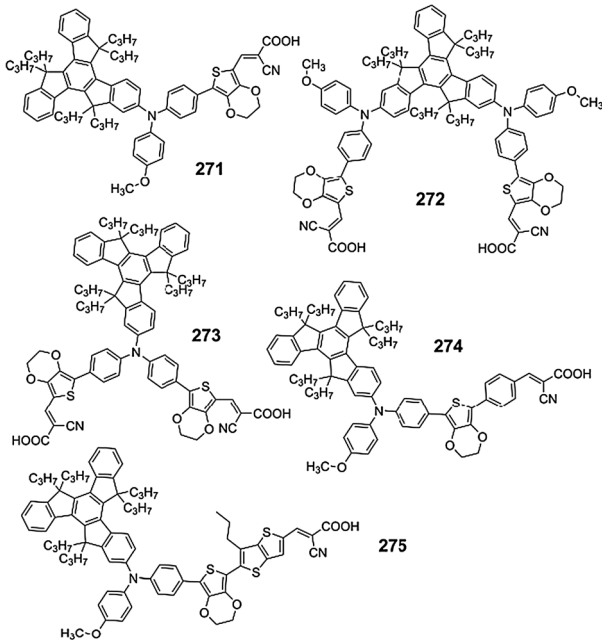

Fig. 34 Representative arylamine organic dyes **271–275** for DSCs employing cobalt electrolytes.

a CPDT bridging unit in the D–π–A structure, exhibited a J_{SC} that is 40% higher than **75**, reaching almost 15 mA cm^{-2} under full sunlight and an unprecedented PCE of up to 9.6% with the $[Co(II)(bpy)_3](B(CN)_4)_2/[Co(III)(bpy)_3](B(CN)_4)_3$ (bpy = 2,2′-bipyridine) redox couple.[219] Later they improved the result by using a tridentate cobalt $[Co(II)(bpy\text{-}pz)_2](PF_6)_2/[Co(III)(bpy\text{-}pz)_2](PF_6)_3$ (bpy-pz = 6-(1*H*-pyrazol-1-yl)-2,2′-bipyridine) complex as a redox mediator. Dye **269** yielded a power conversion efficiency of over 10% at 100 mW cm^{-2} with an unprecedented output voltage exceeding 1000 mV owing to its high oxidation potential of 0.86 V *versus* NHE.[220]

Han and co-workers developed a novel 4,4-ethylenedioxy-4*H*-cyclopenta[2,1-*b*:3,4-*b*′]dithiophene-based D–π–A organic dye (**270**, Fig. 33) and introduced it into a DSC with a $[Co(II)(bpy)_3](PF_6)_2/[Co(III)(bpy)_3](PF_6)_3$ based redox system.[222] It is noteworthy that the IPCE response of the **270**-based cell extended to 820 nm. Finally, **270**-sensitized DSC with a cobalt electrolyte showed an overall conversion efficiency of 4.04%, which was 1.65 times that observed with an iodine electrolyte.

In our development of truxene-based dyes, we noticed that these dyes pose high extinction coefficients apart from their retarding charge recombination, benefiting from the steric hindrance of the hexapropyltruxene group. These features are necessary for organic dyes used in DSCs employing cobalt electrolytes. It is therefore expected that this type dye could show interesting performance in the cobalt redox couple system. Five truxene-based dyes were designed and synthesized (**271–275**, Fig. 34). **272** ($\varepsilon = 8.9 \times 10^4$ M^{-1} cm^{-1}; V_{OC} = 865 mV) with 2(D–π–A) structure and **273** ($\varepsilon = 10.7 \times 10^4$ M^{-1} cm^{-1}; V_{OC} = 870 mV) with D–2(π–A) structure confer an enhanced light absorption coefficient of a stained TiO_2 film and provide an improved V_{OC} in DSCs employing a cobalt redox electrolyte in comparison to **271** ($\varepsilon = 6.4 \times 10^4$ M^{-1} cm^{-1}; V_{OC} = 830 mV) with a D–π–A structure.[223] However, the **271**-sensitized cell exhibited a higher efficiency with respect to those of **272** and **273**, which is primarily due to its superior IPCE. Optimization of DSCs sensitized with **271** in combination with a cobalt electrolyte (0.25 M $[Co(II)(phen)_3](PF_6)_2$, 0.05 M $[Co(III)(phen)_3](PF_6)_3$, 0.5 M 4-tertpyridine (TBP) and 0.1M LiTFSI in acetonitrile) yielded a DSC with a PCE of 7.2% under AM 1.5 irradiation (100 mW cm^{-2}). This work illustrated the importance of introducing sterically bulky groups on the dyes that block the TiO_2 surface from Co(III) species in the electrolyte in DSCs.

We also found that organic dyes with thiophene derivates as linkers are suitable for cobalt DSCs. Dye alteration from **274** to **275** in the iodine cells caused a PCE attenuation of 0.5% (6.1% *vs.* 5.6%), sharply contrasting the 1.4% enhancement (5.5% *vs.* 6.9%) in the cobalt cells (with 0.5 M TBP).[224] Under the optimized conditions, the cobalt electrolyte containing 0.8 M TBP gave the highest efficiency. The lower rate of electron recapture by $[Co(III)(phen)_3]$ for the **275**-sensitized nanocrystalline TiO_2

film allows a high V_{OC} to be realized, with this sensitizer reaching a value of 900 mV in full sunlight without sacrificing J_{SC} or FF. The cumulative increases of J_{SC} or FF gave rise to an efficiency of 7.6% at AM 1.5 irradiation (100 mW cm^{-2}). Our results strongly indicate that the application of truxene-based organic dyes as the photosensitizers in DSCs employing a cobalt electrolyte is promising. Though the efficiency from truxene-based dyes is not satisfying at the current stage, there is much space left for further improvement by enhancing the light harvesting ability to increase the J_{SC} and finding more appropriate cobalt electrolytes to increase the V_{OC}.

12. Exploiting new acceptors for arylamine organic dyes

The acceptor part of a dye behaves as both an electron acceptor, in the charge transfer process from the donor, and as an anchoring group to adsorb onto the TiO_2 surfaces, which is essential for the efficient electron injection from the dye into the TiO_2.[225] Typical acceptors includes cyanoacrylic acid, rhodamine-, and thiazolidinorhodamine-*N*-carboxylic acid moieties. Interesting works to exploit new anchoring groups with strong electron-withdrawing ability have been carried out,[225–233] but they are still limited.

Harima and co-workers have designed and synthesized fluorescent dyes **278–280** (Fig. 35) with a pyridine ring as the electron-withdrawing anchoring group of these new D–π–A dye sensitizers for DSCs.[226,227] The J_{SC} (5.63 to 7.04 mA cm^{-2}) and PCE (1.84 to 2.35%) of DSCs based on the three dyes are greater than those of the conventional D–π–A dye sensitizers **276** (J_{SC} = 2.96 mA cm^{-2}; PCE = 0.91%) and **277** (J_{SC} = 3.07 mA cm^{-2}; PCE = 0.97%) with a carboxyl group as the electron-withdrawing anchoring group. It was demonstrated that the formation of coordinate bonds between the pyridine ring of dyes **278–280** and the Lewis acid sites of the TiO_2 surface leads to an efficient electron injection owing to the good electron communication between them, rather than the formation of an ester linkage between dyes **276** and **277** and the Brønsted acid sites of the TiO_2 surface. This work suggested that the pyridine ring acted not only as the electron-withdrawing anchoring group but also as the electron-injecting group in a D–π–A dye.

Han and co-workers have developed a new method to introduce various electron-withdrawing groups as the acceptor part of D–π–A dyes for the free exploration of acceptor designs. **281**, **282** and **283** (Fig. 35) displayed absorption maxima at around 420 nm with strong extinction coefficients. The DSCs fabricated with these three dyes exhibited efficiencies of 2.51% to 4.05%.[225]

Katono *et al.* designed and synthesized a series of new organic sensitizers with cyano substituted benzoic acid as an acceptor/anchoring group (**284–286**, Fig. 35).[228] They found that the cyano substituent showed an improved DSC performance. The DSC device based on **286**, with a *para*-cyano benzoic acid as the acceptor/anchoring group, revealed a performance with a maximum IPCE of 80% and a PCE of 4.5% at AM 1.5 irradiation (100 mW cm^{-2}).

Yang, Sun and co-workers have successfully synthesized a series of iso-quinoline cationic organic dyes in the absence of a vinyl group for DSCs.[229] The dye **287** (Fig. 35, J_{SC} = 14.4 mA cm^{-2}, V_{OC} = 684 mV and FF = 0.74) showed an efficiency of 7.3% while **N719** yielded an efficiency of 7.9%. Unlike other ionic sensitizers (such as **67** and **68**), **287** did not suffer from low V_{OC}. This indicates that long alkyl chains are indispensable for ionic sensitizers.

Importantly, Hua, Tian and co-workers demonstrated that the electron acceptor 2-(1,1-dicyanomethylene) rhodanine is a promising alternative anchoring group to cyanoacrylic acid for sensitizing dyes.[230] The formation of coordinate bonds between the O and N in the middle acceptor rhodanine of **288** (Fig. 35) tautomers and the Lewis acid sites of the TiO_2 surface guarantees an efficient electron injection from the dyes to TiO_2. **288** based DSCs have obtained a PCE of 7.11%, which is considerably higher than the dye with cyanoacrylic acid as the electron acceptor (**54**, PCE = 6.39%).

Besides the development of new methods to introduce various electron-withdrawing groups as the acceptor part of D–π–A dyes, it is valuable to note that computational chemistry has been used to introduce an element of design in the systematic exploration. Labat *et al.* proposed that model systems containing only the relevant anchoring group and the semiconductor can be used to screen the different adsorption modes of the dye on the surface at low computational cost, since in most cases the anchoring group is electronically and geometrically decoupled from the rest of the dye.[231]

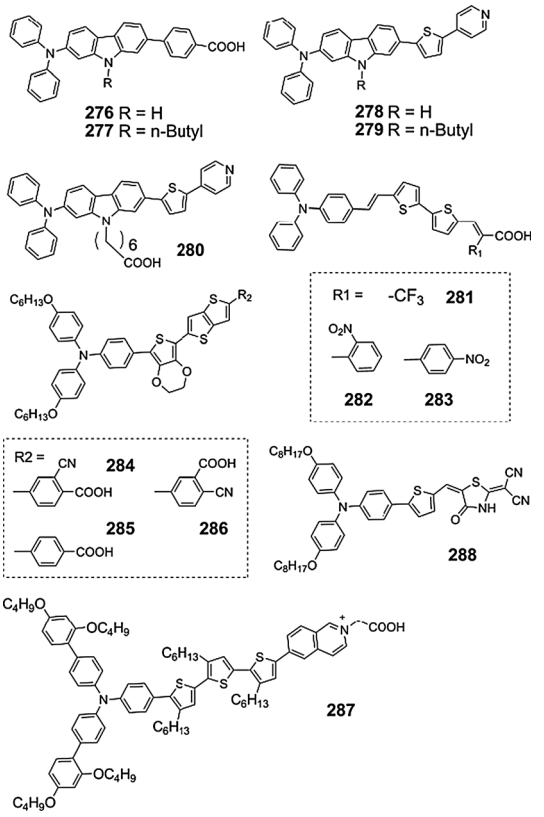

Fig. 35 Representative arylamine organic dyes **276–288** with new acceptors.

Recently, Troisi and co-workers developed a computational procedure to screen the many different anchoring groups used or usable to connect a dye to the semiconducting surface in a dye-sensitized solar cell. The procedure led to a clear identification of the anchoring groups that bind strongly to the surface and facilitate the electron injection at the same time, providing clear-cut indications for the design of new dyes.[232]

13. Arylamine organic compounds as solid-state hole transport materials (HTMs)

As discussed in Section 11, some disadvantages of the iodide/triiodide redox couple have limited the performance of DSCs. In an effort to address these issues, solid-state HTMs with optimized HOMO levels have been the focus of many recent reports. To date, the best performance in such solid-state DSCs (ssDSCs) is based on the HTM termed 2,2′,7,-7′-tetrakis(*N*,*N*-di-*p*-methoxyphenylamine)-9,9′-spirobifluorene (spiro-OMeTAD, **289**, Fig. 36)[234] with an efficiency up to 6.1% using custom synthesized dyes.[235]

Sellinger and co-workers synthesized two new HTMs (**290** and **291**, Fig. 36) for application in ssDSCs.[236] The new HTMs have low glass transition temperatures, low melting points, and high solubility, which makes them promising candidates for increased pore filling into mesoporous titania films. The experimental data demonstrated the superior performance of one of the new HTMs (**291**, PCE = 2.3%) in thicker ssDSCs (6 μm) compared to **289** (PCE = 2.1%).

Johansson *et al.* showed that a small hole-conductor molecule (**292**, Fig. 36) can be used to regenerate the dye molecules in a thick mesoporous electrode of TiO_2.[237] They found that the device efficiency could be improved by employing a combination of **292** and a conducting polymer (P3HT). This addition was thought to enable better transport of the charges to the contact and to reduce recombination and, therefore, increase the photocurrent. They proposed that this device construction with a small hole-conductor regenerating the dye molecules in the small pores and a larger conducting polymer that conducts the holes to the silver contact is promising for further improvement of the ssDSCs.

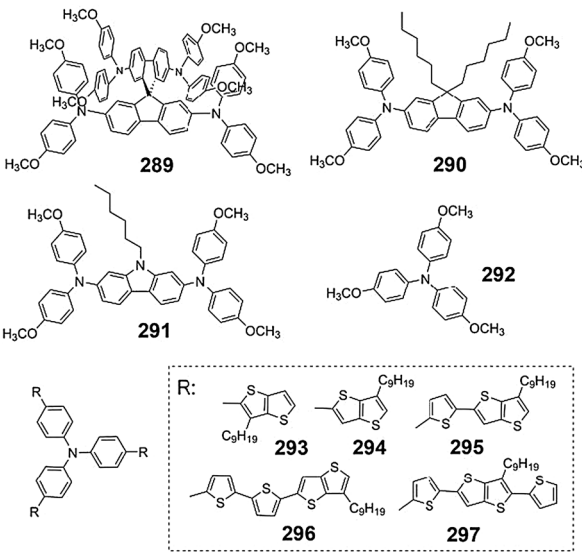

Fig. 36 Representative arylamine organic compounds as solid state hole transport materials.

Metri *et al.* developed five star-shaped π-conjugated molecules (**293–297**, Fig. 36) with a TPA core and various conjugated linkers such as thiophene and thieno[3,2-*b*]–thiophene–C_9H_{19}.[238] They proposed that the compounds **295**, **296** and **297** possess interesting hole-transporting properties and could be good candidates for use in hybrid solar cells.

14. Summary of performance

In summary, we have outlined the development and accomplishments of major types of arylamine-based organic dyes for DSCs. The photophysical properties and cell performance of these sensitizers are summarized for comprehensive comparison, as well as to provide an overview of the field. Detailed cell parameters are summarized in Table 1 (DSCs employing iodine electrolytes) and Table 2 (DSCs employing cobalt electrolytes).

DSCs based on arylamine organic dyes have reached PCE values over 10%, comparable to those of Ru complexes (PCE = 10–11%). The best PCE values of DSCs based on the arylamine-based organic dyes mentioned in this review are as follows: TPA dyes (8.22% for **20**,[31] iodine electrolyte), substituted TPA dyes (10.3% for **60**,[63] iodine electrolyte; over 10% for **266**, **268** and **269**,[217] cobalt electrolyte), branched TPA dyes (7.2% for **92**,[101] iodine electrolyte), fluorene based triarylamine dyes (9.1% for **120**,[114] iodine electrolyte), naphthalene based triarylamine dyes (7.08% for **131**,[129] iodine electrolyte), truxene based triarylamine dyes (6.18% for **158**,[142] iodine electrolyte; 7.6% for **275**,[224] cobalt electrolyte), indoline dyes (9.52% for **164**[146] and 9.04% for **170**,[152] iodine electrolyte), *N*,*N*-dialkylaniline dyes (6.8% for **185**,[163] iodine electrolyte), tetrahydroquinoline dyes (5.1% for **198**,[169] iodine electrolyte), phenothiazine dyes (7.78% for **224**,[183] iodine electrolyte), phenoxazine dyes (7.4% for **234**,[186] iodine electrolyte), and carbazole dyes (8.3% for **238**,[190] iodine electrolyte). These results proved that the rational design of the molecular structure contributes significantly to the performance of arylamine organic dyes. It is thus that some basic guidelines and strategies are outlined for the future design of higher performance sensitizers.

1. Strategies for extending the spectral response region of the sensitizer include the following points. (i) Multiple strongly electron-donating substituents at the arylamine core could induce a bathochromic shift in the absorption spectrum due to the increasing donation from the amino moieties.[50,53,77,88,141,161,186] (ii) Planarization of the donor has proven powerful in extending the red light response of the sensitizer.[20,99,100,150] (iii) The extension of a conjugated bridge by the introduction of strong electron-donating units[22,30,66–68,177] (*e.g.*, thiophene derivatives) or electron-withdrawing units[34,45,46,50,83,84,150] (*e.g.*, benzothiadiazole) significantly contributes to a red shift in the absorption spectra. However, we should bear in mind that organic dyes with an elongation of the π-conjugated linker

Table 1 Arylamine organic dyes tested in DSCs employing liquid iodine electrolytes

Dye	λ_{max}/nm	J_{SC}/mA cm^{-2}	V_{OC}/mV	FF	PCE(%)	Ref.
1	386	6.3	770	0.67	3.3	21
2	417	11.1	730	0.66	5.3	21
3	438	10.39	702	0.785	5.73	22
4	438	7.72	694	0.803	4.3	22
5	490	12.41	663	0.760	6.25	22
6	457	9.60	671	0.776	5.0	22
7	418	8.78	726	0.807	5.14	23
8	464	11.7	766	0.756	6.78	23
9	441	9.4	668	0.69	4.36	24
10	444	8.1	704	0.68	3.86	24
11	500	1.3	480	0.70	0.44	24
12	425	8.1	630	0.68	3.49	24
13	433	13.83	677	0.692	6.49	26
14	—	11.1	585	0.59	3.86	19
15	410	12.8	620	0.66	5.20	30
16	426	15.5	690	0.683	7.30	30
17	420	10.7	750	0.668	5.36	30
18	420	14.73	754	0.65	7.25	31
19	440	15.78	735	0.60	7.00	31
20	420	15.58	787	0.67	8.22	31
21	472	9.38	720	0.64	4.36	32
22	503	10.33	797	0.64	5.30	32
23	435	10.1	750	0.75	5.7	33
24	465	11.9	720	0.73	6.3	33
25	525	5.70	735	0.78	3.27	34
26	362	14.6	676	0.75	7.40	34
27	489	14.4	697	0.73	7.3	35
28	477	14.2	765	0.66	7.17	36
29	465	13.5	715	0.65	6.27	36
30	443	13.97	670	0.62	5.8	37
31	510	12.66	610	0.56	4.4	37
32	469	16.59	690	0.64	7.36	40
33	456	14.16	680	0.66	6.30	40
34	437	13.47	600	0.59	4.77	41
35	472	14.20	570	0.60	4.79	41
36	425	11.29	710	0.65	5.22	42
37	491	10.44	546	0.66	3.77	43
38	502	8.35	524	0.67	2.91	43
39	501	15.2	670	0.66	6.72	44
40	557	16.46	545	0.67	6.04	45
41	625	16.24	480	0.68	5.30	46
42	596	11.29	470	0.69	3.66	46
43	504	11.79	680	0.65	5.30	47
44	457	11.78	810	0.60	5.73	48
45	470	15.69	778	0.61	7.51	49
46	433	12.47	789	0.61	6.01	49
47	563	9.89	559	0.64	3.52	50
48	458	13.0	564	0.59	4.32	53
49	461	18.2	563	0.57	5.84	53
50	486	9.01	631	0.72	4.11	15
51	510	9.89	534	0.66	3.49	15
52	444	8.12	715	0.68	3.94	15
53	486	11.40	692	0.72	5.70	15
54	514	11.88	775	0.747	6.88	65
55	516	13.9	731	0.740	7.54	64
56	524	15.2	720	0.733	8.02	66
57	552	16.1	803	0.759	9.8	66
58	525	13.81	714	0.721	7.11	67
59	555	15.84	769	0.735	8.95	67
60	521	17.94	770	0.730	10.1	68
61	511	13.39	810	0.70	7.60	73
62	472	11.9	713	0.67	5.68	74
63	502	10.65	710	0.68	5.14	75
64	489	7.97	670	0.68	3.63	75
65	459	9.4	810	0.74	5.6	76
66	510	11.59	791	0.76	7.12	77
67	691	11.12	422	0.557	2.61	78
68	650	9.40	432	0.578	2.34	78
69	602	3.61	448	0.63	1.03	80

Table 1 (*continued*)

Dye	λ_{max}/nm	J_{SC}/mA cm^{-2}	V_{OC}/mV	FF	PCE(%)	Ref.
71	570	3.40	489	0.74	1.24	83
72	515	18.47	640	0.69	8.21	83
73	497	11.42	600	0.61	4.18	84
74	514	13.52	620	0.62	5.19	84
75	445	12.96	750	0.61	6.00	85
76	482	12.00	670	0.60	4.83	85
77	487	13.6	615	0.69	5.77	88
78	522	9.05	567	0.56	2.87	88
79	480	13.8	632	0.69	6.02	88
80	411	8.70	710	0.70	4.30	89
81	424	7.3	603	0.74	3.26	91
82	422	9.2	625	0.79	4.54	91
83	425	11.61	766	0.586	5.21	93
84	440	11.71	709	0.592	4.92	93
85	487	14.69	740	0.62	6.77	94
86	576	9.2	660	0.72	4.37	95
87	455	15.2	720	0.72	7.87	99
88	463	16.8	750	0.70	8.71	99
89	558	15.37	651	0.75	7.51	100
90	569	16.09	671	0.74	8.00	100
91	462	14.00	694	0.71	6.90	101
92	458	13.90	744	0.70	7.23	101
93	473	16.0	630	0.61	6.15	102
94	480	15.2	610	0.58	5.41	102
95	462	14.5	680	0.61	5.95	102
96	465	15.6	650	0.60	6.04	102
97	462	11.4	610	0.59	4.11	102
98	426	12.21	650	0.59	4.68	103
99	413	9.68	690	0.60	4.01	103
100	400	10.21	700	0.71	5.07	104
101	413	5.51	630	0.726	2.52	104
102	384	6.56	700	0.75	3.46	105
103	386	10.78	710	0.74	5.67	105
104	489	8.85	639	0.76	4.34	106
105	511	10.45	701	0.77	5.63	106
106	478	10.9	641	0.725	5.05	107
107	480	9.65	662	0.706	4.51	107
108	485	10.34	715	0.722	5.35	108
109	468	6.87	687	0.678	3.20	108
110	495	7.13	670	0.71	3.4	109
111	480	11.25	770	0.76	6.6	109
112	436	12.20	764	0.77	7.20	110
113	452	14.0	753	0.77	8.01	110
114	463	14.39	700	0.66	6.65	111
115	456	15.33	740	0.66	7.43	112
116	480	13.84	790	0.75	8.2	115
117	430	16.13	641	0.718	7.42	113
118	430	17.45	664	0.742	8.60	113
119	480	15.7	690	0.74	8.0	114
120	490	17.6	710	0.72	9.1	114
121	450	13.02	570	0.72	5.34	116
122	466	17.49	700	0.70	8.70	116
123	525	14.33	734	0.76	8.0	123
124	514	13.35	777	0.749	7.8	125
125	525	13.58	708	0.760	7.31	124
126	544	14.85	696	0.736	7.61	124
127	669	13.92	610	0.74	6.29	126
128	662	12.17	509	0.7936	4.91	127
129	534	17.10	610	0.72	7.51	128
130	468	14.80	740	0.74	8.19	128
131	422	16.81	740	0.57	7.08	129
132	427	15.36	690	0.50	5.25	129
133	409	12.28	730	0.67	6.0	130
134	424	11.28	700	0.66	5.23	130
135	441	10.5	595	0.70	4.36	131
136	447	10.4	571	0.69	4.11	131
137	458	17.04	650	0.61	6.72	132
138	460	15.48	690	0.65	6.87	132
139	458	15.16	680	0.68	7.00	132
140	442	9.32	580	0.70	3.37	132

Table 1 (*continued*)

Dye	λ_{max}/nm	J_{SC}/mA cm^{-2}	V_{OC}/mV	FF	PCE(%)	Ref.
141	433	10.55	660	0.65	4.46	133
142	437	11.34	700	0.67	5.27	133
143	430	14.16	650	0.65	5.95	82
144	414	7.16	640	0.67	3.04	136
145	517	14.0	627	0.745	6.6	135
146	500	13.9	618	0.717	6.2	135
147	406	7.75	689	0.73	3.90	139
148	420	7.89	731	0.74	4.27	139
149	430	6.86	752	0.70	3.61	139
150	383	10.13	750	0.72	5.45	140
151	383	7.31	760	0.66	3.64	140
152	398	9.71	690	0.69	4.62	140
153	388	5.53	670	0.67	2.48	140
154	486	9.8	750	0.67	4.92	141
155	498	10.7	745	0.66	5.26	141
156	506	11.5	772	0.68	6.04	141
157	498	10.4	763	0.67	5.32	142
158	519	11.8	771	0.68	6.18	142
159	491	17.76	604	0.57	6.1	143
160	526	18.75	645	0.538	6.51	144
161	532	17.50	584	0.538	5.50	144
162	531	17.38	628	0.513	5.60	144
163	—	19.56	569	0.533	5.93	144
164	532	18.56	717	0.716	9.52	146
165	567	13.07	660	0.65	5.55	148
166	486	10.58	650	0.69	4.72	155
167	533	17.7	650	0.76	8.70	150
168	547	14.3	639	0.75	6.85	151
169	557	10.4	629	0.71	4.64	151
170	536	18.00	696	0.72	9.04	152
171	496	13.18	780	0.78	8.02	153
172	495	13.39	680	0.74	6.74	153
173	442	10.06	748	0.68	5.11	155
174	526	13.40	760	0.73	7.43	156
175	433	8.23	727	0.71	4.26	157
176	385	5.10	772	0.732	2.88	158
177	386	8.23	767	0.735	4.64	158
178	643	13.64	480	0.57	3.75	159
179	440	15.1	640	0.63	6.20	160
180	491	11.63	639	0.68	5.08	161
181	504	15.29	627	0.72	6.84	161
182	523	18.53	649	0.71	8.49	161
183	454	10.4	710	0.74	5.5	163
184	465	9.9	740	0.74	5.4	163
185	501	12.9	710	0.74	6.8	163
186	469	12.5	680	0.69	5.9	163
187	488	15.23	560	0.73	6.23	165
188	513	10.64	520	0.70	3.87	165
189	464	12.33	642	0.64	5.08	20
190	450	11.46	643	0.66	4.93	20
191	521	13.7	606	0.69	5.7	166
192	491	15.2	605	0.68	6.3	166
193	468	8.48	583	0.64	3.17	167
194	441	11.20	600	0.67	4.49	167
195	462	12.00	597	0.63	4.53	167
196	455	10.00	537	0.64	3.44	167
197	610	11.76	464	0.674	3.7	168
198	615	13.35	519	0.73	5.1	169
199	452	10.9	712	0.71	5.5	171
200	481	4.8	532	0.74	1.9	171
201	568	14.4	390	0.54	3.0	172
202	472	3.87	698	0.65	1.8	173
203	462	12.52	675	0.693	7.3	174
204	469	14.96	675	0.682	6.8	174
205	473	15.18	645	0.69	6.72	175
206	496	11.69	708	0.653	5.4	176
207	508	7.14	706	0.556	2.80	176
208	442	12.18	771.7	0.7002	5.29	177
209	448	12.05	724.5	0.7233	6.32	177
210	466	11.68	745.7	0.6995	6.09	177
211	451	11.2	768	0.75	6.53	178

Table 1 (*continued*)

Dye	λ_{max}/nm	J_{SC}/mA cm^{-2}	V_{OC}/mV	FF	PCE(%)	Ref.
212	478	15.2	691	0.70	7.44	178
213	449	10.84	592	0.69	4.41	179
214	450	7.39	505	0.66	2.48	179
215	453	13.66	670	0.61	5.60	180
216	474	11.65	710	0.63	5.22	180
217	442	14.42	690	0.63	6.22	180
218	463	5.99	570	0.60	2.04	180
219	471	11.82	759	0.65	5.84	181
220	474	12.62	789	0.63	6.29	181
221	474	11.41	804	0.63	5.76	181
222	462	10.76	793	0.64	5.51	182
223	466	12.18	826	0.65	6.55	182
224	495	14.33	830	0.65	7.78	183
225	496	13.33	830	0.62	6.87	183
226	439	6.13	709	0.67	2.91	184
227	433	7.86	740	0.71	4.13	184
228	435	8.27	750	0.68	4.22	184
229	439	6.98	740	0.69	3.56	184
230	513	9.13	679	0.71	4.40	185
231	511	12.75	691	0.69	6.06	185
232	491	12.25	760	0.72	6.70	186
233	506	14.38	0.78	0.64	7.17	186
234	500	13.09	800	0.70	7.40	186
235	482	13.7	800	0.63	7.0	187
236	517	14.7	733	0.71	7.7	188
237	480	9.90	750	0.67	4.97	190
238	480	10.67	690	0.68	5.01	190
239	485	10.56	670	0.63	4.46	190
240	483	16.0	710	0.71	8.1	192
241	480	14.5	730	0.69	7.3	192
242	502	13.8	700	0.77	7.4	193
243	496	14.6	700	0.76	7.8	193
244	490	15.0	660	0.74	7.3	193
245	492	15.4	710	0.67	7.3	194
246	501	15.5	700	0.62	6.7	194
247	444	11.67	796	0.68	6.33	195
248	411	9.83	740	0.70	5.02	196
249	435	11.50	680	0.66	5.15	196
250	428	14.63	685	0.67	6.70	197
251	465	10.02	570	0.64	3.62	198
252	429	8.76	621	0.754	4.1	199
253	468	10.9	400	0.57	2.48	200
254	386	13.0	630	0.75	6.14	201
255	441	13.7	680	0.70	6.52	201
276	374	1.99	516	0.59	0.60	226
277	376	1.80	517	0.60	0.56	226
278	394	5.80	540	0.60	1.89	226
279	396	5.63	548	0.60	1.84	226
280	396	7.04	568	0.59	2.35	227
281	430	8.57	540	0.72	3.28	225
282	416	9.91	580	0.70	4.05	225
283	422	7.03	520	0.69	2.51	225
284	437	7.04	682	0.691	3.32	228
285	432	5.78	688	0.718	2.87	228
286	443	8.05	756	0.733	4.50	228
287	485	14.4	684	0.74	7.3	229
288	519	13.94	746	0.68	7.11	230

are liable to experience dye aggregation through strong intermolecular π–π interactions and charge recombination, which will bring down the electron injection efficiency and electron lifetime. It is very critical to balance between the light harvesting and cell performance of dyes. In addition, electron-donating and electron-withdrawing units as spacers have a profound effect on the molar extinction coefficient. Generally, the former evokes an improved ε, but the latter bring a lower ε.[150] (iv) A successful approach to obtain a

Table 2 Arylamine organic dyes tested in DSCs employing liquid cobalt electrolytes

Dye	λ_{max}/nm	J_{SC}/mA cm^{-2}	V_{OC}/mV	FF	PCE(%)	Ref.
75	—	10.7	920	0.68	6.7	208
59		13.3	950	0.74	9.3	214
256	497	10.54	950	0.77	7.7	213
257	504	12.05	930	0.75	8.4	213
258	503	11.41	870	0.77	7.6	213
259	429	6.91	1050	0.76	5.5	214
260	514	12.17	990	0.75	9.0	214
261	511	12.92	860	0.72	8.0	214
262	—	7.99	815	0.76	5.0	215
263	—	12.98	837	0.74	8.0	215
264	—	15.31	850	0.73	9.4	216
265	—	14.86	840	0.753	9.4	217
266	—	14.81	930	0.730	10.1	217
267	—	14.67	830	0.750	9.1	217
268	—	14.55	930	0.743	10.1	217
269	—	13.06	998	0.774	10.08	220
270	488	8.38	747	0.648	4.04	222
271	498	12.0	830	0.72	7.2	223
272	520	9.0	865	0.71	5.5	223
273	501	11.2	870	0.71	6.9	223
274	498	9.6	870	0.70	5.8	224
275	500	11.9	900	0.71	7.6	224

panchromatic response in the visible region is to employ ionic units such as squaraines.[78,80,126,127,159] The key issue to make the most of the advantage of ionic sensitizers is to avoid their V_{OC} defects.[81,82] (v) An anchoring group with a strong electron-withdrawing ability is effective for bathochromic shift of the absorption spectra.[55,144,230]

2. Apart from the good spectral response, the suppression of charge recombination and dye aggregation are necessary for achieving high J_{SC}. DCA or CDCA have been proven to prevent aggregation and hence to improve the photovoltaic performance by means of improving both J_{SC} and V_{OC}.[86,150] However, improved dye design incorporating the properties of a coadsorbent into the dye structure is important for the future economization of cost and simplification of the coadsorbent-free DSCs assembly process.[86] Thus, the strategic structural modification of organic sensitizers through the introduction of sterically hindered substituents (bulky groups) such as long alkyl chains and aromatic units onto the donors[68,86,99,116,137–142,182,183,186] or π-bridges[67,77,113,114,146,152,153,173,189–194] are indispensable. It is necessary to point out that having a 3D structure to increase the distance between dyes and acceptors is important to increase the electron lifetime and, hence, V_{OC}. A twisted structure on the spacer may induce a blue-shift of the absorption maximum because a larger energy is necessary to undergo an intramolecular charge transfer. In contrast, a twisted structure on the end of dyes is preferred because a high V_{OC} can be realized without sacrificing light harvesting and, hence, J_{SC}. Furthermore, D–π–A branched dyes are favorable to reduce intermolecular interaction and retard charge recombination.[101–109]

3. The exploration of arylamine organic dyes for iodine-free DSCs brought forth a new opportunity for the efficiency enhancement of DSCs. Photosensitizers with high extinction coefficients, suitable electronic structures and steric properties are warranted.[208–224]

15. Conclusions

The development of arylamine organic dyes for DSCs including triphenylamine (TPA) dyes, substituted TPA dyes, triarylamine dyes (fluoren-substituted aniline dyes, truxene-substituted aniline dyes and naphthalene-substituted aniline dyes), *N*,*N*-dialkylaniline dyes, tetrahydroquinoline dyes, indoline dyes, phenothiazine (PTZ)/phenoxazine (POZ) dyes and carbazole dyes has been summarized. Some basic design rationales of arylamine organic dyes and information about the relationship between the chemical structures and photovoltaic performance of DSCs have also been presented. Arylamine organic dyes have exhibited an especially excellent performance and are regarded as one of the most promising classes of organic sensitizers. It should be noted, however, that it is still challenging for arylamine organic dyes to achieve higher efficiency. The further investigations include: (1) the discovery of panchromatic arylamine organic dyes possessing broad absorption characteristics extending throughout the visible and NIR regions; (2) the exploration of arylamine organic dyes to match suitable iodine-free redox couples; (3) a deeper understanding of the essential processes based on experiments and computational chemistry. New breakthroughs would be expected through the design of new photosensitizers with high extinction coefficients, suitable electronic structures and steric properties based on fundamental insights into the interface processes.

Acknowledgements

The authors acknowledge financial support from the National MOST (2011CBA00702, 2011CB935900, 2012AA051901), NSFC (21003096), and 111 Project (B12015).

Notes and references

1 B. O'Regan and M. Gratzel, *Nature*, 1991, **353**, 737–740.
2 A. Yella, H. W. Lee, H. N. Tsao, C. Yi, A. K. Chandiran, M. K. Nazeeruddin, E. W. G. Diau, C. Y. Yeh, S. M. Zakeeruddin and M. Grätzel, *Science*, 2011, **334**, 629–634.
3 M. Grätzel, *J. Photochem. Photobiol., C*, 2003, **4**, 145–153.
4 A. Hagfeldt, G. Boschloo, L. Sun, L. Kloo and H. Pettersson, *Chem. Rev.*, 2010, **110**, 6595–6663.
5 K. Hara, T. Sato, R. Katoh, A. Furube, Y. Ohga, A. Shinpo, S. Suga, K. Sayama, H. Sugihara and H. Arakawa, *J. Phys. Chem. B*, 2003, **107**, 597–606.
6 S. Wenger, P. A. Bouit, Q. Chen, J. Teuscher, D. Di Censo, R. Humphry-Baker, J. E. Moser, J. L. Delgado, N. Martin, S. M. Zakeeruddin and M. Grätzel, *J. Am. Chem. Soc.*, 2010, **132**, 5164–5169.
7 J. H. Yum, E. Baranoff, S. Wenger, Md. K. Nazeeruddin and M. Grätzel, *Energy Environ. Sci.*, 2011, **4**, 842–857.
8 A. Hagfeldt, G. Boschloo, L. Sun, L. Kloo and H. Pettersson, *Chem. Rev.*, 2010, **110**, 6595–6663.

9 W. Zeng, Y. Cao, Y. Bai, Y. Wang, Y. Shi, M. Zhang, F. Wang, Y. Pan and P. Wang, *Chem. Mater.*, 2010, **22**, 1915–1925.
10 H. Yan, P. Lee, N. R. Armstrong, A. Graham, G. A. Evmenenko, P. Dutta and T. J. Marks, *J. Am. Chem. Soc.*, 2005, **127**, 3172–3183.
11 B. Lim, Y. C. Nah, J. T. Hwang, J. Ghim, D. Vak, J. M. Yuna and D. Y. Kim, *J. Mater. Chem.*, 2009, **19**, 2380–2385.
12 H. J. Snaith, *Adv. Funct. Mater.*, 2010, **20**, 13–19.
13 H. N. Tian and L. C. Sun, *J. Mater. Chem.*, 2011, **21**, 10592–10601.
14 X. F. Wang, H. Tamiaki, L. Wang, N. Tamai, O. Kitao, H. S. Zhou and S. I. Sasaki, *Langmuir*, 2010, **26**, 6320–6327.
15 Y. Liang, B. Peng and J. Chen, *J. Phys. Chem. C*, 2010, **114**, 10992–10998.
16 Z. S. Wang, T. Yamaguchi, H. Sugihara and H. Arakawa, *Langmuir*, 2005, **21**, 4272–4276.
17 A. Usami, S. Seki, Y. Mita, H. Kobayashi, H. Miyashiro and N. Sol. Terada, *Sol. Energy Mater. Sol. Cells*, 2009, **93**, 840–842.
18 D. Zhou, Q. Yu, N. Cai, Y. Bai, Y. Wang and P. Wang, *Energy Environ. Sci.*, 2011, **4**, 2030–2034.
19 T. Marinado, K. Nonomura, J. Nissfolk, M. K. Karlsson, D. P. Hagberg, L. C. Sun, S. Mori and A. Hagfeldt, *Langmuir*, 2010, **26**, 2592–2598.
20 B. Liu, W. H. Zhu, Q. Zhang, W. J. Wu, M. Xu, Z. J. Ning, Y. S. Xie and H. Tian, *Chem. Commun.*, 2009, 1766–1768.
21 T. Kitamura, M. Ikeda, K. Shigaki, T. Inoue, N. A. Anderson, X. Ai, T. Q. Lian and S. Yanagida, *Chem. Mater.*, 2004, **16**, 1806–1812.
22 C. Teng, X. C. Yang, C. Yang, H. N. Tian, S. F. Li, X. N. Wang, A. Hagfeldt and L. C. Sun, *J. Phys. Chem. C*, 2010, **114**, 11305–11313.
23 C. Teng, X. C. Yang, C. Yang, S. F. Li, M. Cheng, A. Hagfeldt and L. C. Sun, *J. Phys. Chem. C*, 2010, **114**, 9101–9110.
24 H. N. Tian, X. C. Yang, R. K. Chen, R. Zhang, A. Hagfeldt and L. C. Sun, *J. Phys. Chem. C*, 2008, **112**, 11023–11033.
25 S. Hwang, J. H. Lee, C. Park, H. Lee, C. Kim, C. Park, M. H. Lee, W. Lee, J. Park, K. Kim, N. G. Park and C. Kim, *Chem. Commun.*, 2007, 4887–4889.
26 H. Im, S. Kim, C. Park, S. H. Jang, C. J. Kim, K. Kim, N. G. Park and C. Kim, *Chem. Commun.*, 2010, **46**, 1335–1337.
27 K. Hara, M. Kurashige, Y. Dan-oh, C. Kasada, A. Shinpo, S. Suga, K. Sayama and H. Arakawa, *New J. Chem.*, 2003, **27**, 783–785.
28 D. P. Hagberg, T. Marinado, K. M. Karlsson, K. Nonomura, P. Qin, G. Boschloo, T. Brinck, A. Hagfeldt and L. C. Sun, *J. Org. Chem.*, 2007, **72**, 9550–9556.
29 D. P. Hagberg, T. Edvinsson, T. Marinado, G. Boschloo, A. Hagfeldt and L. C. Sun, *Chem. Commun.*, 2006, 2245–2247.
30 W. H. Liu, I. C. Wu, C. H. Lai, C. H. Lai, P. T. Chou, Y. T. Li, C. L. Chen, Y. Y. Hsu and Y. Chi, *Chem. Commun.*, 2008, 5152–5154.
31 B. S. Chen, D. Y. Chen, C. L. Chen, C. W. Hsu, H. C. Hsu, K. L. Wu, S. H. Liu, P. T. Chou and Y. Chi, *J. Mater. Chem.*, 2011, **21**, 1937–1945.
32 Y. Liang, B. Peng, J. Liang, Z. Tao and J. Chen, *Org. Lett.*, 2010, **12**, 1204–1207.
33 J. I. Nishida, T. Masuko, Y. Cui, K. Hara, H. Shibuya, M. Ihara, T. Hosoyama, R. Goto, S. Mori and Y. Yamashita, *J. Phys. Chem. C*, 2010, **114**, 17920–17925.
34 X. Lu, Q. Feng, T. Lan, G. Zhou and Z. S. Wang, *Chem. Mater.*, 2012, **24**, 3179–3187.
35 T. H. Kwon, V. Armel, A. Nattestad, D. R. MacFarlane, U. Bach, S. J. Lind, K. C. Gordon, W. H. Tang, D. J. Jones and A. B. Holmes, *J. Org. Chem.*, 2011, **76**, 4088–4093.
36 E. Kozma, I. Concina, A. Braga, L. Borgese, L. E. Depero, A. Vomiero, G. Sberveglieri and M. Catellani, *J. Mater. Chem.*, 2011, **21**, 13785–13788.
37 C. G. Wu, M. F. Chung, H. H. G. Tsai, C. J. Tan, S. C. Chen, C. H. Chang and T. W. Shih, *ChemPlusChem*, 2012, **77**, 832–843.
38 P. Shen, Y. H. Tang, S. H. Jiang, H. J. Chen, X. Y. Zheng, X. Y. Wang, B. Zhao and S. T. Tan, *Org. Electron.*, 2011, **12**, 125–135.
39 G. Zhou, N. Pschirer, J. C. Schoneboom, F. Eickemeyer, M. Baumgarten and K. Mullen, *Chem. Mater.*, 2008, **20**, 1808–1815.
40 J. T. Lin, P. C. Chen, Y. S. Yen, Y. C. Hsu, H. H. Chou and P. M. C. Yeh, *Org. Lett.*, 2009, **11**, 97–100.
41 Y. S. Yen, Y. C. Hsu, J. T. Lin, C. W. Chang, C. P. Hsu and D. J. Yin, *J. Phys. Chem. C*, 2008, **112**, 12557–12567.
42 Q. Q. Li, J. Shi, H. Y. Li, S. Li, C. Zhong, F. L. Guo, M. Peng, J. L. Hua, J. G. Qina and Z. Li, *J. Mater. Chem.*, 2012, **22**, 6689–6696.
43 M. Velusamy, K. R. J. Thomas, J. T. Lin, Y. C. Hsu and K. C. Ho, *Org. Lett.*, 2005, **7**, 1899–1902.
44 H. H. Chou, Y. C. Chen, H. J. Huang, T. H. Lee, J. T. Lin, C. T. Tsai and K. Chen, *J. Mater. Chem.*, 2012, **22**, 10929–10938.
45 Z. M. Tang, T. Lei, K. J. Jiang, Y. L. Song and J. Pei, *Chem.–Asian J.*, 2010, **5**, 1911–1917.
46 X. F. Lu, G. Zhou, H. Wang, Q. Y. Feng and Z. S. Wang, *Phys. Chem. Chem. Phys.*, 2012, **14**, 4802–4809.
47 J. Shi, J. N. Chen, Z. F. Chai, H. Wang, R. L. Tang, K. Fan, M. Wu, H. W. Han, J. G. Qin, T. Y. Peng, Q. Q. Li and Z. Li, *J. Mater. Chem.*, 2012, **22**, 18830–18838.
48 J. X. He, W. J. Wu, J. L. Hua, Y. H. Jiang, S. Y. Qu, J. Li, Y. T. Long and H. Tian, *J. Mater. Chem.*, 2011, **21**, 6054–6062.
49 J. X. He, F. L. Guo, X. Li, W. J. Wu, J. B. Yang and J. L. Hua, *Chem.–Eur. J.*, 2012, **18**, 7903–7915.
50 W. Ying, F. Guo, J. Li, Q. Zhang, W. Wu, H. Tian and J. Hua, *ACS Appl. Mater. Interfaces*, 2012, **4**, 4215–4224.
51 J. S. Song, F. Zhang, C. H. Li, W. L. Liu, B. S. Li, Y. Huang and Z. S. Bo, *J. Phys. Chem. C*, 2009, **113**, 13391–13397.
52 D. W. Chang, H. J. Lee, J. H. Kim, S. Y. Park, S. M. Park, L. M. Dai and J. B. Baek, *Org. Lett.*, 2011, **13**, 3880–3883.
53 M. Liang, W. Xu, F. S. Cai, P. Q. Chen, B. Peng, J. Chen and Z. M. Li, *J. Phys. Chem. C*, 2007, **111**, 4465–4472.
54 W. Xu, B. Peng, J. Chen, M. Liang and F. S. Cai, *J. Phys. Chem. C*, 2008, **112**, 874–880.

55 W. Xu, J. Pei, J. F. Shi, S. J. Peng and J. Chen, *J. Power Sources*, 2008, **183**, 792–798.
56 J. Pei, S. J. Peng, J. F. Shi, Y. L. Liang, Z. L. Tao, J. Liang and J. Chen, *J. Power Sources*, 2009, **187**, 620–626.
57 J. Shi, L. Wang, Y. Liang, S. Peng, F. Cheng and J. Chen, *J. Phys. Chem. C*, 2010, **114**, 6814–6821.
58 J. Shi, S. Peng, J. Pei, Y. Liang, F. Cheng and J. Chen, *ACS Appl. Mater. Interfaces*, 2009, **1**, 944–950.
59 M. Liang, X. Zong, H. Han, C. Chen, Z. Sun and S. Xue, *Mater. Lett.*, 2011, **65**, 1331–1333.
60 Y. Xu, M. Liang, X. Liu, H. Han, Z. Sun and S. Xue, *Synth. Met.*, 2011, **161**, 496–503.
61 J. Wiberg, T. Marinado, D. P. Hagberg, L. C. Sun, A. Hagfeldt and B. J. Albinsson, *J. Phys. Chem. C*, 2009, **113**, 3881–3886.
62 B. Peng, S. Yang, L. Li, F. Cheng and J. Chen, *J. Chem. Phys.*, 2010, **132**, 034305.
63 M. F. Xu, R. Z. Li, N. Pootrakulchote, D. Shi, J. Guo, Z. H. Yi, S. M. Zakeeruddin, M. Grätzel and P. Wang, *J. Phys. Chem. C*, 2008, **112**, 19770–19776.
64 G. L. Zhang, Y. Bai, R. Z. Li, D. Shi, S. Wenger, S. M. Zakeeruddin, M. Grätzel and P. Wang, *Energy Environ. Sci.*, 2009, **2**, 92–95.
65 R. Z. Li, X. J. Lv, D. Shi, D. F. Zhou, Y. M. Cheng, G. L. Zhang and P. Wang, *J. Phys. Chem. C*, 2009, **113**, 7469–7479.
66 G. L. Zhang, H. Bala, Y. M. Cheng, D. Shi, X. J. Lv, Q. J. Yu and P. Wang, *Chem. Commun.*, 2009, 2198–2200.
67 R. Z. Li, J. Y. Liu, N. Cai, M. Zhang and P. Wang, *J. Phys. Chem. B*, 2010, **114**, 4461–4464.
68 W. Zeng, Y. Cao, Y. Bai, Y. Wang, Y. Shi, M. Zhang, F. Wang, C. Pan and P. Wang, *Chem. Mater.*, 2010, **22**, 1915–1925.
69 J. Y. Liu, R. Z. Li, X. Y. Si, D. F. Zhou, Y. S. Shi, Y. H. Wang, X. Y. Jing and P. Wang, *Energy Environ. Sci.*, 2010, **3**, 1924–1928.
70 J. Y. Liu, D. F. Zhou, F. F. Wang, F. Fabregat-Santiago, S. G. Miralles, X. Y. Jing, J. Bisquert and P. Wang, *J. Phys. Chem. C*, 2011, **115**, 14425–14430.
71 J. Y. Liu, D. F. Zhou, M. F Xu, X. Y. Jing and P. Wang, *Energy Environ. Sci.*, 2011, **4**, 3545–3551.
72 D. F. Zhou, N. Cai, H. J. Long, M. Zhang, Y. G. Wang and P. Wang, *J. Phys. Chem. C*, 2011, **115**, 3163–3171.
73 L. Y. Lin, C. H. Tsai, K. T. Wong, T. W. Huang, L. Hsieh, S. H. Liu, H. W. Lin, C. C. Wu, S. H. Chou, S. H. Chen and A. I. Tsai, *J. Org. Chem.*, 2010, **75**, 4778–4785.
74 X. Hao, M. Liang, X. Cheng, X. Pian, Z. Sun and S. Xue, *Org. Lett.*, 2011, **13**, 5424–5427.
75 E. Longhi, A. Bossi, G. Di Carlo, S. Maiorana, F. De Angelis, P. Salvatori, A. Petrozza, M. Binda, V. Roiati, P. R. Mussini, C. Baldoli and E. Licandro, *Eur. J. Org. Chem.*, 2013, 84–94.
76 P. Gao, H. N. Tsao, M. Grätzel and M. K. Nazeeruddin, *Org. Lett.*, 2012, **14**, 4330–4333.
77 X. Zhu, H. Tsuji, A. Yella, A. S. Chauvin, M. Grätzel and E. Nakamura, *Chem. Commun.*, 2013, **49**, 582–584.
78 J. Y. Li, C. Y. Chen, C. P. Lee, S. C. Chen, T. H. Lin, H. H. Tsai, K. C. Ho and C. G. Wu, *Org. Lett.*, 2010, **12**, 5454–5457.
79 A. Mishra, M. K. R. Fischer and P. Bäuerle, *Angew. Chem., Int. Ed.*, 2009, **48**, 2474–2499.
80 Y. L. Liang, F. Y. Cheng, J. Liang and J. Chen, *J. Phys. Chem. C*, 2010, **114**, 15842–15848.
81 J. H. Yum, S. R. Jang, P. Walter, T. Geiger, F. Nüesch, S. Kim, J. Ko, M. Grätzel and M. K. Nazeeruddin, *Chem. Commun.*, 2007, 4680–4682.
82 R. Y. Y. Lin, Y. S. Yen, Y. T. Cheng, C. P. Lee, Y. C. Hsu, H. H. Chou, C. Y. Hsu, Y. C. Chen, J. T. Lin, K. C. Ho and C. Tsai, *Org. Lett.*, 2012, **14**, 3612–3615.
83 S. Haid, M. Marszalek, A. Mishra, M. Wielopolski, J. Teuscher, J.-E. Moser, R. Humphry-Baker, S. M. Zakeeruddin, M. Grätzel and P. Bäuerle, *Adv. Funct. Mater.*, 2012, **22**, 1291–1302.
84 X. B. Cheng, M. Liang, S. Y. Sun, Y. B. Shi, Z. J. Ma, Z. Sun and S. Xue, *Tetrahedron*, 2012, **68**, 5375–5385.
85 D. P. Hagberg, X. Jiang, E. Gabrielsson, M. Linder, T. Marinado, T. Brinck, A. Hagfeldtbd and L. C. Sun, *J. Mater. Chem.*, 2009, **19**, 7232–7238.
86 X. Jiang, T. N. Marinado, E. Gabrielsson, D. P. Hagberg, L. Sun and A. Hagfeldt, *J. Phys. Chem. C*, 2010, **114**, 2799–2805.
87 X. Jiang, K. M. Karlsson, E. Gabrielsson, E. M. J. Johansson, M. Quintana, M. Karlsson, L. C. Sun, G. Boschloo and A. Hagfeldt, *Adv. Funct. Mater.*, 2011, **21**, 2944–2952.
88 Z. J. Ning, Q. Zhang, W. J. Wu, H. C. Pei, B. Liu and H. Tian, *J. Org. Chem.*, 2008, **73**, 3791–3797.
89 J. Tang, J. Hua, W. Wu, J. Li, Z. Jin, Y. Long and H. Tian, *Energy Environ. Sci.*, 2010, **3**, 1736–1745.
90 J. Tang, W. Wu, J. Huan, J. Li, X. Li and H. Tian, *Energy Environ. Sci.*, 2009, **2**, 982–990.
91 Z. Q. Wan, C. Y. Jia, Y. D. Duan, L. L. Zhou, J. Q. Zhang, Y. Lin and Y. Shi, *RSC Adv.*, 2012, **2**, 4507–4514.
92 Z. Q. Wan, C. Y. Jia, J. Q. Zhang, Y. D. Duan, Y. Lin and Y. Shi, *J. Power Sources*, 2012, **199**, 426–431.
93 M. D. Zhang, H. Pan, X. H. Ju, Y. J. Ji, L. Qin, H. G. Zheng and X. F. Zhou, *Phys. Chem. Chem. Phys.*, 2012, **14**, 2809–2815.
94 J. Shi, J. Huang, R. Tang, Z. Chai, J. Hua, J. Qin, Q. Li and Z. Li, *Eur. J. Org. Chem.*, 2012, 5248–5255.
95 S. P. Singh, M. S. Roy, K. R. J. Thomas, S. Balaiah, K. Bhanuprakash and G. D. Sharma, *J. Phys. Chem. C*, 2012, **116**, 5941–5950.
96 H. Han, M. Liang, K. Tang, X. Cheng, X. Zong, Z. Sun and S. Xue, *J. Photochem. Photobiol., A*, 2011, **217**, 169–176.
97 J. H. Yum, D. P. Hagberg, S. J. Moon, K. M. Karlsson, T. Marinado, L. C. Sun, A. Hagfeldt, M. K. Nazeeruddin and M. Grätzel, *Angew. Chem., Int. Ed.*, 2008, **48**, 1576–1580.
98 L. Alibabaei, J. H. Kim, M. Wang, N. Pootrakulchote, J. Teuscher, D. Di Censo, R. Humphry-Baker, J. E. Moser, Y. J. Yu, K. Y. Kay, S. M. Zakeeruddin and M. Grätzel, *Energy Environ. Sci.*, 2010, **3**, 1757–1764.
99 K. Do, D. Kim, N. Cho, S. Paek, K. Song and J. Ko, *Org. Lett.*, 2012, **14**, 222–225.
100 L. Cai, H. N. Tsao, W. Zhang, L. Wang, Z. Xue, M. Grätzel and B. Liu, *Adv. Energy Mater.*, 2012, DOI: 10.1002/aenm.201200435.

101 D. P. Hagberg, J. H. Yum, H. Lee, F. D. Angelis, T. Marinado, K. M. Karlsson, R. Humphry-Baker, L. C. Sun, A. Hagfeldt, M. Grätzel and M. K. Nazeeruddin, *J. Am. Chem. Soc.*, 2008, **130**, 6259–6266.
102 K. R. J. Thomas, Y. C. Hsu, J. T. Lin, K. M. Lee, K. C. Ho, C. H. Lai, Y. M. Cheng and P. T. Chou, *Chem. Mater.*, 2008, **20**, 1830–1840.
103 M. S. Tsai, Y. C. Hsu, J. T. Lin, H. C. Chen and C. P. Hsu, *J. Phys. Chem. C*, 2007, **111**, 18785–18793.
104 H. J. Chen, H. Huang, X. W. Huang, J. N. Clifford, A. Forneli, E. Palomares, X. Y. Zheng, L. P. Zheng, X. Y. Wang, P. Shen, B. Zhao and S. T. Tan, *J. Phys. Chem. C*, 2010, **114**, 3280–3286.
105 D. W. Chang, H. N. Tsao, P. Salvatori, F. D. Angelis, M. Grätzel, S. M. Park, L. Dai, H. J. Lee, J. B. Baek and M. K. Nazeeruddin, *RSC Adv.*, 2012, **2**, 6209–6215.
106 G. Li, Y. F. Zhou, X. B. Cao, P. Bao, K. J. Jiang, Y. Lin and L. M. Yang, *Chem. Commun.*, 2009, 2201–2203.
107 A. Abbotto, V. Leandri, N. Manfredi, F. D. Angelis, M. Pastore, J.-H. Yum, M. K. Nazeeruddin and M. Grätzel, *Eur. J. Org. Chem.*, 2011, 6195–6205.
108 Y. Numata, A. Islam, H. Chen and L. Han, *Energy Environ. Sci.*, 2012, **5**, 8548–8552.
109 X. Ren, S. Jiang, M. Cha, G. Zhou and Z. S. Wang, *Chem. Mater.*, 2012, **24**, 3493–3499.
110 S. Kim, J. K. Lee, S. O. Kang, J. Ko, J. H. Yum, S. Frantacci, F. D. Angelis, D. D. Censo, M. K. Nazeeruddin and M. Grätzel, *J. Am. Chem. Soc.*, 2006, **128**, 16701–16707.
111 I. Jung, J. K. Lee, K. H. Song, K. Song, S. O. Kang and J. Ko, *J. Org. Chem.*, 2007, **72**, 3652–3658.
112 H. Choi, J. K. Lee, K. Song, S. O. Kang and J. Ko, *Tetrahedron*, 2007, **63**, 3115–3121.
113 H. Choi, C. Baik, S. O. Kang, J. Ko, M. S. Kang, M. K. Nazeeruddin and M. Grätzel, *Angew. Chem., Int. Ed.*, 2008, **47**, 327–330.
114 H. Choi, I. Raabe, D. Kim, F. Teocoli, C. Kim, K. Song, J. H. Yum, J. Ko, M. K. Nazeeruddin and M. Grätzel, *Chem.–Eur. J.*, 2010, **16**, 1193–1201.
115 K. Lim, C. Kim, J. Song, T. Yu, W. Lim, K. Song, P. Wang, N. N. Zu and J. Ko, *J. Phys. Chem. C*, 2011, **115**, 22640–22646.
116 S. Paek, H. Choi, H. Choi, C. W. Lee, M. S. Kang, K. Song, M. K. Nazeeruddin and J. Ko, *J. Phys. Chem. C*, 2010, **114**, 14646–14653.
117 S. Kim, D. Kim, H. Choi, M. S. Kang, K. Song, S. O. Kang and J. Ko, *Chem. Commun.*, 2008, 4951–4953.
118 C. Kim, H. Choi, S. Kim, C. Baik, K. Song, M. S. Kang, S. O. Kang and J. Ko, *J. Org. Chem.*, 2008, **73**, 7072–7079.
119 H. Choi, J. K. Lee, K. Song, S. O. Kang and J. Ko, *Tetrahedron*, 2007, **63**, 3115–3121.
120 S. Kim, H. Choi, D. Kim, K. Song, S. O. Kang and J. Ko, *Tetrahedron*, 2007, **63**, 9206–9212.
121 S. Ko, H. Choi, M. S. Kang, H. H. wang, H. Ji, J. Kim, J. Ko and Y. J. Kang, *J. Mater. Chem.*, 2010, **20**, 2391–2399.
122 S. Q. Fan, C. Kim, B. Fang, K. X. Liao, G. J. Yang, C. J. Li, J. J. Kim and J. Ko, *J. Phys. Chem. C*, 2011, **115**, 7747–7754.
123 H. Qin, S. Wenger, M. Xu, F. Gao, X. Jing, P. Wang, S. M. Zakeeruddin and M. Grätzel, *J. Am. Chem. Soc.*, 2008, **130**, 9202–9203.
124 M. F. Xu, S. Wenger, H. Bala, D. Shi, R. Z. Li, Y. Z. Zhou, S. M. Zakeeruddin, M. Grätzel and P. Wang, *J. Phys. Chem. C*, 2009, **113**, 2966–2973.
125 M. K. Wang, M. F. Xu, D. Shi, R. Z. Li, F. F. Gao, G. L. Zhang, Z. H. Yi, R. Humphry-Baker, P. Wang, S. M. Zakeeruddin and M. Grätzel, *Adv. Mater.*, 2008, **20**, 4460–4463.
126 S. Paek, H. Choi, C. Kim, N. Cho, S. So, K. Song, M. K. Nazeeruddinc and J. Ko, *Chem. Commun.*, 2011, **47**, 2874–2876.
127 H. Choi, J. J. Kim, K. Song, J. Ko, Md. K. Nazeeruddinc and M. Grätzel, *J. Mater. Chem.*, 2010, **20**, 3280–3286.
128 J. J. Kim, H. Choi, J. W. Lee, M. S. Kang, K. Song, S. O. Kang and J. Ko, *J. Mater. Chem.*, 2008, **18**, 5223–5229.
129 Y. J. Chang and T. J. Chow, *Tetrahedron*, 2009, **65**, 4726–4734.
130 A. Baheti, P. Tyagi, K. R. J. Thomas, Y. C. Hsu and J. T. Lin, *J. Phys. Chem. C*, 2009, **113**, 8541–8547.
131 A. Baheti, P. Singh, C. P. Lee, K. R. J. Thomas and K. C. Ho, *J. Org. Chem.*, 2011, **76**, 4910–4920.
132 Y. J. Chang and T. J. Chow, *J. Mater. Chem.*, 2011, **21**, 9523–9531.
133 Y. D. Lin and T. J. Chow, *J. Mater. Chem.*, 2011, **21**, 14907–14916.
134 K. F. Chen, Y. C. Hsu, Q. Y. Wu, M. C. P. Yeh and S. S. Sun, *Org. Lett.*, 2009, **11**, 377–380.
135 C. Olivier, F. Sauvage, L. Ducasse, F. Castet, M. Grätzel and T. Toupance, *ChemSusChem*, 2011, **4**, 731–736.
136 Y. C. Chen, Y. H. Chen, H. H. Chou, S. Chaurasia, Y. S. Wen, J. T. Lin and C. F. Yao, *Chem.–Asian J.*, 2012, **7**, 1074–1084.
137 X. Y. Cao, W. B. Zhang, J. L. Wang, X. H. Zhou, H. Lu and J. Pei, *J. Am. Chem. Soc.*, 2003, **125**, 12430–12431.
138 Y. Sun, K. Xiao, Y. Liu, J. Wang, J. Pei, G. Yu and D. Zhu, *Adv. Funct. Mater.*, 2005, **15**, 818–822.
139 Z. Ning, Q. Zhang, H. Pei, J. Luan, C. Lu, Y. Cui and H. Tian, *J. Phys. Chem. C*, 2009, **113**, 10307–10313.
140 S. H. Lin, Y. C. Hsu, J. T. Lin, C. K. Lin and J. S. Yang, *J. Org. Chem.*, 2010, **75**, 7877–7886.
141 M. Liang, M. Lu, Q. Wang, W. Chen, H. Han, Z. Sun and S. Xue, *J. Power Sources*, 2011, **196**, 1657–1664.
142 M. Lu, M. Liang, H. Han, Z. Sun and S. Xue, *J. Phys. Chem. C*, 2011, **115**, 274–281.
143 T. Horiuchi, H. Miura and S. Uchida, *Chem. Commun.*, 2003, 3036–3037.
144 T. Horiuchi, H. Miura, K. Sumioka and S. Uchida, *J. Am. Chem. Soc.*, 2004, **126**, 12218–12219.
145 S. Ito, S. M. Zakeeruddin, R. Humphry-Baker, P. Liska, R. Charvet, P. Comte, M. K. Nazeeruddin, P. Péchy, M. Takata, H. Miura, S. Uchida and M. Grätzel, *Adv. Mater.*, 2006, **18**, 1202–1205.
146 S. Ito, H. Miura, S. Uchida, M. Takata, K. Sumioka, P. Liska, P. Comte, P. Péchy and M. Grätzel, *Chem. Commun.*, 2008, 5194–5196.

147 D. Kuang, S. Uchida, R. Humphry-Baker, S. K. Zakeeruddin and M. Grätzel, *Angew. Chem., Int. Ed.*, 2008, **47**, 1923–1927.
148 S. Higashijima, Y. Inoue, H. Miura, Y. Kubota, K. Funabiki, T. Yoshida and M. Matsui, *RSC Adv.*, 2012, **2**, 2721–2724.
149 M. Matsui, T. Fujita, Y. Kubota, K. Funabiki, J. Jin, T. Yoshida and H. Miura, *Dyes Pigm.*, 2010, **86**, 143–148.
150 W. Zhu, Y. Wu, S. Wang, W. Li, X. Li, J. Chen, Z. S. Wang and H. Tian, *Adv. Funct. Mater.*, 2011, **21**, 756–763.
151 Y. Z. Wu, X. Zhang, W. Q. Li, Z.-S. Wang, H. Tian and W. H. Zhu, *Adv. Energy Mater.*, 2012, **2**, 149–156.
152 Y. Z. Wu, M. Marszalek, S. M. Zakeeruddin, Q. Z. H. Tian, M. Grätzel and W. H. Zhu, *Energy Environ. Sci.*, 2012, **5**, 8261–8272.
153 Y. Cui, Y. Wu, X. Lu, X. Zhang, G. Zhou, F. B. Miapeh, W. Zhu and Z. S. Wang, *Chem. Mater.*, 2011, **23**, 4394–4401.
154 Z. Ning, Y. Fu and H. Tian, *Energy Environ. Sci.*, 2010, **3**, 1170–1181.
155 W. Q. Li, Y. Z. Wu, Q. Zhang, H. Tian and W. H. Zhu, *ACS Appl. Mater. Interfaces*, 2012, **4**, 1822–1830.
156 S. Y. Qu, C. J. Qin, A. Islam, Y. Z. Wu, W. H. Zhu, J. L. Hua, H. Tian and L. Y. Han, *Chem. Commun.*, 2012, **48**, 6972–6974.
157 W. Q. Li, Y. Z. Wu, X. Li, Y. S. Xie and W. H. Zhu, *Energy Environ. Sci.*, 2011, **4**, 1830–1837.
158 M. Akhtaruzzaman, Y. Seya, N. Asao, A. l. Islam, E. Kwon, A. E. Shafei, L. Y. Han and Y. Yamamoto, *J. Mater. Chem.*, 2012, **22**, 10771–10778.
159 K. Funabiki, H. Mase, Y. Saito, A. Otsuka, A. Hibino, N. Tanaka, H. Miura, Y. Himori, T. Yoshida, Y. Kubota and M. Matsui, *Org. Lett.*, 2012, **14**, 1246–1249.
160 M. Akhtaruzzaman, A. Islam, F. Yang, N. Asao, E. Kwon, S. P. Singh, L. Y. Han and Y. Yamamoto, *Chem. Commun.*, 2011, **47**, 12400–12402.
161 B. Liu, Q. B. Liu, D. You, X. Y. Li, Y. Naruta and W. H. Zhu, *J. Mater. Chem.*, 2012, **22**, 13348–13356.
162 B. Liu, W. J. Wu, X. Y. Li, L. Li, S. F. Guo, X. R. Wei, W. H. Zhu and Q. B. Liu, *Phys. Chem. Chem. Phys.*, 2011, **13**, 8985–8992.
163 K. Hara, T. Sato, R. Katoh, A. Furube, T. Yoshihara, M. Murai, M. Kurashige, S. Ito, A. Shinpo, S. Suga and H. Arakawa, *Adv. Funct. Mater.*, 2005, **15**, 246–252.
164 K. Hara, M. Kurashige, S. Ito, A. Shinpo, S. Suga, K. Sayama and H. Arakawa, *Chem. Commun.*, 2003, 252–253.
165 S. L. Li, K. J. Jiang, K. F. Shao and L. M. Yang, *Chem. Commun.*, 2006, 2792–2794.
166 X. B. Cheng, S. Y. Sun, M. Liang, Y. B. Shi, Z. Sun and S. Xue, *Dyes Pigm.*, 2012, **92**, 1292–1299.
167 R. Chen, X. Yang, H. Tian, X. Wang, A. Hagfeldt and L. Sun, *Chem. Mater.*, 2007, **19**, 4007–4015.
168 Y. Hao, X. Yang, J. Cong, H. Tian, A. Hagfeldt and L. Sun, *Chem. Commun.*, 2009, 4031–4033.
169 Y. Hao, X. C. Yang, M. Z. Zhou, J. Y. Cong, X. N. Wang, A. Hagfeldt and L. Sun, *ChemSusChem*, 2011, **4**, 1601–1605.
170 N. S. Cho, J. H. Park, S. K. Lee, J. Lee and H. K. Shim, *Macromolecules*, 2006, **39**, 177–183.
171 H. Tian, X. Yang, R. Chen, Y. Pan, L. Li, A. Hagfeldt and L. Sun, *Chem. Commun.*, 2007, 3741–3743.
172 H. N. Tian, X. C. Yang, R. K. Chen, A. Hagfeldt and L. C. Sun, *Energy Environ. Sci.*, 2009, **2**, 674–677.
173 T. Meyer, D. Ogermann, A. Pankrath, K. Kleinermanns and T. J. J. Müller, *J. Org. Chem.*, 2012, **77**, 3704–3715.
174 S. S. Park, Y. S. Won, Y. C. Choi and J. H. Kim, *Energy Fuels*, 2009, **23**, 3732–3736.
175 M. H. Tsao, T. Y. Wu, H. P. Wang, I. W. Sun, S. G. Su, Y. C. Lin and C. W. Chang, *Mater. Lett.*, 2011, **65**, 583–586.
176 Z. B. Xie, A. Midya, K. P. Loh, S. Adams, D. J. Blackwood, J. Wang, X. J. Zhang and Z. k. Chen, *Prog. Photovoltaics*, 2010, **18**, 573–581.
177 S. H. Kim, H. W. Kim, C. Sakong, J. W. Namgoong, S. W. Park, M. J. Ko, C. H. Lee, W. I. Lee and J. P. Kim, *Org. Lett.*, 2011, **13**, 5784–5787.
178 M. Marszalek, S. Nagane, A. Ichake, R. Humphry-Baker, V. Paul, S. M. Zakeeruddin and M. Grätzel, *J. Mater. Chem.*, 2012, **22**, 889–894.
179 W. J. Wu, J. B. Yang, J. N. Hua, J. Tang, L. Zhang, Y. T. Long and H. Tian, *J. Mater. Chem.*, 2010, **20**, 1772–1779.
180 C. J. Yang, Y. J. Chang, M. Watanabe, Y. S. Hon and T. J. Chow, *J. Mater. Chem.*, 2012, **22**, 4040–4049.
181 C. J. Chen, J. Y. Liao, Z. G. Chi, B. J. Xu, X. Q. Zhang, D. B. Kuang, Y. Zhang, S. W. Liu and J. R. Xu, *RSC Adv.*, 2012, **2**, 7788–7797.
182 C. J. Chen, J. Y. Liao, Z. G. Chi, B. J. Xu, X. Q. Zhang, D. B. Kuang, Y. Zhang, S. W. Liu and J. R. Xu, *J. Mater. Chem.*, 2012, **22**, 8994–9005.
183 Y. J. Chang, P. T. Chou, Y. Z. Lin, M. Watanabe, C. J. Yang, T. M. Chin and T. J. Chow, *J. Mater. Chem.*, 2012, **22**, 21704–21712.
184 D. Cao, J. Peng, Y. Hong, X. Fang, L. Wang and H. Meier, *Org. Lett.*, 2011, **13**, 1610–1613.
185 Y. Hong, J. Y. Liao, D. Cao, X. Zang, D. B. Kuang, L. Wang, H. Meier and C. Y. Su, *J. Org. Chem.*, 2011, **76**, 8015–8021.
186 K. M. Karlsson, X. Jiang, S. K. Eriksson, E. Gabrielsson, H. Rensmo, A. Hagfeldt and L. C. Sun, *Chem.–Eur. J.*, 2011, **17**, 6415–6424.
187 H. Tian, I. Bora, X. Jiang, E. Gabrielsson, K. M. Karlsson, A. Hagfeldt and L. C. Sun, *J. Mater. Chem.*, 2011, **21**, 12462–12472.
188 H. Tian, X. C. Yang, J. Y. Cong, R. K. Chen, J. Liu, Y. Hao, A. Hagfeldt and L. C. Sun, *Chem. Commun.*, 2009, 6288–6290.
189 N. Koumura, Z. S. Wang, S. Mori, M. Miyashita, E. Suzuki and K. Hara, *J. Am. Chem. Soc.*, 2006, **128**, 14256–14257.
190 Z. S. Wang, N. Koumura, Y. Cui, M. Takahashi, H. Sekiguchi, A. Mori, T. Kubo, A. Furube and K. Hara, *Chem. Mater.*, 2008, **20**, 3993–4003.
191 K. Hara, Z. S. Wang, Y. Cui, A. Furube and N. Koumura, *Energy Environ. Sci.*, 2009, **2**, 1109–1114.
192 N. Koumura, Z. S. Wang, M. Miyashita, Y. Uemura, H. Sekiguchi, Y. Cui, A. Mori, S. Mori and K. Hara, *J. Mater. Chem.*, 2009, **19**, 4829–4836.
193 X. H. Zhang, Y. Cui, R. Katoh, N. Koumura and K. Hara, *J. Phys. Chem. C*, 2010, **114**, 18283–18290.

194 X. H. Zhang, Z. S. Wang, Y. Cui, N. Koumura, A. Furube and K. Hara, *J. Phys. Chem. C*, 2009, **113**, 13409–13415.
195 H. Lai, J. Hong, P. Liu, C. Yuan, Y. X. Li and Q. Fang, *RSC Adv.*, 2012, **2**, 2427–2432.
196 D. Kim, J. K. Lee, S. O. Kang and J. Ko, *Tetrahedron*, 2007, **63**, 1913–1922.
197 Y. J. Chang, P. T. Chou, S. Y. Lin, M. Watanabe, Z. Q. Liu, J. L. Lin, K. Y. Chen, S. S. Sun, C. Y. Liu and T. J. Chow, *Chem.–Asian J.*, 2012, **7**, 572–581.
198 T. Duan, K. Fan, C. Zhong, T. Y. Peng, J. G. Qin and X. G. Chen, *RSC Adv.*, 2012, **2**, 7081–7086.
199 C. Teng, X. Yang, C. Yuan, C. Li, R. Chen, H. Tian, S. Li, A. Hagfeldt and L. Sun, *Org. Lett.*, 2009, **11**, 5542–5545.
200 E. M. Barea, C. Zafer, B. Gultekin, B. Aydin, S. Koyuncu, S. Icli, F. F. Santiago and J. Bisquert, *J. Phys.Chem. C*, 2010, **114**, 19840–19848.
201 W. Lee, N. Cho, J. Kwon, J. Ko and J. I. Hong, *Chem.–Asian J.*, 2012, **7**, 343–350.
202 G. Boschloo and A. Hagfeldt, *Acc. Chem. Res.*, 2009, **42**, 1819–1826.
203 B. C. O'Regan, I. López-Duarte, M. V. Martínez-Díaz, A. Forneli, J. Albero, A. Morandeira, E. Palomares, T. Torres and J. R. Durrant, *J. Am. Chem. Soc.*, 2008, **130**, 2906–2907.
204 T. Marinado, K. Nonomura, J. Nissfolk, M. K. Karlsson, D. P. Hagberg, L. Sun, S. Mori and A. Hagfeldt, *Langmuir*, 2010, **26**, 2592–2598.
205 M. Planells, L. Pellejà, J. N. Clifford, M. Pastore, D. Angelis, F. López, N. Marder and S. R. Palomares, *Energy Environ. Sci.*, 2011, **4**, 1820–1829.
206 A. Hagfeldt and M. Grätzel, *Chem. Rev.*, 1995, **95**, 49–68.
207 H. Nusbaumer, S. M. Zakeeruddin, J. E. Moser and M. Grätzel, *Chem.–Eur. J.*, 2003, **9**, 3756–3763.
208 S. M. Feldt, E. A. Gibson, E. Gabrielsson, L. Sun, G. Boschloo and A. Hagfeldt, *J. Am. Chem. Soc.*, 2010, **132**, 16714–16724.
209 S. M. Feldt, G. Wang, G. Boschloo and A. Hagfeldt, *J. Phys. Chem. C*, 2011, **115**, 21500–21507.
210 H. Nusbaumer, J. E. Moser, S. M. Zakeeruddin, M. K. Nazeeruddin and M. Grätzel, *J. Phys. Chem. B*, 2001, **105**, 10461–10464.
211 H. X. Wang, P. G. Nicholson, L. Peter, S. M. Zakeeruddin and M. Grätzel, *J. Phys. Chem. C*, 2010, **114**, 14300–14306.
212 Y. Liu, J. R. Jennings, Y. Huang, Q. Wang, S. M. Zakeeruddin and M. Grätzel, *J. Phys. Chem. C*, 2011, **115**, 18847–18855.
213 M. Xu, D. Zhou, N. Cai, J. Liu, R. Li and P. Wang, *Energy Environ. Sci.*, 2011, **4**, 4735–4742.
214 M. F. Xu, M. Zhang, M. Pastore, R. Z. Li, F. D. Angelis and P. Wang, *Chem. Sci.*, 2012, **3**, 976–983.
215 M. Zhang, J. Y. Liu, Y. H. Wang, D. F. Zhou and P. Wang, *Chem. Sci.*, 2011, **2**, 1401–1406.
216 Y. Bai, J. Zhang, D. Zhou, Y. Wang, M. Zhang and P. Wang, *J. Am. Chem. Soc.*, 2011, **133**, 11442–11445.
217 Y. M. Cao, N. Cai, Y. L. Wang, R. Z. Li, Y. Yuan and P. Wang, *Phys. Chem. Chem. Phys.*, 2012, **14**, 8282–8286.
218 J. Liu, J. Zhang, M. Xu, D. Zhou, X. Jing and P. Wang, *Energy Environ. Sci.*, 2011, **4**, 3021–3029.
219 H. N. Tsao, C. Y. Yi, T. Moehl, J. H. Yum, S. M. Zakeeruddin, M. K. Nazeeruddin and M. Grätzel, *ChemSusChem*, 2011, **4**, 591–594.
220 J. H. Yum, E. Baranoff, F. Kessler, T. Mmoehl, S. Ahmad1, T. Bessho, A. Mmarchioro, E. Ghadiri, J. E. Mmoser, C. Y. Yi, M. K. Nnazeeruddin and M. Grätzel, *Nat. Commun.*, 2012, **3**, 631–638.
221 J. Burschka, A. Dualeh, F. Kessler, E. Baranoff, N. Lê Cevey-Ha, C. Yi, M. K. Nazeeruddin and M. Grätzel, *J. Am. Chem. Soc.*, 2011, **133**, 18042–18045.
222 C. Qin, W. Peng, K. Zhang, A. Islam and L. Han, *Org. Lett.*, 2012, **14**, 2532–2535.
223 X. P. Zong, M. Liang, C. R. Fan, K. Tang, G. Li, Z. Sun and S. Xue, *J. Phys. Chem. C*, 2012, **116**, 11241–11250.
224 X. P. Zong, M. Liang, T. Chen, J. N. Jia, L. N. Wang, Z. Sun and S. Xue, *Chem. Commun.*, 2012, **48**, 6645–6647.
225 Y. Numata, I. Ashraful, Y. Shirai and L. Han, *Chem. Commun.*, 2011, **47**, 6159–6161.
226 Y. Oyama, S. Inoue, T. Nagano, K. Kushimoto, J. Ohshita, I. Imae, K. Komaguchi and Y. Harima, *Angew. Chem., Int. Ed.*, 2011, **50**, 7429–7433.
227 Y. Ooyama, T. Nagano, S. Inoue, I. Imae, K. Komaguchi, J. Ohshita and Y. Harima, *Chem.–Eur. J.*, 2011, **17**, 14837–14843.
228 M. Katono, T. Bessho, M. Wielopolski, M. Marszalek, J. E. Moser, R. H. Baker, S. M. Zakeeruddin and M. Grätzel, *J. Phys. Chem. C*, 2012, **116**, 16876–16884.
229 J. Zhao, X. Yang, M. Cheng, S. Li, X. Wang and L. Sun, *J. Mater. Chem. A*, 2013, **1**, 2441–2446.
230 J. Mao, N. He, Z. Ning, Q. Zhang, F. Guo, L. Chen, W. Wu, J. Hua and H. Tian, *Angew. Chem., Int. Ed.*, 2012, **51**, 9873–9876.
231 F. Labat, T. Le Bahers, I. Ciofini and C. Adamo, *Acc. Chem. Res.*, 2012, **45**, 1268–1277.
232 F. Ambrosio, N. Martsinovich and A. Troisi, *J. Phys. Chem. Lett.*, 2012, **3**, 1531–1535.
233 K. Srinivas, K. Yesudas, K. Bhanuprakash, V. J. Rao and L. Giribabu, *J. Phys. Chem. C*, 2009, **113**, 20117–20126.
234 U. Bach, D. Lupo, P. Comte, J. E. Moser, F. Weissortel, J. Salbeck, H. Spreitzer and M. Grätzel, *Nature*, 1998, **395**, 583–585.
235 N. Cai, S. J. Moon, N. L. Cevey-Ha, T. Moehl, R. Humphry-Baker, P. Wang, S. M. Zakeeruddin and M. Grätzel, *Nano Lett.*, 2011, **11**, 1452–1456.
236 T. Leijtens, I. K. Ding, T. Giovenzana, J. T. Bloking, M. D. McGehee and A. Sellinger, *ACS Nano*, 2012, **6**, 1455–1462.
237 E. M. J. Johansson, L. Yang, E. Gabrielsson, P. W. Lohse, G. Boschloo, L. Sun and A. Hagfeldt, *J. Phys. Chem. C*, 2012, **116**, 18070–18078.
238 N. Metri, X. Sallenave, C. Plesse, L. Beouch, P.-H. Aubert, F. Goubard, C. Chevrot and G. Sini, *J. Phys. Chem. C*, 2012, **116**, 3765–3772.

